

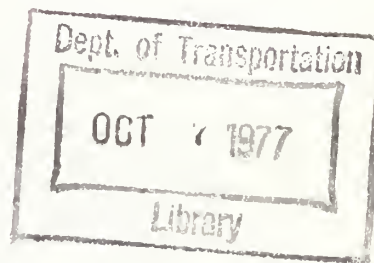
PS 232-57
HE
18.5
.A37
no.
DOT-
TSC-
UMTA-
77-15

NO. UMTA-MA-06-0044-77-1

FLYWHEEL PROPULSION SIMULATION

Charles M. King
Alexander Kusko

Alexander Kusko, Inc.
161 Highland Avenue
Needham Heights MA 02194



MAY 1977

FINAL REPORT

DOCUMENT IS AVAILABLE TO THE U.S. PUBLIC
THROUGH THE NATIONAL TECHNICAL
INFORMATION SERVICE, SPRINGFIELD,
VIRGINIA 22161

Prepared for

U.S. DEPARTMENT OF TRANSPORTATION
Urban Mass Transportation Administration
Office of Technology Development
and Deployment
Washington DC 20590

NOTICE

This document is disseminated under the sponsorship of the Department of Transportation in the interest of information exchange. The United States Government assumes no liability for its contents or use thereof.

NOTICE

The United States Government does not endorse products or manufacturers. Trade or manufacturers' names appear herein solely because they are considered essential to the object of this report.

1. Report No. UMTA-MA-06-0044-77-1	2. Government Accession No.	3. Recipient's Catalog No.
4. Title and Subtitle FLYWHEEL PROPULSION SIMULATION	5. Report Date May 1977	6. Performing Organization Code
7. Author(s) Charles M. King, Alexander Kusko	8. Performing Organization Report No. DOT-TSC-UMTA-77-15	
9. Performing Organization Name and Address Alexander Kusko, Inc. 161 Highland Avenue Needham Heights MA 02194	10. Work Unit No. (TRAIS) UM730/R7724	11. Contract or Grant No. DOT-TSC-1180
12. Sponsoring Agency Name and Address U.S. Department of Transportation Urban Mass Transportation Administration Office of Technology Development and Deployment Washington DC 20590	13. Type of Report and Period Covered Final Report May 1, 1975-March 30, 1977	14. Sponsoring Agency Code
15. Supplementary Notes *Under Contract to: DOT/Transportation Systems Center Kendall Square Cambridge MA 02142 Technical Monitor: Frank L. Raposa		
16. Abstract This report was prepared in support of the Urban Mass Transportation Administration's program in flywheel energy storage. This report develops and describes the analytical models and digital computer simulations that can be used for the evaluation of flywheel-electric propulsion systems employed with urban transit vehicles operating over specified routes and with predetermined velocity profiles. The computer simulation is divided into two sections. The first section simulates the dynamic behavior of the vehicle enroute, computes the energy and power requirements, and the power losses of each of the propulsion system components. The second section utilizes thermal models to compute the temperature rises of each of the propulsion system components. The simulations can be used to determine the suitability of a given flywheel-electric propulsion system for an intended mission.		
<div data-bbox="868 1268 1245 1526" data-label="Image"> </div>		
17. Key Words Flywheel Propulsion System Urban Transit Vehicle Digital Computer Simul. Velocity Profile Power Losses - Component Temperature Rises - Component	18. Distribution Statement DOCUMENT IS AVAILABLE TO THE U.S. PUBLIC THROUGH THE NATIONAL TECHNICAL INFORMATION SERVICE, SPRINGFIELD, VIRGINIA 22161	
19. Security Classif. (of this report) Unclassified	20. Security Classif. (of this page) Unclassified	21. No. of Pages 204
		22. Price

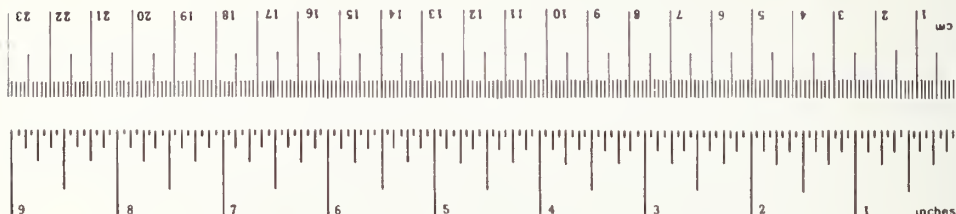
PREFACE

The work described in this report was performed by Alexander Kusko, Inc. of Needham Heights, MA., under contract DOT/ TSC-1180 for the Transportation Systems Center, Department of Transportation, Cambridge, MA., under the auspices of the Urban Mass Transportation Administration, Department of Transportation, Washington, D. C.

Mr. Frank Raposa of the Electrical Power and Propulsion Branch, Vehicles and Engineering Division of the Office of Ground Systems at the Transportation Systems Center provided many valuable suggestions as technical monitor. Mr. Roger Flanders of Kentron Hawaii, Ltd. worked closely with the authors to develop a working simulation on the Transportation Systems Center computer. Ms. Ruth Weinstock of Word Guild did much to make this report more readable and more interesting.

Approximate Conversions to Metric Measures

Symbol	When You Know	Multiply by	To Find	Symbol
LENGTH				
in	inches	2.5	centimeters	cm
ft	feet	30	meters	m
yd	yards	0.9	kilometers	km
mi	miles	1.6		
AREA				
in ²	square inches	6.5	square centimeters	cm ²
ft ²	square feet	0.09	square meters	m ²
yd ²	square yards	0.8	square meters	m ²
mi ²	square miles	2.6	square kilometers	km ²
	acres	0.4	hectares	ha
MASS (weight)				
oz	ounces	28	grams	g
lb	pounds	0.45	kilograms	kg
	short tons (2000 lb)	0.9	tonnes	t
VOLUME				
tsp	teaspoons	5	milliliters	ml
Tabsp	tablespoons	15	milliliters	ml
fl oz	fluid ounces	30	milliliters	ml
c	cups	0.24	liters	l
pt	pints	0.47	liters	l
qt	quarts	0.95	liters	l
gal	gallons	3.8	liters	l
ft ³	cubic feet	0.03	cubic meters	m ³
yd ³	cubic yards	0.76	cubic meters	m ³
TEMPERATURE (exact)				
°F	Fahrenheit temperature	5/9 (after subtracting 32)	Celsius temperature	°C

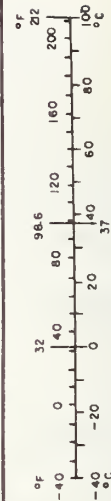


Approximate Conversions from Metric Measures

Symbol	When You Know	Multiply by	To Find	Symbol
LENGTH				
mm	millimeters	0.04	inches	in
cm	centimeters	0.4	inches	in
m	meters	3.3	feet	ft
	meters	1.1	yards	yd
km	kilometers	0.6	miles	mi
AREA				
cm ²	square centimeters	0.16	square inches	in ²
m ²	square meters	1.2	square yards	yd ²
km ²	square kilometers	0.4	square miles	mi ²
ha	hectares (10,000 m ²)	2.5	acres	
MASS (weight)				
g	grams	0.035	ounces	oz
kg	kilograms	2.2	pounds	lb
t	tonnes (1000 kg)	1.1	short tons	
VOLUME				
ml	milliliters	0.03	fluid ounces	fl oz
l	liters	2.1	pints	pt
	liters	1.06	quarts	qt
	liters	0.26	gallons	gal
m ³	cubic meters	35	cubic feet	ft ³
	cubic meters	1.3	cubic yards	yd ³

TEMPERATURE (exact)

°C	Celsius temperature	9/5 (then add 32)	Fahrenheit temperature	°F
----	---------------------	-------------------	------------------------	----



CONTENTS

<u>Section</u>	<u>Page</u>
EXECUTIVE SUMMARY	xii
1. INTRODUCTION	1-1
Research Context	1-1
Performance Criteria for Flywheel Electric-Drive Systems	1-5
Simulation Approach	1-9
Scope of Analysis	1-13
2. BASELINE SYSTEM: COMPONENTS AND MODES OF OPERATION	2-1
Configuration of Major Components	2-1
The Mission Profile	2-6
Modes of Operation	2-9
Wayside Charging Mode	2-9
Traveling Mode	2-13
3. COMPUTER SIMULATION PROCEDURES	3-1
Scope of Simulation	3-1
Operation of Computer Program	3-1
Calculation of Propulsion Power and Auxiliary Power Requirements	3-12
4. MODELS	4-1
Procedure	4-1
Dynamic and Power Loss Models	4-2
DC Traction Motor	4-4
Solid-State Controller	4-8
Alternator	4-8
Ratings	4-10
Phasor diagrams	4-14
Power loss model	4-20
Propulsion System Losses	4-24
Thermal Models	4-26
Rotating Electric Machines	4-28
Solid-State Controller	4-34
Changing Ratings of Major Components	4-37
Changes in Electrical Ratings of Electric Machine	4-38
Changes in Speed Ratings of Electric Machines	4-40
Changes in Electrical Rating of Solid-State Controller	4-42
Changes in Thermal Parameters	4-42

CONTENTS (CONTINUED)

<u>Section</u>	<u>Page</u>
5. RESULTS	5-1
Sample Run	5-1
Mission Profile	5-1
Tractive Force	5-6
Electrical Operation	5-8
Component Temperature	5-10
System Redesign	5-11
Extension to Other Systems	5-14
Conclusions	5-15
6. CONCLUSIONS	6-1
REFERENCES	R-1

CONTENTS (CONTINUED)

<u>Section</u>		<u>Page</u>
APPENDIX A.	MATHEMATICAL MODELS	A-1
	Part I Dynamic and Power Loss Models	A-1
	A. Propulsion Requirements	A-1
	B. Gearbox (Transmission)	A-3
	C. DC Traction Motor	A-4
	D. Solid-State Controller	A-8
	E. Alternator	A-9
	F. Flywheel	A-15
	Part II Thermal Models	A-17
	G. DC Traction Motor	A-17
	H. Alternator	A-19
	I. Solid-State Controller	A-21
	Part III Wayside Charging Mode	A-22
APPENDIX B.	INPUT CONSTANTS FOR COMPUTER PROGRAM	B-1
	Part I Constants for a Computer Run	B-1
	Part II Other Constants	B-8
APPENDIX C.	PARAMETER LISTING FOR COMPUTER PROGRAM	C-1
APPENDIX D.	TABULAR OUTPUTS FOR SAMPLE RUN (ONE ROUND TRIP)	D-1
	Part I Dynamics and Power Loss Outputs (FOR ϕ 3.DAT)	D-1
	Flywheel Vehicle Propulsion System Loss Model	D-2
	Charging Mode Data (Station A, Initial)	D-4
	Traveling Mode Data (Outbound Leg)	D-6
	Charging Mode Data (Station B)	D-8
	Traveling Mode Data (Return Leg)	D-9
	Charging Mode Data (Station A, Final)	D-11
	Part II Thermal Outputs (FOR 26.DAT)	D-12
	Flywheel Vehicle Propulsion System Thermal Model	D-13
	Charging Mode Data (Station A, Initial)	D-14
	Traveling Mode Data (Outbound Leg)	D-16
	Charging Mode Data (Station B)	D-18
	Traveling Mode Data (Return Leg)	D-19
	Charging Mode Data (Station A, Final)	D-21

CONTENTS (CONTINUED)

<u>Section</u>		<u>Page</u>
APPENDIX E.	MANUFACTURERS' DATA FOR MAJOR COMPONENTS	E-1
	Part I Alternator Data	E-1
	Part II DC Traction Motor Data	E-3
	Part III Solid-State Controller Data	E-10
APPENDIX F.	REPORT OF INVENTIONS	F-1

LIST OF FIGURES

<u>Figure</u>		<u>Page</u>
1.	Oerlikon Electrogyro Bus	1-2
2.	Morgantown Vehicle	2-2
3.	Major Components of Baseline Propulsion System	2-4
4.	Roadway Elevation and Vehicle Velocity Profiles for the Morgantown Route	2-7
5.	Wayside Charging Mode: System Diagram	2-10
6.	Wayside Charging Mode for Basline System: Input Power and Input Voltage vs. Alternator Speed	2-12
7.	Traveling Mode: Direction of Power Flow During Motoring and Full Regenerative Braking	2-16
8.	Flowchart for Flywheel Propulsion Simulation	3-4
9.	Flowchart for Computing Tractive Force F and Propulsion Power P_2	3-17
10.	Saturation Curves for Alternator	4-13
11.	Alternator Phasor Diagram, Traveling Mode: Generator Operation at Alternator Base Conditions	4-15
12.	Alternator Phasor Diagrams, Traveling Mode: Generator Operation at DC Traction Motor Base Conditions	4-17
13.	Alternator Phasor Diagrams, Wayside Charging Mode: Alternator Operating as a Synchronous Motor	4-19
14.	Power and Efficiency of Electric Propulsion System Components	4-25
15.	Thermal Circuit Model for DC Traction Motor	4-30
16.	Flowchart of Thermal Computations for DC Traction Motor	4-33
17.	Thermal Circuit Model for Solid-State Controller	4-35
18.	Vehicle Speed, Roadway Grade Profile and Vehicle Tractive Force Requirements	5-2

LIST OF FIGURES (CONTINUED)

<u>Figure</u>	<u>Page</u>
19. Power and Loss Performance	5-3
20. Controller, Flywheel, and DC Traction Motor Performance	5-4
21. Electric Machine and Controller Temperatures	5-5
A-1. Circuit Diagram for Solid-State Controller	A-8
E-1. Cross Section of 70 HP-DC Traction Motor	E-4
E-2. Performance Curve for 70 HP-DC Traction Motor	E-8

LIST OF TABLES

<u>Table</u>	<u>Page</u>
1. Dynamic and Power Loss Outputs During Wayside Charging Mode (FOR 03. DAT)	3-6
2. Dynamic and Power Loss Outputs During Traveling Mode (FOR 03.DAT)	3-7
3. Thermal Outputs During Wayside Charging and Traveling Modes (FOR26.DAT)	3-8
4. Tabular Summary of Key Parameters and Their Peak Values	3-9
5. Key System Parameter Listing (Masthead for Output Plots)	3-10
6. DC Traction Motor Base Quantities	4-5
7. DC Traction Motor Loss Components at Base Conditions	4-7
8. Alternator Per-Unit Impedances	4-10
9. Alternator Base Quantities	4-12
10. Alternator Loss Components at Base Conditions	4-21
11. Alternator Loss Components During Traveling Mode	4-22
12. Alternator Losses During Wayside Charging Mode	4-23
13. Thermal-to-Electric Analogs	4-28
14. Weighting Coefficients for Thermal Models of Electric Machines	4-32
15. Thermal Resistances and Time Constants for Electric Machines	4-34
16. Thermal Resistances and Time Constants for Solid-State Controller	4-36
E-1. Parts List for 70 HP-DC Traction Motor	E-5
E-2. Test Data for 70 HP-DC Traction Motor	E-7
E-3. Power Pack Thyristor Data	E-10

EXECUTIVE SUMMARY

This report develops and describes the analytical models and digital computer simulations of the electric propulsion systems for flywheel energy storage vehicles. The simulation described facilitates a critical evaluation of candidate flywheel-powered electric vehicles operating over urban transit routes. The computer program provides dynamic or time-varying information on voltages, currents, tractive effort, flywheel speed, etc., as the vehicle traverses a given roadway profile and conforms to a specified velocity profile. The specific flywheel electric-drive propulsion system is well defined in the computer model, and is based on manufacturers' data for the actual hardware. The power losses in the major components are computed at each time interval and used as inputs for the thermal models, which determine the temperature rises of the components. The wayside recharge of the flywheel, using the on-board alternator as a motor, is simulated and the use of regenerative braking to recover energy and store it in the flywheel is also featured.

This simulation can be used to determine whether or not the component ratings have been properly selected, based on the temperature rises observed after a run of several round trips or mission cycles. Scaling laws are provided to change the loss models and the thermal models in accordance with changes in the machine ratings or sizes.

The simulation can also be used to determine:

1. If the flywheel size, i. e. energy storage capacity, is adequate for the vehicle/ mission profile.
2. The energy efficiency of the propulsion system in terms of average kWh required per vehicle route mile.
3. The effectiveness of regenerative braking energy recovery in reducing the propulsion energy requirement, i. e. is the extra complexity of regenerative braking worthwhile in terms of energy savings?
4. The time required to recharge the flywheel at each stop, so that inconveniently long recharge intervals are identified. Alternate recharge strategies can then be simulated to minimize the longest recharge time. One such scheme makes all recharge intervals of equal time.

Finally, this simulation can be used to determine suitability of a given system configuration for an intended mission. Also, changes in the ratings of components and different configurations of components can be analyzed in order to optimize the drive system. Furthermore, the simulation method can be applied to electric-drive systems for battery energy-storage vehicles, to hybrid vehicles, and to vehicles operating from wayside power.

1. INTRODUCTION

Research Context

Development of a bus propelled by a flywheel instead of by an engine or storage battery has long interested urban transportation planners.

The kinetic energy stored in a flywheel supplants the need for petroleum-derived fuels and minimizes negative environmental impacts. Flywheel-driven vehicles depend on fossil-fuel, nuclear, or hydroelectric central station power. They have no emission fumes and low noise levels.

The flywheel propulsion concept is not new. As early as 1935, an Electrogyro Bus¹ powered by a kinetic energy wheel was placed in service by Oerlikon of Switzerland (see Fig. 1). Designs that combine flywheel energy-storage with conventional electric-drive systems, however, have not been actively developed until recently. Renewed interest in this type of vehicle stems from the dual concern with reducing pollution from fuel-burning vehicles and, following the 1974 oil embargo, with developing alternative energy sources.

Basically, a flywheel is a spinning disc which stores kinetic energy. Carried on board a rubber-tired vehicle, it can be charged or recharged using electric power at selected wayside stations. The stored

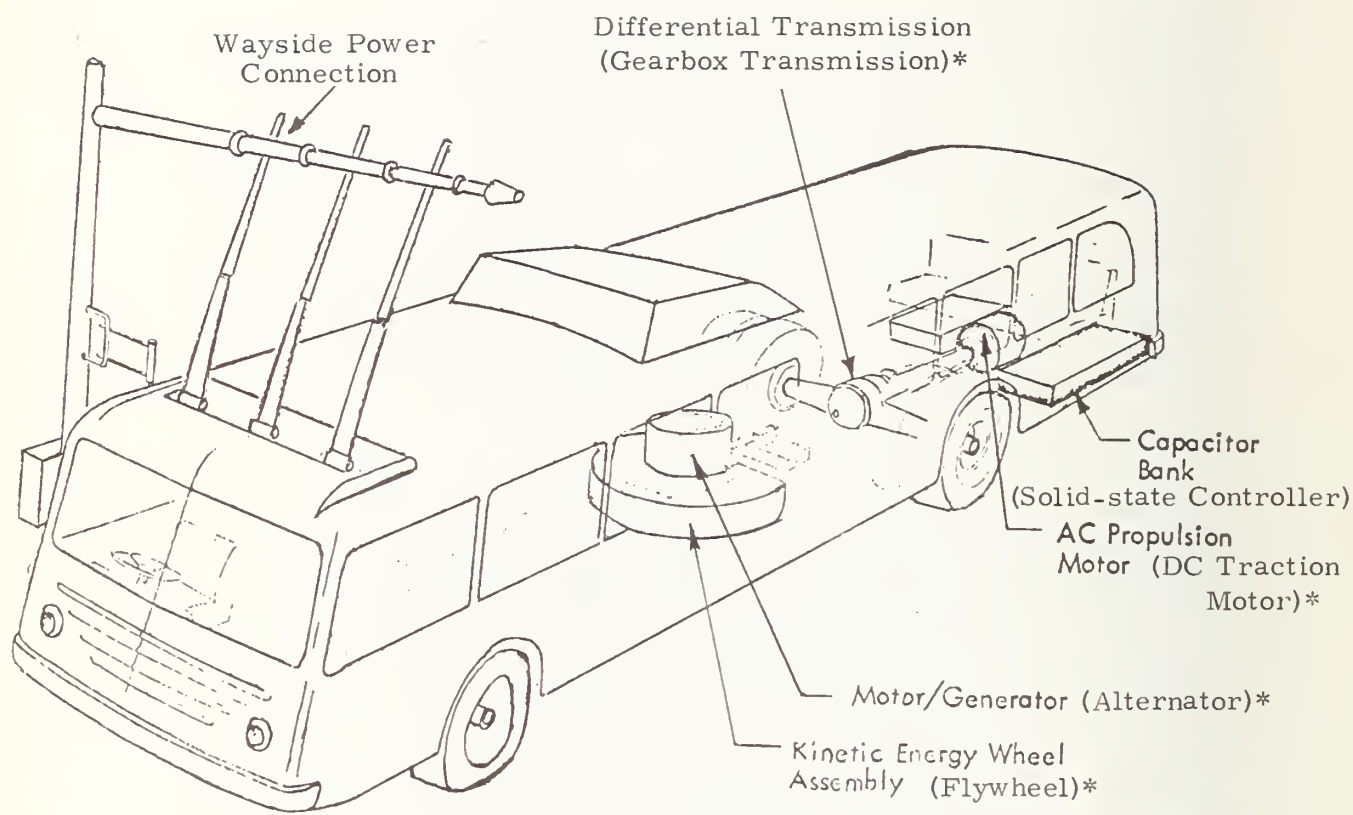


Fig. 1

Oerlikon Electrogyro Bus

*Parenthetical names refer to major components of the baseline system modeled in this report. While roughly equivalent to those used in the Swiss bus, these components have been varied somewhat, for reasons which will be explained in Section 2 of the report. (Solid-state controllers, for example, were not available in 1935.

energy is expended between stations to supply: (1) traction power for propelling the vehicle along the roadway; (2) power for overcoming the power losses incurred by the major system components; and (3) auxiliary power for on-board lighting, heating, cooling, and other passenger comforts. The sum of these three power components is the total power delivered by the flywheel at each instant of travel time. The energy required to propel the vehicle between charging stations, plus the losses and auxiliaries, must be equal to the energy drain on the flywheel during the same time interval. The main purpose of the drive system is to convert the energy stored in the flywheel to useful propulsion power at the vehicle drivewheels.

Flywheel energy-storage systems are now under serious consideration for use not only in buses but also in subway cars, trolleys, and other vehicles. For example, an R-32 energy-storage unit built by the Garrett Corporation is currently being evaluated in-service on selected New York City subways.² Also, the Urban Mass Transportation Administration recently sponsored the design of a flywheel electric-drive system to propel trackless trolley coaches for the San Francisco Municipal Railway.³ Hybrid electric-drive systems for off-highway vehicles have been seriously studied by the U.S. Army.⁴

Further development of flywheel-driven vehicles can be facilitated by establishment of criteria and procedures for measuring the performance of alternative proposed systems. Since the energy stored in the flywheel must be sufficient for the vehicle to reach the next charging station, effective design procedures will be needed to accurately compute the sums of the three power and energy requirements cited earlier. In addition, procedures for selecting properly sized components for the system configuration will require realistic assessment of (1) both peak power delivered and maximum power dissipated as losses within these components; and (2) the temperature rises resulting therefrom.

Techniques for calculating both the required propulsion power and the required auxiliary power of any electric-drive system are already well established. Flywheel electric-drive systems are more complex, however, than the conventional electric-drive systems used for battery- and wayside-powered vehicles. Application of standard design techniques could result in erroneous estimation of (1) flywheel energy-storage requirements and (2) the temperature rises of the system components. Despite the cited advantages of flywheel propulsion, the losses in the major components of such systems often constitute a substantial portion of the output. Procedures more accurate than the standard design

techniques will thus be needed, first, to calculate these losses and then, to use these calculations for determining the total energy required from the flywheel and the temperature rises of the major system components.

Performance Criteria for Flywheel Electric-Drive Systems

This report can be used for evaluating the degree to which the configuration of major components and the component ratings selected for a proposed propulsion system will optimize its performance.⁵ The report presents a procedure for developing computer models of the electric-drive system for a flywheel energy-storage vehicle. The computer simulates the overall operation of the vehicle and its drive system as well as the electromechanical and thermal operation of the drive system components. The "baseline" system modeled was patterned after an existing vehicle traveling a known route in accordance with a predetermined velocity profile. Any parameter of the route, of the vehicle, or of the drive system components could, however, be varied and the overall effect on system performance easily determined. These modeling techniques can be applied to conventional battery-powered as well as flywheel electric-drive systems, and to any vehicle operating from wayside power.

To evaluate the performance of a proposed system, two primary factors should be considered:

Proper ratings of the major components

Adequacy of the flywheel energy-storage capacity .

The ratings selected for the major components determine how heavily they are loaded in actual use. If a selected rating is too small, the undersized unit is overloaded and operates less efficiently, i. e. , with larger power losses. This larger loss is dissipated in the form of heat within the component and thus produces a higher temperature rise than "allowable by the manufacturer." The excess temperature shortens the life expectancy of the unit.* Allowable temperature rises, determined on the basis of the class of insulation used, typically range from 80 °C to 160 °C. As a rough rule-of-thumb, for every 10 °C a component operates over the allowable temperature, its life expectancy is halved.

If a selected rating is too large, the temperature rise is minimal but the penalties of increased size, weight, and cost reduce the attractiveness of the design. Optimal sizing of a major component is achieved when the final temperature rise that occurs after several round trips is 5 to 10

* Sudden and complete failures of major components are also possible when the allowable temperatures are exceeded. The likelihood of such breakdowns depends on the type of major component in question (e. g. motor or solid-state device) and the degree of excess temperature.

degrees below the manufacturer's allowable temperature rise.

Misspecification of the flywheel size can have varied effects: underspecifying will not allow for sufficient energy to propel the vehicle from station to station; overspecifying will increase flywheel weight at the expense of the vehicle's passenger capacity. Accurate determination of the flywheel size in the early stages of design is particularly important since correcting a misspecification involves time-consuming and costly changes in vehicle design.

This time and cost constraint is considerably more stringent than that on the design of other forms of propulsion. For example, minor modifications can usually accomplish major changes in the power ratings of batteries or engines. If underpowered, a vehicle that operates on electric batteries can have more batteries added; one powered by a gasoline engine can have minor changes made to the spark advance or air intake. Any flywheel modifications, by contrast, would entail not only changing the containment ring used to isolate the flywheel in case of mishap (and thus the size of the envelope) but also redesigning the vehicle layout.

Optimal flywheel sizing procedures should determine the energy-storage capacity needed by accurately computing all known energy

requirements. A margin of 40 to 50 percent should then be added to these requirements to allow for contingencies, such as high winds, and to prevent flywheel spin-down below half speed.

The key to designing a system that fulfills all performance criteria is careful determination of the power losses of each major system component. Power losses directly determine the temperature rises of the components; the losses are required to derive the component efficiencies and to calculate the energy drain from the flywheel. Inaccurate determinations of losses, then, can lead to poor sizing both of the major components and of the flywheel. In the computer simulation, power losses are calculated at each instant of time, as a function of the dynamic state of the system.

Two additional criteria evaluated by the simulation are: usage constraints, particularly the time required to recharge the flywheel at a station; and the overall efficiency by which flywheel energy is converted to useful propulsion power. Energy-conversion efficiency is clearly important in a time of increasing costs for all forms of energy and will influence the projected operating costs for the vehicle. Although both these factors are usually determined only from actual test data,

computer evaluation is possible primarily as a byproduct of the "dynamic" simulation described in the next section.

Simulation Approach

The main computer program is divided into two major portions. The first portion simulates the dynamic behavior of the vehicle as it makes a run over the route. Using as input the velocity profile of the vehicle and the grade profile of the roadway, the computer calculates at each time increment: the electrical and mechanical quantities of the drive system (such as power, voltage, current, and speed); the required propulsion power; the power losses of the major components; and the power required from the flywheel. The calculated power losses are used to determine the efficiencies of the components at any given instant; flywheel power requirements are summed while the vehicle is traveling to find the flywheel energy drain (spin-down) between stations.

In the second thermal portion of the main program, the power losses already determined are used as inputs to thermal models in order to compute the temperature rises of individual components. Thermal models are developed only for those major components whose temperature rises are expected to be significant.

These modeling procedures are more applicable to the design of flywheel energy-storage vehicles than techniques traditionally used for electric-drive systems. The critical data requirement for designing a properly-sized flywheel is the total energy required from the flywheel. The methods used in the Flywheel Propulsion Simulation to calculate this quantity as well as to evaluate the selected ratings of other major components either expand on or depart from the traditional approach in a number of important respects.

Any approach to designing an electric-drive system starts with a vehicle propelled over a roadway in accordance with the desired velocity profile. Data on either an existing or a hypothetical vehicle may be used, and aerodynamic drag may be taken into account if desired. In a first step, the required tractive force is determined on the basis of these data as a function of time, usually by using a computer simulation to insure greater accuracy. The required propulsion power is also calculated as the product of tractive force and velocity.

Following this step, however, the basic assumptions and calculation procedures of the Flywheel Propulsion Simulation differ significantly from the traditional approach. Traditionally, component ratings are selected by approximating both the average and the peak power that

the component will have to deliver in order to get the vehicle over the route on schedule. To determine the average loading of the electric-drive-system components, either the time-averaged or the root-mean-square (rms) value of the propulsion power is used along with an efficiency factor, which is assigned to each component on the basis of manufacturers' test data obtained under steady-state rated conditions.

This procedure assumes that efficiency values will remain meaningful as the load undergoes large variations during the mission. To determine whether the thermal heating of a component will be within allowable limits, it furthermore relies heavily on the designer's judgment of the effect of average and peak power losses on service life of the component. The traditional methodology, in sum, does not take into account the effects of wide variation of operating conditions and losses during a typical run of a vehicle.

In contrast, one of the basic assumptions of this report is that component efficiency will vary widely under the dynamic conditions of the roadway. Because the modeling techniques compute power losses at each instant of time, the Flywheel Propulsion Simulation can determine average and peak losses more realistically and can more accurately calculate on the basis of these losses both the flywheel energy-storage

capacity required and the thermal heating that will occur in the major components.

The inclusion of detailed loss models for each component and the development of thermal models for the major components, thus, constitute a significant expansion of the technology available for designing electric-drive systems. Because the simulation includes thermal models, it can both track temperatures and evaluate the suitability of components of different ratings and designs for inclusion in a proposed system. Because it includes highly detailed loss models, the simulation is particularly applicable to flywheel energy-storage systems, where losses are so significant a part of the output. Though traditional techniques necessarily take losses into account, the actual loss calculations for each component are embodied in only one, approximated, efficiency factor.

It should be noted that while the accuracy of the modeling procedure derives from the dynamic approach, the credibility of the loss models depends not only on their detail but also on their use of manufacturers' loss data for existing hardware. The manufacturers' efficiency data, traditionally employed, were not used in this simulation except to confirm the accuracy of the loss components of the models.

Scope of Analysis

The Flywheel Propulsion Simulation, in summary, can be considered both an evaluation tool and a design tool. On one hand, it can be used for comparing proposed flywheel electric-drive systems with respect to specific performance criteria. On the other hand, it can determine selection of the correct ratings for major system components.

Such changes in the size of units do not necessarily require basic redesign of the system, however. More fundamental changes in a system configuration -- e.g., substituting an ac for a dc traction motor or using a chopper instead of a phase-controlled rectifier -- are also possible with this simulation method. Variations in sizes of components are therefore considered, but detailed evaluation of alternatives at this time, however, would have demanded extensive reprogramming of the simulation, a change clearly not permitted by the time constraints of this study.

Also excluded from the scope of analysis was the possibility of coupling a flywheel energy-storage unit with a mechanical- rather than an electric-drive system. The baseline electric-drive system modeled offered a number of advantages: the flexibility and high efficiency of solid-state control; the availability of electric machines of reasonably

high efficiencies; and greater flexibility in the arrangement of the major components within the vehicle. It furthermore bypassed several disadvantages. A mechanical-drive system would have required an additional auxiliary power generator and entailed a more complex and expensive process for recharging the flywheel.

A description of the baseline system modeled -- the components and prototype existing vehicle as well as the modes of system operation -- is presented in the next chapter of this report, followed by a description of modeling procedures in Section 3. The parameters for the power loss and thermal models are detailed in Section 4. Because the simulation results were necessarily constrained by the baseline parameters modeled, selected variations in those parameters were considered, though not actually modeled, and are also discussed in Section 4. Results of a sample run for the baseline system, as well as recommendations for the use of the simulation, and the design of electric-drive systems, are given in Section 5. Several appendices provide the mathematical equations which are the dynamic, loss and thermal models of the drive system; definitions of the variables used in the report; typical printouts of a computer run, and manufacturers' data on the components for the baseline system.

2. BASELINE SYSTEM: COMPONENTS AND MODES OF OPERATION

Configuration of Major Components

The baseline flywheel energy-storage vehicle was patterned after an existing vehicle: the 21-passenger, rubber-tired PRT (personal rapid transit system)⁶ vehicle built by Boeing for the Morgantown, West Virginia transportation project, which was sponsored by the Urban Mass Transportation Administration. This vehicle (see Fig. 2) was selected for modeling mainly because it is already operant. While the propulsion system modeled for the baseline vehicle has several components in common with the existing vehicle, its configuration is more complex since it adds a flywheel and an alternator.

The configuration of components selected to develop the modeling procedure is that most frequently proposed by other designers for flywheel energy-storage vehicles.⁷ It includes five major units (see Fig. 3), which serve the following general functions:

The flywheel stores energy that is charged into it at a wayside power connection and delivers energy when the vehicle is traveling between stations. The component

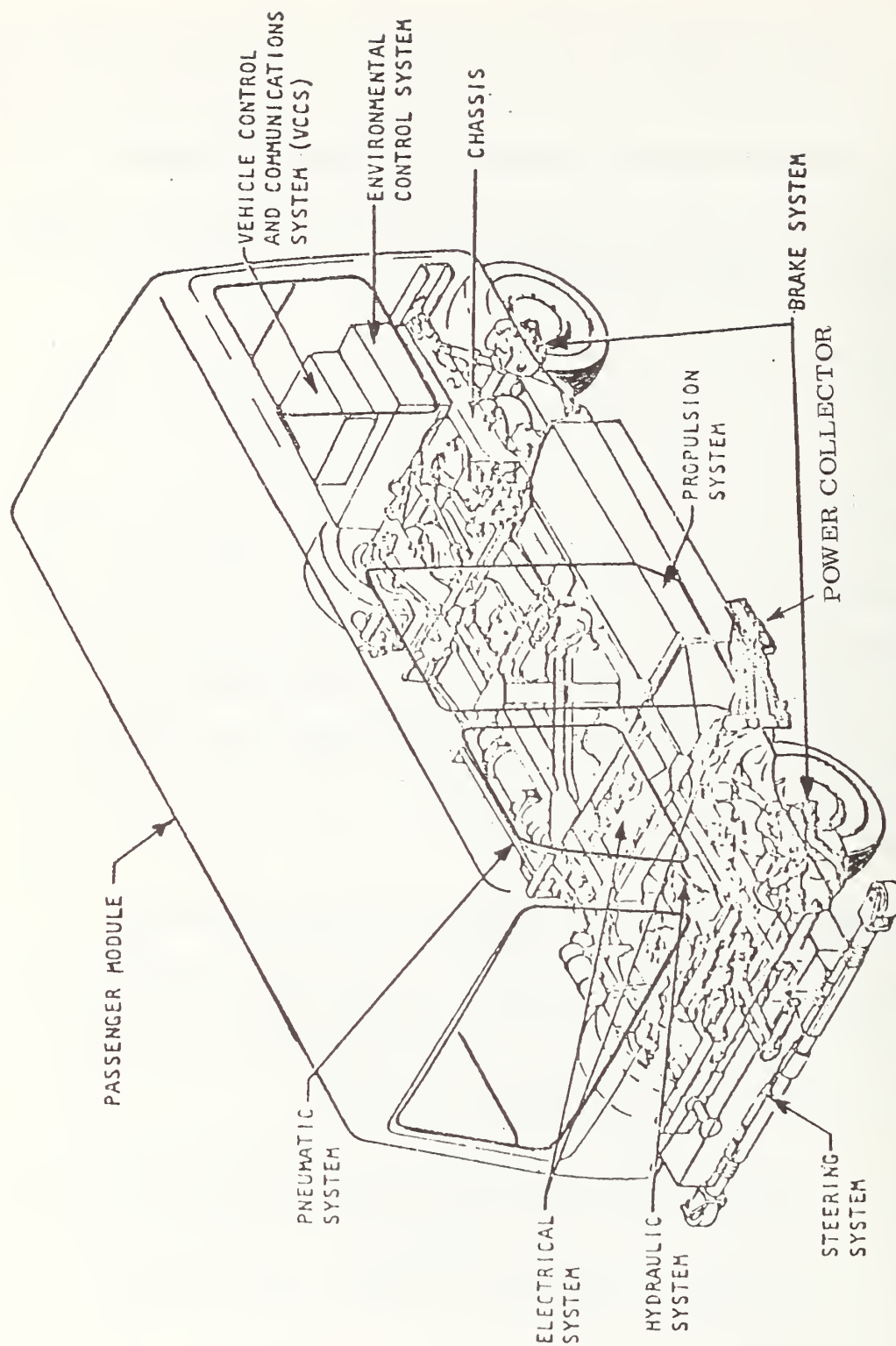


Fig.2

Morgantown Vehicle

modeled is characterized by only two parameters:

maximum speed (12,000 r/min), and moment of inertia (45 slug-ft^2), equivalent to 13.4 kWh.

The alternator directly coupled to the flywheel,

supplies the auxiliary load and generates ac power for vehicle propulsion as the flywheel slows down. During recharge, it accepts ac wayside power as a motor.

The component modeled is a Westinghouse brushless, 3-phase, 4-pole, synchronous machine that is rated at 75.8 kVA unity power factor and 12,000 r/min.⁸ The alternator was selected to match the power rating of the dc traction motor and the maximum speed of the flywheel. The alternator-flywheel is similar to that for the San Francisco Municipal Railway prototype flywheel energy-storage trolley coach.³

The solid-state controller consists of a 6-thyristor (SCR),

3-phase, full-wave phase-controlled bridge rectifier.

It normally modulates and rectifies the ac power for use in the dc motor but may also, during braking, convert dc to ac power. The F-400 Power Pack⁹ manufactured by Power Semiconductors, Inc. was modeled.

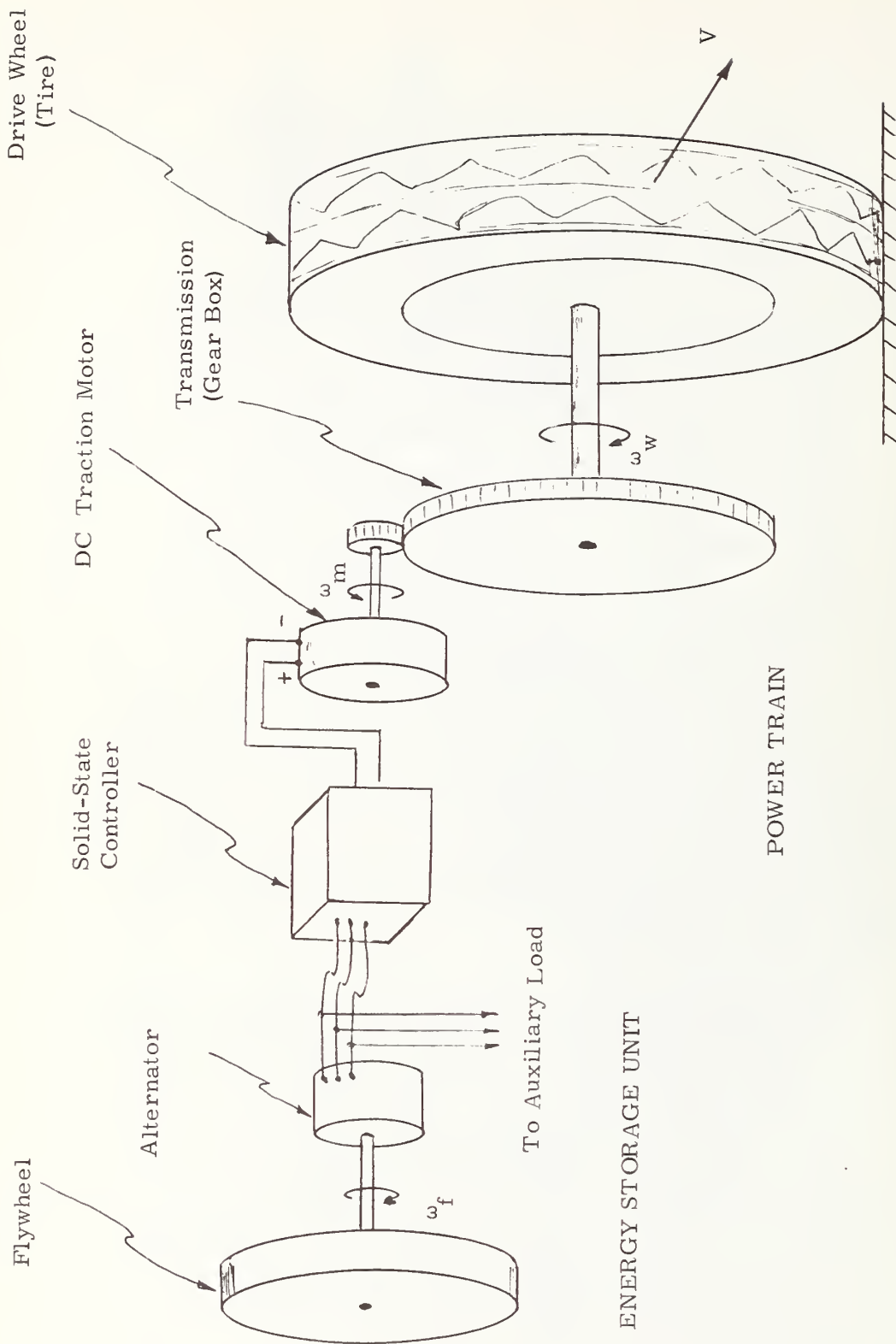


Fig. 3

Major Components of Baseline Propulsion System

The dc traction motor provides the torque to drive the vehicle. The component modeled is a compound-wound, 4-pole machine that is rated at 70 hp and 2,730 r/min. This type ASEA-built motor was installed by Rand-tronics¹⁰ in the Morgantown vehicle.

The single-stage transmission, a simple gearbox, provides a speed reduction of 7.17:1 as it couples the dc motor to the vehicle drive-wheels.

The first two components comprise the energy-storage unit; the last three can be called the "power train," which is subdivided into electrical and mechanical parts. The transmission and drive-wheels comprise the mechanical part. As the vehicle is propelled along the roadway, the direction of power is usually from the energy-storage unit via the power train to the drive-wheels. During braking, if that operation is performed electrically rather than with friction brakes, this direction of power is reversed.

The data used in the computer simulation for these components were derived from two sources: for the dc traction motor and gearbox, from published data on the components actually used in the Morgantown vehicle; for the alternator and solid-state controller, from

manufacturers' equipment catalogs and from personal communications with manufacturers' personnel. Manufacturers' data on all components are detailed in Appendix E.

Of the components modeled, the ac and the dc machines typically have the lowest efficiencies -- each about 0.88 at base conditions and considerably lower under adverse combinations of load and speed. Efficiency of the gearbox can be expected to remain above 0.90 at all times; of the solid-state controller, above 0.97. Hence, the two components with lower efficiencies (i.e., larger power losses) required more elaborate loss models; the loss models for the gearbox and the solid-state controller were much less complex. The flywheel losses were neglected; they could be included as part of the alternator friction and windage losses.

The Mission Profile

The Morgantown PRT vehicle modeled was assumed to traverse the route between the Walnut and Engineering stations on which that vehicle is presently operating. The Flywheel Propulsion Simulation adopted both the route elevation and the vehicle velocity profiles currently in use (see Fig. 4). The vehicle covers a distance of 2.065 mi one-way (4.13 mi round-trip) and travels at a maximum speed of 30 mi/h. One-way travel time between the two stations, which are

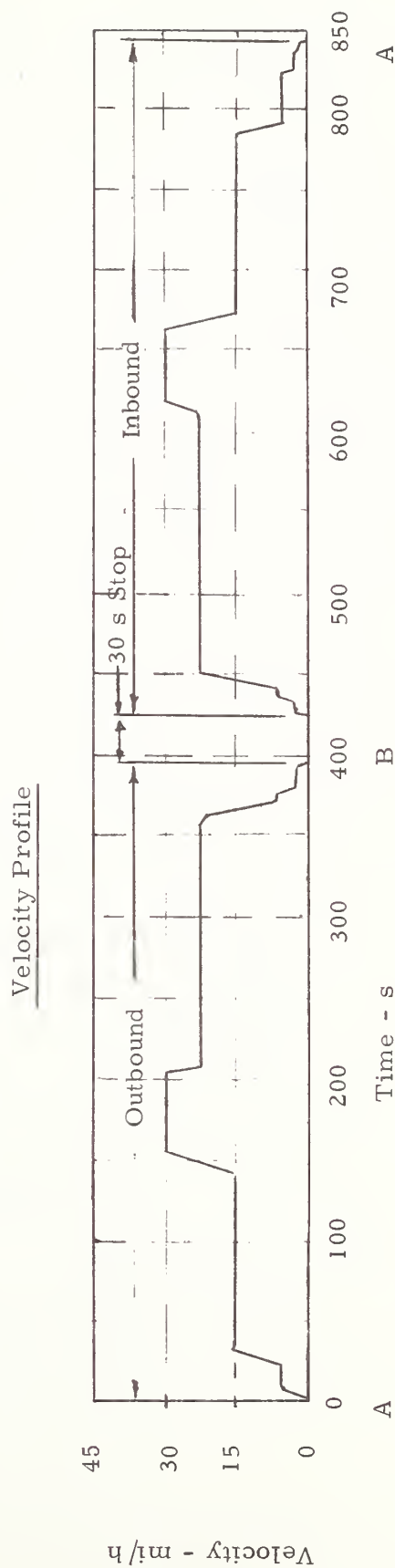
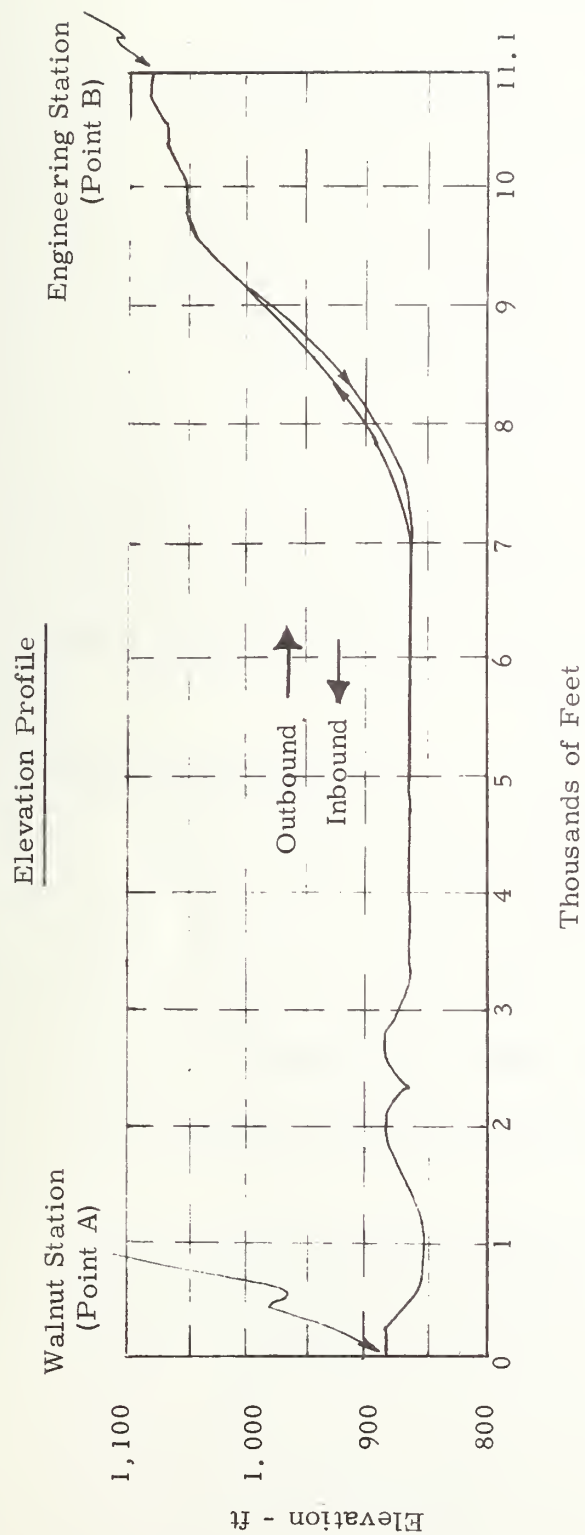


Fig. 4

Roadway Elevation and Vehicle Velocity Profiles for the Morgantown Route

labeled A and B respectively, is roughly seven minutes. The portion A-to-B is the outbound segment of the route; B-to-A, the inbound segment.

The complete round-trip between these stations can be called the "mission cycle" of the vehicle. Initially, the flywheel is charged to maximum speed at the Walnut station (Point A). The vehicle then travels under flywheel propulsion to the Engineering station (Point B), where the flywheel is recharged during passenger boarding. Finally, the vehicle returns to the starting point, and the mission cycle is repeated following a flywheel recharge at Point A.

In the computer simulation, both mission profile parameters and vehicle parameters are used to compute the required tractive force and the required propulsion power at each instant of travel. The three mission profile parameters are:

Roadway grade (slope of roadway elevation plot)

Vehicle velocity

Wind velocity .

Prestored values of these parameters are used at each instant of elapsed travel time. The following vehicle parameters are prestored at the start of a computer run:

Effective weight

Tire friction coefficients (rolling and coulomb friction)

Aerodynamic drag forces (drag coefficient and frontal area).

Headwinds and/ or tailwinds may be used in the drag calculation.

The Flywheel Propulsion Simulation is capable of modeling a more elaborate mission cycle (one with three or more stations, for example) and any number of successive round-trips (i.e., extended missions). In modeling the continuous performance of the vehicle, this multiple-trip capability is needed to find the final temperature rises of those components, i.e., the electric machines that have long thermal time constants.

Modes of Operation

The flywheel propulsion system operates alternately in two different modes. In the traveling mode, flywheel energy is expended between stations to supply the three major requirements of the system. In the wayside charging mode, that energy is replaced at each stop as the flywheel is recharged to maximum speed.

Wayside Charging Mode. The charging or recharging process (see Fig. 5) begins when the vehicle is parked at a station and passengers

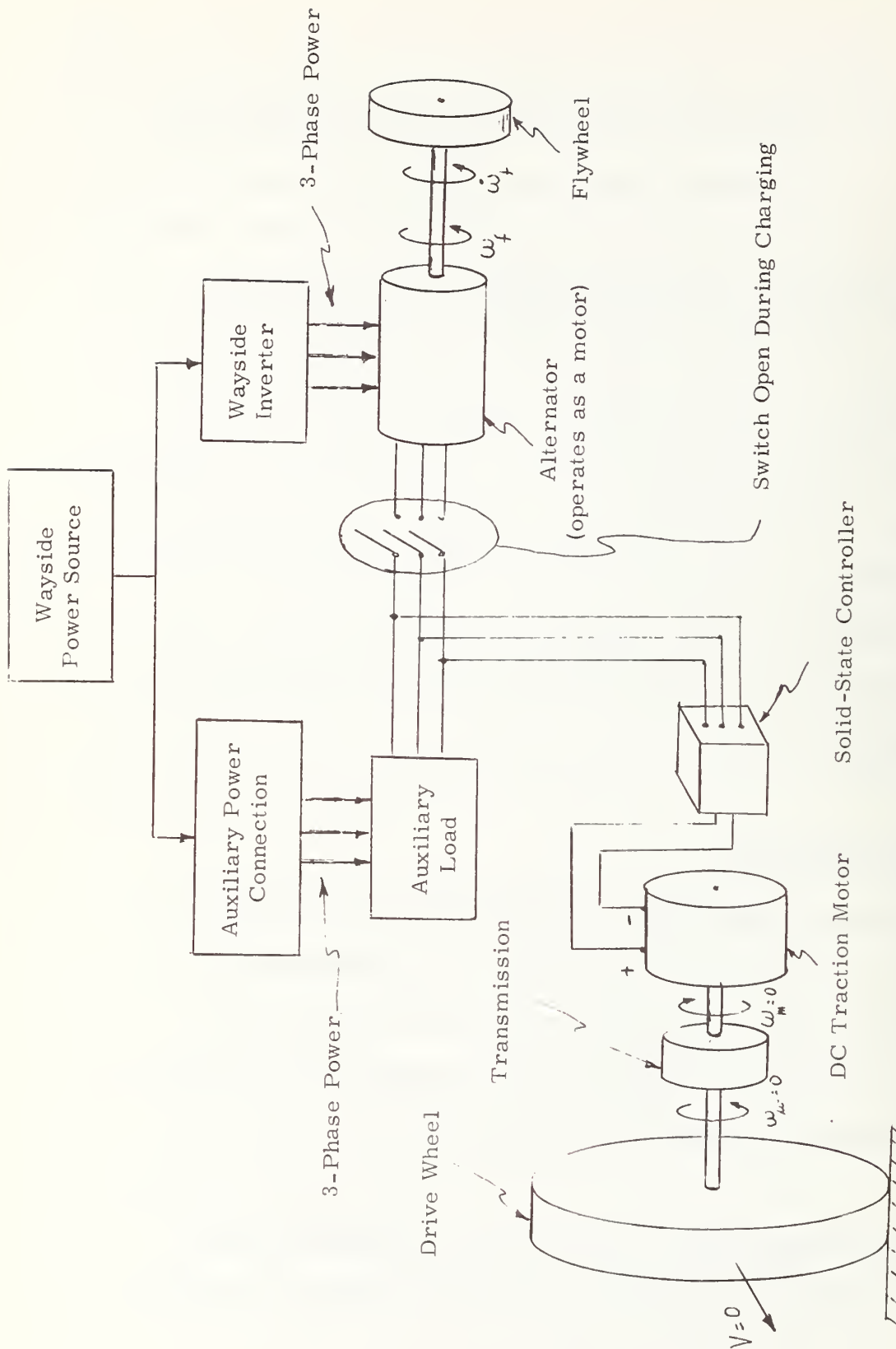


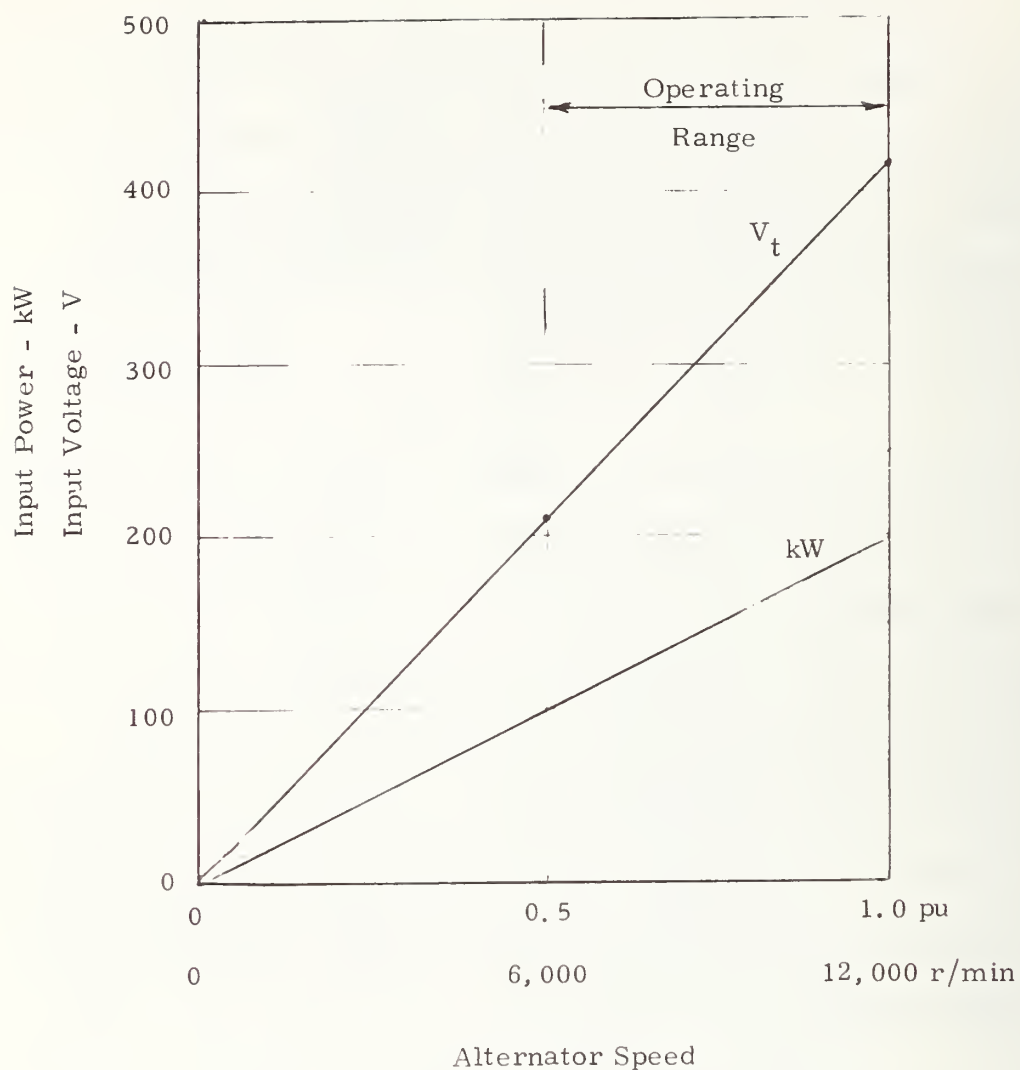
Fig. 5

Wayside Charging Mode: System Diagram

are boarding. The dc traction motor and solid-state controller are electrically disconnected; the auxiliary load is supplied by wayside power. A stationary charging-station inverter provides 3-phase adjustable-frequency electric power to the alternator operating as a motor to accelerate the flywheel.

As the flywheel speeds up, the input power delivered to the ac machine is controlled to be proportional to the alternator-flywheel speed (i.e., the ac frequency), while the armature current and the power factor are held constant (see Fig. 6). Input voltage increases in proportion to the speed of the alternator; at maximum speed, this voltage is assumed to be 20 percent higher than the rated terminal voltage of the alternator. The 20 percent higher charging voltage is used to reduce the armature current and to minimize alternator overheating during each recharge.

The charging process usually continues until the maximum (rated) speed of the alternator and flywheel (12,000 r/min) has been reached. It could, however, be stopped at any point if additional constraints on charging are introduced (such as an arbitrary upper bound on the time available for recharging the flywheel at each station). The charging terminated, the vehicle proceeds down the roadway in the traveling mode.



*Alternator operating as a motor at constant armature current of 2.2 pu and constant power factor of -1.

Fig. 6

Wayside Charging Mode for Baseline System:
Input Power and Input Voltage vs. Alternator Speed*

A critical problem with flywheel electric-propulsion systems is the long recharge time. For the baseline system modeled, recharge to full flywheel speed and energy required 215 s after the vehicle traveled an uphill outbound segment and 80 s after a downhill inbound segment. The longer recharge interval is about 50 percent of the one-way travel time; the shorter interval, about 20 percent. However, the charging intervals could be made equal, at about 157 s each, corresponding to 39 percent of the one-way travel time. The flywheel would not be fully charged when the vehicle starts its downhill inbound segment. Since the alternator would be running at less than its full speed, as well, its extra field-circuit losses would cause the overall energy losses for that segment to be greater than for the baseline system. These recharge times would probably be an unacceptable inconvenience to the general public. In fact, long recharge time caused abandonment of the early Swiss Electrogyro Bus. The charging time can be reduced by increasing the size of the alternator and by raising the power delivered from the wayside to the alternator and flywheel.

Traveling Mode. Using flywheel energy, the vehicle moves along the roadway in accordance with the predetermined velocity profile. To supply the correct tractive force required for maintaining this velocity, the firing angle of the solid-state controller is adjusted continuously, which in turn determines the load on the alternator at each instant of

travel. These adjustments are required to account for time-varying changes in required velocity and tractive force that occur as the vehicle travels between stations. For a given vehicle configuration, these variations result from changes in:

Inertia force (proportional to vehicle acceleration)

Gravity force (proportional to roadway grade or slope)

Tire friction force (nearly constant-changes slightly with vehicle velocity)

Aerodynamic drag force (proportional to square of sum of vehicle velocity and wind velocity).

In the computer simulation, then, the velocity, grade, and wind profiles are pre-stored as the mission profile. Tractive force is calculated at each instant of travel as the sum of four components: 1) inertia; 2) gravity; 3) tire friction; and 4) aerodynamic drag.

The field current of the alternator is regulated to maintain constant terminal voltage, even though the alternator slows down from 12,000 r/min to as low as 6,000 r/min. The auxiliary load is thus supplied at constant ac voltage, but at a frequency from 400 Hz to as low as 200 Hz.

The traveling mode has two mutually exclusive forms, either motoring or braking, depending on the positive or negative sign of the tractive

force required at the drive-wheels. During motoring, positive tractive force is required to push the vehicle in the direction of travel. When the vehicle slows down, e. g. , before a station or on a steep downgrade, negative tractive force is required.

Regenerative braking, rather than either dynamic braking or friction braking used on the Morgantown vehicle was selected for the simulation, since it is potentially more energy-efficient. The type of braking used in a flywheel energy-storage vehicle can influence total energy consumption and therefore the amount of flywheel energy expended. Regenerative braking can transfer some of the vehicle's kinetic energy to the flywheel; in both friction and dynamic braking, that energy would be dissipated in the form of heat. The energy savings from regenerative braking are potentially greatest for heavy vehicles (which have greater kinetic energy) and for vehicles that: stop frequently for passengers (i. e. , over five times per mile); require high braking decelerations; or travel routes with steep grades. These are conditions for the largest negative tractive force and generally the largest negative propulsion power at the drive-wheels.

During regenerative braking, the direction of power is the opposite of that during motoring (see Fig. 7). The direction of the current in the field windings is also reversed, but that in the armature winding

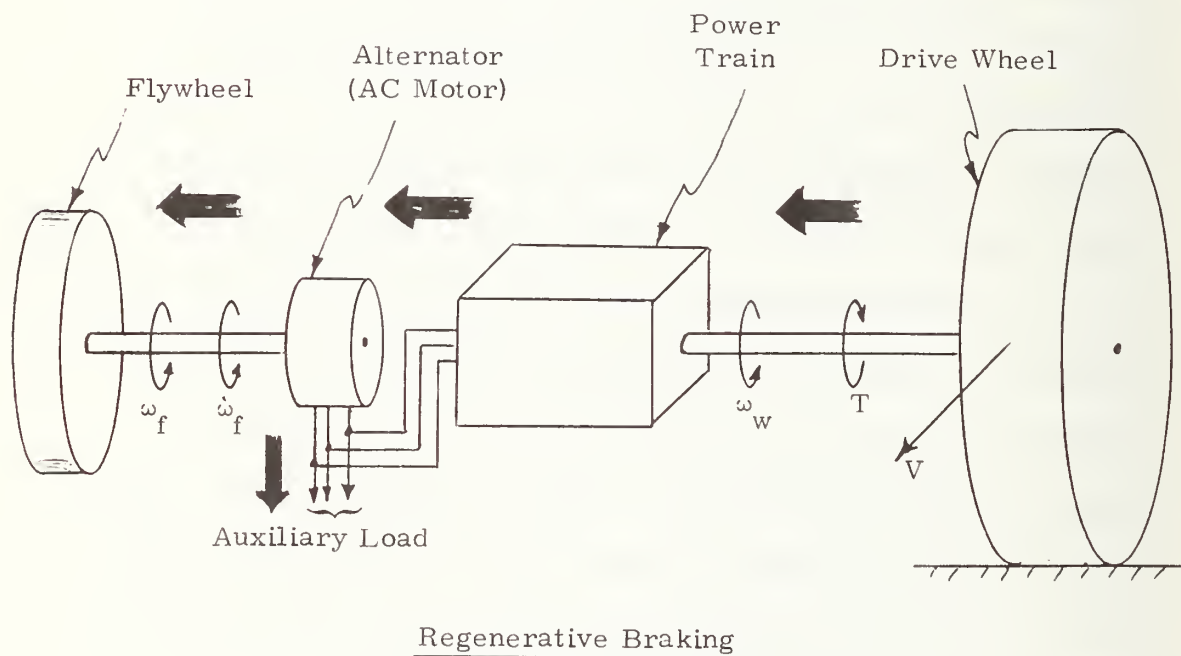
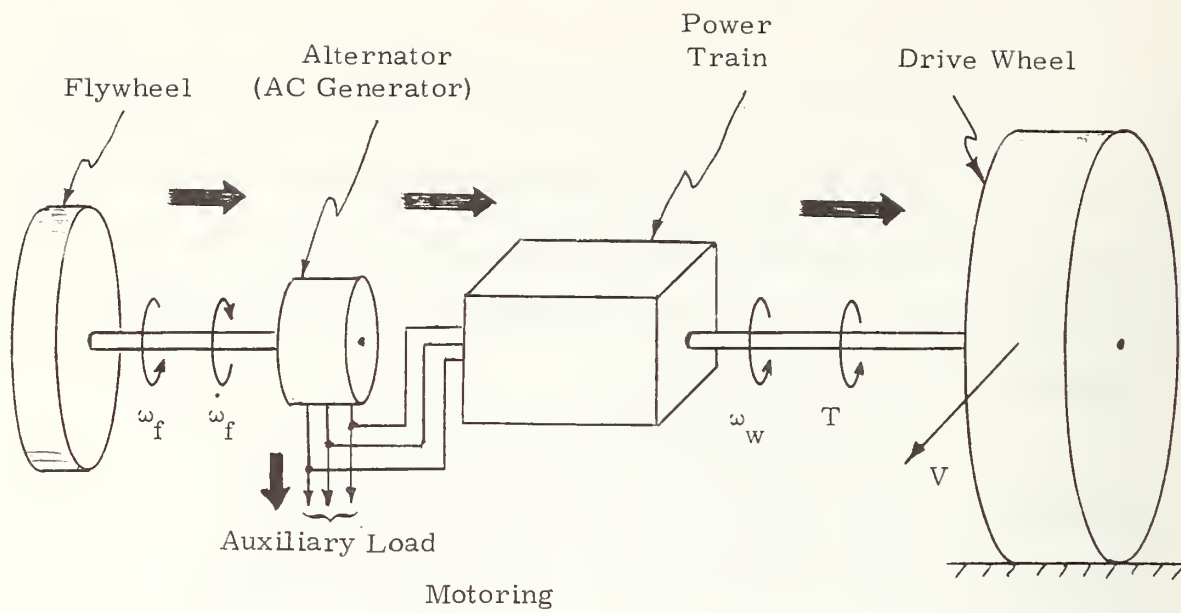


Fig. 7

Traveling Mode: Direction of Power Flow During
Motoring and Full Regenerative Braking

remains the same as in motoring. In motoring, the dc traction motor receives energy for propelling the vehicle from the solid-state controller; in braking, it operates rather as a dc generator, receiving energy from the drive-wheels and sending it into the controller, where it is converted into ac power. This ac power is used primarily to provide the auxiliary load. Any surplus power, after the component losses have been accounted for, is used to drive the alternator as a motor and thus, to supply the torque that accelerates the flywheel during regenerative braking.

Two types of regenerative braking -- either full or partial -- are possible. If the traction power is greater than or equal to the auxiliary load plus the sum of all the losses in the major components, full regenerative braking occurs; if not, the braking is only partial. During partial braking, the dc motor operates as a generator; the alternator, however, does not operate as a motor. Rather, it also operates as a generator but supplies a reduced electrical load. This reduction of the electrical load on the alternator diminishes the energy drain on the flywheel. Even in partial regenerative braking, this energy drain is less than in friction braking.

In sum, the direction of power can be either from the flywheel to the drive-wheels (during motoring), or in the reverse direction (during regenerative braking). Regardless of the direction, the losses of the major components must always be computed and their effects on flywheel speed properly accounted for. In the Flywheel Propulsion Simulation, however, the sequence in which losses are computed always proceeds from the drive-wheels to the flywheel. To determine the power required from the flywheel, which is also the rate of flywheel energy discharge, the required traction power is worked back through the loss models. This sequence of computations holds for both the motoring and regenerative-braking modes; in braking, however, the tractive force and the traction power are negative.

3. COMPUTER SIMULATION PROCEDURES

Scope of Simulation

The Flywheel Propulsion Simulation has been implemented in the Digital Equipment Corporation DEC System-10 computer located at the Transportation System Center, Cambridge, Massachusetts. Because the simulation is programmed in Fortran IV, a universal language, the program can be used on most other large-scale machines with little or no modification. This section describes the operation of the computer program and the procedures for calculating propulsion power and auxiliary power requirements. More complex portions of the simulation, including the power loss and thermal models as well as alternative ratings of major components, are detailed in the next chapter; a sample run of the program for the baseline system is described in Section 5.

Operation of Computer Program

The Flywheel Propulsion Simulation consists of an executive program, a main program, and nine subroutines. The executive program is called VSPC (Vehicle System Performance Calculator); it serves as

the program controller, since it calls in the main program and subroutines as needed. The main program is called FLY (Flywheel); it performs all the computations required for simulating operation of the baseline system, including the following:

- Required tractive force and propulsion power
- Power losses in all major components
- Total power at flywheel during discharge and recharge
- Flywheel speed and its kinetic energy
- Electric currents and voltages
- Thermal heating of select major components .

Nine auxiliary subroutines are used in conjunction with the main program: the two subroutines that process input data are:

- FLY ϕ 1 a listing of all input constants
- PROF 1 a subroutine to process "raw" mission profile data .

The five subroutines that collect, label or summarize the output data are:

- FORM 1 prepares comment statements for the tabular dynamic and power loss printout (FOR ϕ 3)
- FORM 2 prepares page titles for the FOR ϕ 3 printout

- FORM 3 prepares a summary output to follow
 tabular outputs
- FORM 4 prepares page titles for the tabular thermal
 output (FOR 26.DAT)
- FORM 5 prepares comment statements for the
 FOR 26.DAT output .

The tabular outputs for a run are stored in the two subroutines used as data storage files:

- FOR ϕ 3.DAT dynamics and power loss tabular output
- FOR 26.DAT thermal tabular output .

The flowchart for the Flywheel Propulsion Simulation, shown in Fig. 8, indicates the overall sequence of computations and the decisions made at each time increment of the simulation. A computation step-size of one second was used.

The flowchart contains two major loops, for the wayside charging and traveling modes. The program is begun in the wayside charging loop, with the flywheel initially at low speed, and remains there until the flywheel reaches its rated or full speed. It then switches to the traveling loop and calls in new mission profile inputs (i. e., vehicle velocity,

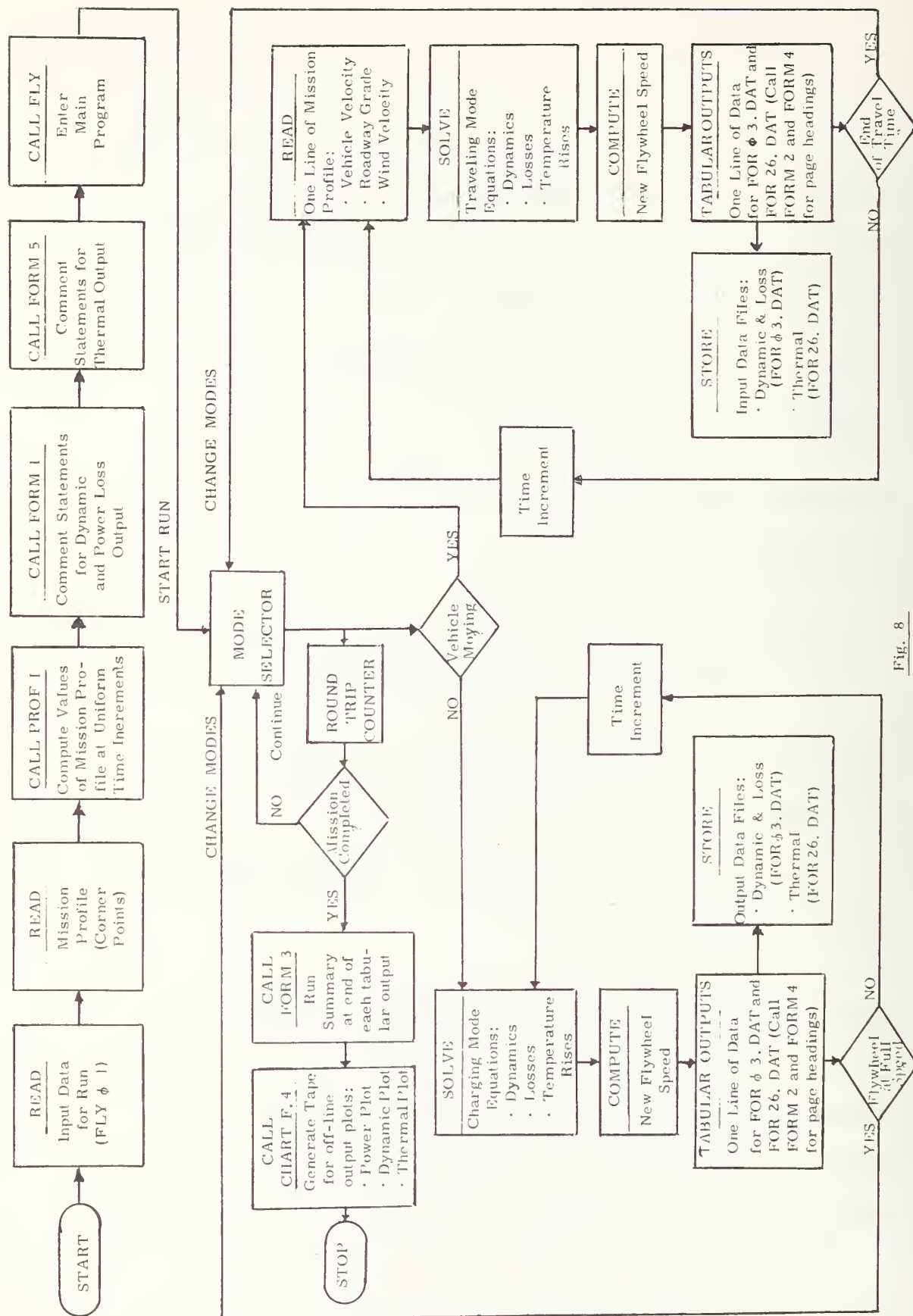


Fig. 8

Flowchart for Flywheel Propulsion Simulation

Vehicle System Performance Calculator (VSPC)
is the computer code name for the overall program.

roadway grade, and wind velocity) at each time increment. At the end of the traveling mode (a known traveling time), the simulation switches back to the charging loop for flywheel recharging. These alternating loops are both repeated until the desired number of cycles of the extended mission have been completed.

The program tabular outputs are prepared at each time increment and stored in the two output data files. Listings of the dynamics and power loss outputs during the wayside charging and traveling modes are given in Tables 1 and 2, and of the thermal outputs during both modes, in Table 3. Outputs are available in either one-second or five-second time increments. Sample outputs are provided in Appendix D, which includes comment statements as well as output data.

At the end of each complete computer run, subroutine FORM 3 prints for ready reference a tabular summary of key parameters and their peak values. This summary appears at the end of each of the two outputs. The tabular summary shown in Table 4 is for a run of five consecutive mission cycles, to insure that the electric machine temperatures have stabilized.

Finally, the simulation provides a plotting program, Chart F.4, that displays significant system parameters in a 6-channel strip-chart fashion. A table (see Table 5) describing the key system parameters

Table 1
Dynamic and Power Loss Outputs During
Wayside Charging Mode (FOR ϕ 3. DAT)*

<u>Parameter</u>	<u>Symbol</u>	<u>Units</u>
Flywheel speed	ω_o	pu
Flywheel acceleration	$\dot{\omega}_f$	rad/s ²
Alternator power input	P_{in_w}	kW
Alternator terminal voltage	V_t	V
Alternator armature current (per phase)	I_4	pu
Alternator field current	I_5	pu
Alternator efficiency	η_{ac}	pu
Alternator armature copper loss	A_1	kW
Alternator field copper loss	A_2	kW
Alternator core loss	A_3	kW
Alternator friction and windage loss	A_4	kW
Alternator stray load loss	A_5	kW
Alternator total loss	P_7	kW
Alternator power angle	δ	deg
Alternator power factor angle	θ	deg

* The order of the output quantities in the table corresponds to the sequence in which they appear in the computer tabular outputs.

Table 2
Dynamic and Power Loss Outputs During
Traveling Mode (FOR ϕ 3.DAT)*

<u>Parameter</u>	<u>Symbol</u>	<u>Units</u>
Vehicle velocity	V	mi/h
Propulsion (tractive) force	F	lb
Flywheel speed	ω_o	pu
Power required from flywheel	P	kW
Propulsion power (at wheels)	P_2	kW
Alternator power factor angle	θ	deg
DC traction motor total loss	P_5	kW
Alternator total loss	P_7	kW
DC traction motor terminal voltage	E_o	pu
DC traction motor armature current	I_o	pu
Alternator power angle	δ	deg
Alternator field excitation voltage	E_5	pu
Alternator field excitation current	I_5	pu
Alternator efficiency	η_{ac}	pu
DC traction motor efficiency	η_{dc}	pu
Solid-state controller total loss	P_6	kW
Solid-state controller firing angle	α	deg
Net propulsion energy	$E_{2 \text{ to } 4}$	kWh
Net energy for all losses	$E_{3 \text{ to } 4}$	kWh
Alternator armature current (per phase)	I_4	pu

* The order of the output quantities in the table corresponds to the sequence in which they appear in the computer tabular outputs.

Table 3
Thermal Outputs During
Wayside Charging and Traveling Modes (FOR 26. DAT)*

<u>Parameter</u>	<u>Symbol</u>	<u>Units</u>
DC traction motor total loss	P_5	kW
DC traction motor rotor input power	$P_{r_{dc}}$	kW
DC traction motor stator input power	$P_{s_{dc}}$	kW
DC traction motor gap cooling power	$P_{dc_{out}}$	kW
DC traction motor rotor temperature rise	$T_{r_{dc}}$	°C
DC traction motor stator temperature rise	$T_{s_{dc}}$	°C
DC traction motor gap temperature rise	$T_{g_{dc}}$	°C
Solid-state controller (PDR) heating rate	P_6	kW
Solid-state controller (PDR) cooling rate	$P_{6_{out}}$	kW
Solid-state controller (PDR) junction temp. rise	T_{6_t}	°C
Alternator total loss	P_7	kW
Alternator rotor input power	$P_{r_{ac}}$	kW
Alternator stator input power	$P_{s_{ac}}$	kW
Alternator gap cooling power	$P_{ac_{out}}$	kW
Alternator rotor temperature rise	$T_{r_{ac}}$	°C
Alternator stator temperature rise	$T_{s_{ac}}$	°C
Alternator gap temperature rise	$T_{g_{ac}}$	°C

* The order of the output quantities in the table corresponds to the sequence in which they appear in the computer tabular outputs.

Table 4
Tabular Summary of Key Parameters and
Their Peak Values*

FLYWHEEL VEHICLE SIMULATION

VEHICLE EQUIVALENT WEIGHT = 13222. LBS

VEHICLE FRONTAL AREA = 53.20 SQ-FT

I = 45.0 SLUG-FT-SQ

RESISTANCE COEFFICIENTS :

A = .023000

B = .000175

C = .610000

TOTAL TRAVELING TIME = 1.1319 HRS

TOTAL DIST. TRAVELED = 20.67 MI.

PEAK HEADWIND = 30.0 MPH

PEAK VELOCITY = 30.0 MPH

PEAK ACCEL. = 1.00 MPH/SEC

PEAK DECEL. = -1.00 MPH/SEC

PEAK GRADE = -10.0 PERCENT

PEAK THRUST = 1903. LBS

PEAK PROPULSION POWER = 84.96 KW

PEAK DC LOSS = 22.02 KW

PEAK AC LOSS = 74.04 KW

PEAK TOTAL POWER = 196.4 KW

PEAK DC ARM. CURRENT = 2.186 PU

PEAK AC ARM. CURRENT = 3.563 PU

PEAK AC POWER FACTOR ANGLE = 180.0 DEG

PEAK AC POWER ANGLE = -70.2 DEG

PEAK AC FIELD CURRENT = 8.967 PU

PEAK AC FIELD VOLTAGE = 7.805 PU

PEAK DC ROTOR TEMP ABOVE AMB. = 51.3 DEG C

PEAK DC STATOR TEMP ABOVE AMB. = 23.6 DEG C

PEAK AC ROTOR TEMP ABOVE AMB. = 321.5 DEG C

PEAK AC STATOR TEMP ABOVE AMB. = 372.8 DEG C

PEAK PDR JUNCTION TEMP ABOVE AMB. = 155.8 DEG C

PEAK HEAT SINK TEMP ABOVE AMB. = 36.5 DEG C

*Total traveling time and distance traveled for a computer run of five consecutive mission cycles.

Table 5
Key System Parameter Listing

(Masthead for Output Plots)

FLYWHEEL VEHICLE SIMULATION
PADS* CONFIGURATION NO. 1
THERMAL PLOTS

VEHICLE EQUIV. WT. : 13222. LB
FRONTAL AREA : 53.0 SQ-FT
DRAG COEFF. : 0.610
TIRE FRICT. COEFF. : ROLLING = 0.0230
COULOMB = 0.000175 PER MPH
WIND VELOCITY : 30. MPH (RETARDING)-OUTBOUND LEG
-30. MPH (AIDING) - RETURN LEG
FLYWHEEL : I = 45.0 SLUG-FT-SQD
MAX SPEED = 12000. RPM
INITIAL SPEED = 6000. RPM
ROADWAY/VELOCITY : MAX SPEED = 30. MPH
PROFILE NO. 1 TOTAL DISTANCE = 4.13 MILES
MAX GRADE = 10.0 PERCENT
TOTAL TRAVEL TIME = 0.2264 HR
TRACTION MOTOR : 70.2 HP RATING AT 2730 RPM
TERM. VOLT. = 420. V
BASE ARM. CUR. = 140. A
PDR : FULL WAVE 3-PHASE TYPE
ALTERNATOR : 75.8 KVA AT 12000. RPM, 3-PHASE
L-TO-N TERM. VOLT.= 215. V (CONST.)
BASE ARM. CUR. = 73.2 A/PHASE

WAYSIDE RECHARGE AT CONSTANT ARMATURE CURRENT

PROPULSION ENERGY	MOTORING	BRAKING
WALNUT TO ENGR. STA; KW-HRS = 3.4739		-0.1018
ENGR. TO WALNUT STA; KW-HRS = 1.8396		-0.4916
ROUND TRIP; KW-HRS = 5.3136		-0.5934

DATE OF RUN : 28-JUNE-76

* Propulsion and Distribution System

for a plot is also provided on left side of each output plot. The actual plotting is done off-line by a Calcomp plotter. The three following sets of plots are generated, all using mission time as the abscissa:

A power plot shows: propulsion power during the traveling mode and charging power during the way-side charging mode; power from the flywheel; and total power losses in the major components.

A dynamic plot shows: the flywheel energy; the dc traction motor armature current; and the solid-state controller firing angle.

A thermal plot shows the temperature rise of the hottest element of each thermally-modeled component: the armature of the dc traction motor; the stator of the alternator; and one thyristor junction of the solid-state controller.

To facilitate comparisons among these three plots, the first three channels of each plot show the vehicle velocity profile, roadway grade profile, and computed tractive force. Samples of these plots are shown in Figs. 18 thru 21.

If flywheel-spin-down, which results either from an undersized flywheel, or from too much drain, does not permit the alternator to generate the required ac voltage, a special feature of the simulation stops the program and prints an error message that prevents further useless computation.

Calculation of Propulsion Power and Auxiliary Power Requirements

The total power required from the flywheel at any instant of travel time is the sum of three requirements:

Propulsion power
Auxiliary power
Total power losses

Because the detailed simulation of the loss process for all of the major components represents a basic departure from a conventional approach, it will be described in a separate section. The methods for computing the auxiliary and propulsion power requirements at each instant of time are more conventional. Since auxiliary power is the least significant power requirement, it warrants only brief discussion.

The required auxiliary power has been estimated in the simulation. Its value can vary widely as a function of the ambient temperature of the day and related heating or cooling requirements of the vehicle interior. The requirement is modeled as a constant 3-phase load of 6 kW, 0.8 PF lag, during the traveling and charging modes. It is supplied from the alternator during motoring, from the solid-state controller during regenerative braking, and from the wayside power connector during wayside charging.

The methods used to determine the required propulsion power are well-known. The propulsion power at any instant of travel time is the product of the tractive force and the vehicle velocity. Velocity is a known input to the simulation. Tractive force is calculated as the sum of four component forces:

Inertia

Gravity

Tire friction

Aerodynamic drag .

Inertia forces are the forces required to change vehicle velocity to conform to the velocity profile. They are the product of the vehicle equivalent mass and the slope of the vehicle velocity/time profile

(acceleration). The vehicle equivalent mass is the sum of the actual vehicle mass and the referred value of the rotary inertia of those rotating parts whose speed is directly proportional to vehicle speed, such as the drive-wheels and the dc traction motor. For example, for an equivalent vehicle mass of 13,222 lb and an acceleration of 1.4 mi/h/s, the inertia force is 884 lb.

Gravity forces equal the product of the vehicle equivalent weight and the sine of the roadway grade angle above the horizontal. For the same vehicle on a 5 percent grade, the gravity force is 661 lb.

Tire friction forces result from the resistance of the roadway to tire motion. They depend on vehicle weight and velocity, tire pressure, and tire design. The tire friction model used here, which is based on nominal conditions, is:

$$F_{\text{tire}} = \mu W (1 + C_c V) (MF) \quad \text{lb}$$

where:

μ = rolling friction coefficient (0.0230 lb/lb)

W = vehicle weight (12,238 lb)

C_c = coulomb friction coefficient (1.75×10^{-4} h/mi)

V = vehicle velocity (ft/s)

MF = mass factor-ratio of equivalent to actual mass.

For example, for a vehicle velocity of 30 mi/h, the tire friction force is 306 lb.

Aerodynamic drag forces result from the air resistance to vehicle velocity and wind velocity. For this simulation, the wind speed is taken as constant (30 mi/h) in a vehicle frame of reference. The wind speed opposes vehicle motion during the uphill outbound segment of the trip and aids it during the downhill inbound segment. The drag force model is:

$$F_{\text{drag}} = 1/2 \rho (V + V_w)^2 \frac{(V + V_w)}{|V + V_w|} C_d A \quad \text{lb}$$

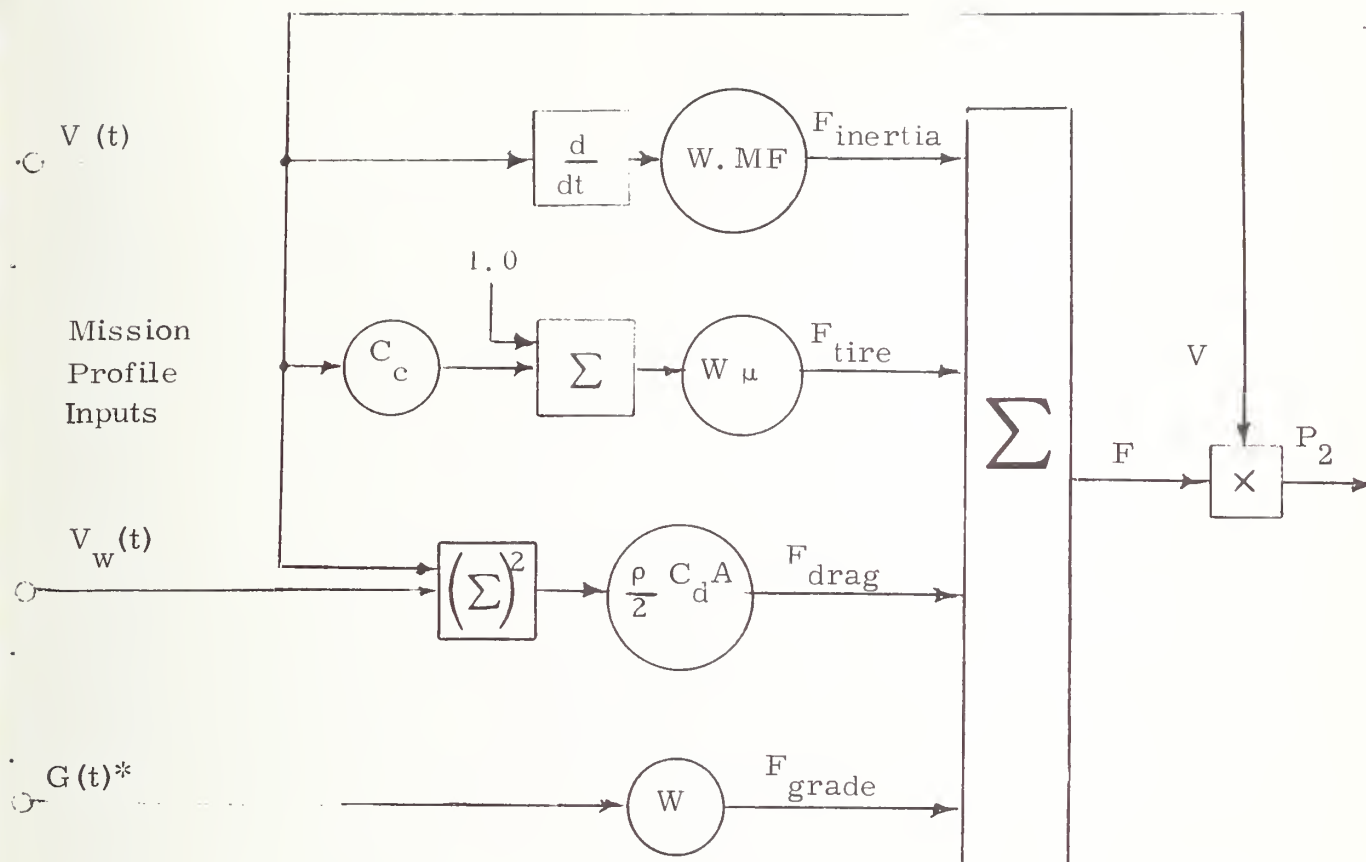
where:

- ρ = air density at sea level (0.002378 slugs/ft³)
- V = vehicle velocity (ft/s)
- V_w = wind velocity (ft/s) (negative for tailwind)
- C_d = vehicle drag coefficient (0.61)
- A = vehicle frontal area (53.0 ft²).

For example, for the same vehicle at a velocity of 30 mi/h and a headwind of 30 mi/h, the aerodynamic drag force is 298 lb.

The sum of the force components for the 13,222 lb vehicle accelerating at 1.4 mi/h/s, at a velocity of 30 mi/h, on a 5 percent grade and against a

headwind of 30 mi/h, is 2,109 lb. A flowchart for computing the tractive force and propulsion power is shown in Fig. 9.



*If grade profile input is provided in the form of $G(x)$ rather than $G(t)$,
 then $G(t) = G(x)_t \times V(t)$.

Fig. 9

Flowchart for Computing

Tractive Force F and Propulsion Power P_2

4, MODELS

Procedure

Calculation of the power losses in the energy-storage unit and the power train is required in the simulation in order to compute the power delivered by the flywheel and the temperatures of the components at each instant of travel time. The power loss for each component is calculated by a two-step process, using first the dynamic model, then the power loss model for the component. The power loss model utilizes as inputs the electrical variables and speeds which are the outputs of the dynamic model. The temperature rises for the electric machines and the thyristors in the controller are calculated in a third step, using thermal models for the components and the losses from the power loss models. These models are derived in this section; numerical values for the parameters are given for the components of the baseline system. In order to use the simulation as a design tool, and to vary the machine ratings, the relationships are given in terms of the linear dimension of the electric machines between the power ratings, loss components and electrical parameters.

Dynamic and Power Loss Models

The dynamic models of each component of the electric propulsion system are basically the equations that relate the input and output variables. The dynamic models of the electric machines are more complicated than the other components. The models are sets of equations that relate the speed and torque of the electric machines to the electrical variables of current and voltage. These equations are based on the machine parameters of resistance, reactance, and saturation, which are either obtained from the manufacturer or calculated from the per-unit quantities for machines of the same type and size.

The power loss models are sets of equations that relate the electrical variables and speeds of the major components to their power losses. These models are generally more elaborate for the baseline system components that are expected to exhibit the largest losses, i. e., the lowest efficiencies. The most elaborate loss models, each including five separate loss terms, are for the alternator and the dc traction motor. A two-term loss model describes the solid-state controller losses. The model that represents the transmission losses is simplest, since a constant percentage of the input is assumed lost in that component power. The flywheel mechanical losses (friction and windage)

were not modeled, since test data for representative flywheels running in evacuated enclosures were not available, but could be added at a later date if necessary. Flywheel losses are expected to be small and could be lumped with the alternator friction and windage losses.

As the flywheel is spun-up in the wayside charging mode, the only losses occur in the alternator, which is used as a motor, while the solid-state controller, dc traction motor, and transmission are not in operation. The auxiliary load is assumed to be supplied from the wayside power connector. During the traveling mode, regardless of the direction of power, all four major components develop losses.

Part of the output of the simulation is a tabulation of all of the electrical variables, machine speeds, loss terms, component losses, and total losses. In a further calculation, the component losses are used with the thermal models to obtain the temperatures of the components at each instant of travel time.

The dynamic and loss models are developed in this section in the order of calculation at each time increment of the computer program,

that is, from the drive wheels through the propulsion system to the flywheel. Hence the dc traction motor model, which effectively includes the gear box is addressed first, followed by the controller and the alternator. The alternator is the most complicated of the component models.

DC Traction Motor. The equations for the dynamic model of the dc traction motor are given in Appendix A. Basically, the armature current is computed from the tractive force at the drive-wheels as reflected through the gearbox. The motor speed is also related to the drive-wheel speed.

The equations can be written in per-unit terms or in terms of the variables in ohms, volts, amps, r/min, etc. The per-unit terms are more convenient because the value of the variable conveys its proportion to the rating of the machine; $I_0 = 0.5$ pu, for example, means that the armature current is at half its base value. An additional advantage is that for small changes of the power rating of the machine, the per-unit parameters hardly change; the same equations can usually be used.

Before the per-unit equations for the dynamic model can be written, the base quantities, corresponding to 1.0 pu, must be given for the machine. Usually, these quantities are the nameplate rated quantities. The base quantities for the dc traction motor used in the base-line system are given in Table 6.

Table 6

DC Traction Motor Base Quantities

Armature current	I_o	= 140 A
Armature voltage	V_{dc}	= 420 V
Armature resistance	R_{adc}	= 3.0 Ω
Speed	N	= 2730 r/ min
Torque	T	= 135 lb/ ft
Mechanical power	P_m	= 52.3 kW (70 hp)

The five equations for the power loss model are written in terms of the per-unit variables but yield the power loss components in kW.

The equations for the armature circuit copper and independent field losses (D_1 and D_2) are derived from the circuit resistances. The equation for friction, windage, and iron losses (D_3) assumes a variation with speed to the 2.5 power. The stray load loss (D_4) is taken as 1 percent of the mechanical power. The brush loss (D_5) is derived from a constant 2-V brush drop. The five equations in per-unit variables yield the following loss components in kW:

$$\begin{aligned}
 D_1 &= 4.10 I_a^2 && \text{- Armature circuit copper loss} \\
 D_2 &= 0.288 (N)^{2.5} && \text{- Independent field loss} \\
 D_3 &= 1.56 (N/2730) && \text{- Friction, windage, and iron losses} \\
 D_4 &= 10^{-2} P_m^* && \text{- Stray load loss} \\
 D_5 &= 0.280 I_0 && \text{- Brush loss}
 \end{aligned}$$

* In the computer program, the variable P_m (in D_4) is expressed as P_2/η_{gb} for motoring and $P_2 \times \eta_{gb}$ for braking, where P_2 is the propulsion power at the wheels and η_{gb} is the gearbox efficiency (0.92).

The sum of the loss components calculated at the base conditions from the power-loss equations must yield the losses at the base conditions calculated from the efficiency. The loss components for the baseline system's dc traction motor are shown in Table 7. The manufacturer usually supplies the armature resistance, field resistance, and full-load efficiency.

Table 7

DC Traction Motor Loss Components at Base Conditions

D_1	= 4.10 kW	- Armature circuit copper loss
D_2	= 0.29 kW	- Independent field loss
D_3	= 1.56 kW	- Friction, windage, and iron losses
D_4	= 0.52 kW	- Stray load loss
D_5	= 0.28 kW	- Brush loss
P_5	= 6.75 kW	- Total loss

The stray load and brush loss components can be found as previously described. The friction, windage, and iron loss component makes up the remainder of the losses, which can be calculated from the efficiency, i. e. once the efficiency is known.

Solid-State Controller. The equations for the dynamic model of the controller relate the dc output voltage and current to the ac input voltage and current and yield the controller firing angle as a dependent variable. The power loss model does not require the results of the dynamic model calculation. The power losses consist of two components: the thyristor forward drop losses and the snubber network losses. Forward drop loss of this 6-thyristor controller are based on typical values. Forward drop loss is assumed to vary with direct current and is taken at 0.3 kW/100 A, i.e., 3 V drop. Snubber network losses are assumed to be 1 percent of the output power of the solid-state controller. When the dc traction motor delivers its rated output, the sum of both loss terms is roughly 1 kW.

Alternator. The dynamic model for the alternator is much more complicated than the model for the traction motor, for the following reasons. First, since the alternator is an ac machine, the stator electrical quantities must be expressed in complex numbers to identify magnitude and phase of the currents and voltages. Second, the baseline alternator operates over a range of speeds, typically from 0.5 to 1.0 pu; practically all conventional alternator analysis is based on constant-speed operation. Third, to obtain a sufficiently accurate dynamic model, the alternator must be represented in its

direct and quadrature (d-q) axes. Fourth, because the alternator will operate down to a speed of 0.5 pu and at high field current to maintain terminal voltage, saturation of the magnetic circuit must be included in the model.

The equations for the dynamic model, which are given in Appendix A, use the standard machine impedance, d-q axis representation, and the Kingsley method for saturation correction.^{11,12} They describe the operation of the alternator in the traveling mode, as the flywheel and alternator speed declines from 1.0 pu to as low as 0.5 pu; or in the wayside charging mode, with the alternator operating as a synchronous motor as the speed rises from 0.5 pu to 1.0 pu. In the traveling mode, the alternator delivers energy to the solid-state controller and supplies the auxiliary load; the terminal voltage is held constant over the speed range. In the wayside charging mode, the alternator receives power from the wayside inverter.

The per-unit system used for the dynamic model defines the currents, voltages, and reactances at the base $\omega_0 = 1.0$ pu. At other than base speed, the per-unit reactance is multiplied by the per-unit speed to reflect the effect of the frequency on the reactances. If the per-unit

impedances are not provided by the manufacturer for a specific alternator, typical per-unit values can be obtained for alternators of the same similar rating and speed from a handbook.¹³ The per-unit impedances for the baseline alternator -- a 75-kVA, 12,000-r/min, 4-pole unit -- have been provided by Westinghouse and are given in Table 8.

Table 8

Alternator Per-Unit Impedances

$r_{a\ ac}$	= 0.0495	- Resistance (200°C)
x_d	= 3.40	- D-axis unsaturated reactance
x_q	= 1.24	- Q-axis reactance
x_a	= 0.085	- Leakage reactance
x_d''	= 0.145	- Subtransient reactance

Ratings - The power and speed rating of the alternator determine its physical size and its ability to carry continuous load. Selection of an alternator should be based on three criteria: (1) its ability to provide peak power at some point in the mission; (2) its energy losses between wayside charging stations; and (3) its maximum internal temperature

as compared to the allowable temperature. For an alternator running at one speed and variable load, the rating can be selected by calculating the rms current over an operating period. However, for an alternator operating over a range of speed and load, as in a flywheel energy-storage vehicle, the selection can best be made by using the dynamic, loss, and thermal models described in this report.

After power and speed ratings are determined, the alternator voltage rating must be selected. For a given power rating and frame, the voltage and current ratings of the machine are like scale factors. Any values can be used, provided their product yields the given power rating. However, the ratings selected will significantly affect the alternator power losses. In the traveling mode, the alternator is assumed to operate at constant terminal voltage, while the speed ranges from 1.0 pu to 0.5 pu. If, on one hand, the rated voltage is set equal to the required voltage, then at 0.5 pu speed the alternator must be capable of twice the air-gap flux density developed at 1.0 pu speed. The field current and field losses will be high at low speed. If, on the other hand, the rated voltage is set equal to twice the required voltage, then the increase of stator turns will raise the armature resistance and make the armature losses high at all speeds. In the baseline alternator, the rated voltage was expressed as a rewind

factor (RWF) times the original 115 V/phase rating of the machine.

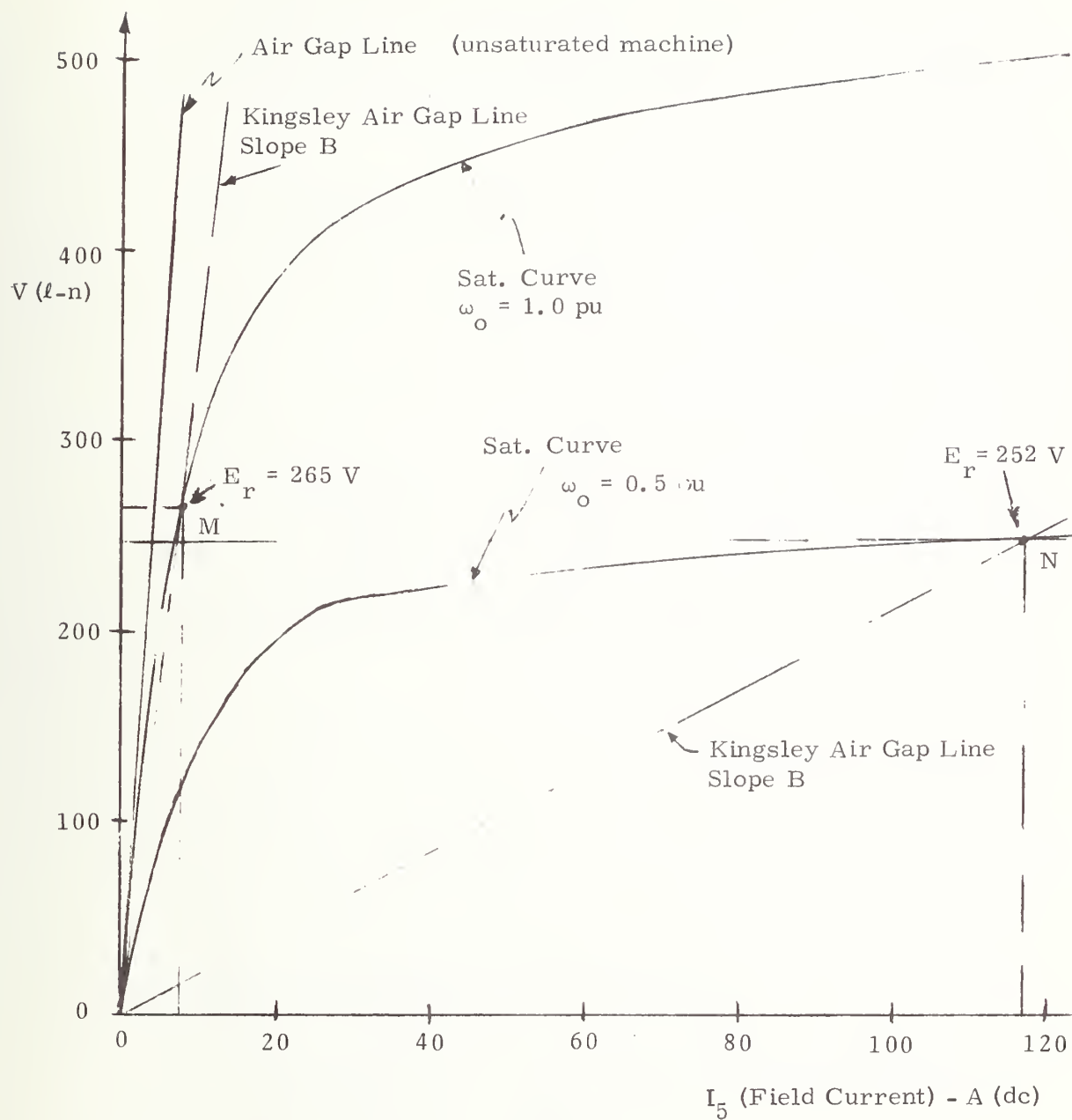
A rewind factor of 3.0 was selected.

The base quantities for the alternator used in the baseline system are shown in Table 9.

Table 9
Alternator Base Quantities

Power	$P = 75.8 \text{ kVA}$
Voltage	$V_t = 345 \text{ V (l-n)}$
Armature current	$I_4 = 73.2 \text{ A}$
Speed	$\omega_o = 12,000 \text{ r/min}$
Field current	$I_5 = 14.3 \text{ A}$
Base impedance	$Z_o = 4.70\Omega$

The saturation curves for the baseline alternator are shown in Fig. 10 for $\omega_o = 1.0 \text{ pu}$ and 0.5 pu . The saturation curve for $\omega_o = 1.0 \text{ pu}$ was supplied by the manufacturer. The saturation curve for $\omega_o = 0.5 \text{ pu}$, or for any other speed, is merely scaled down vertically by $\omega_o \text{ pu}$ for each value of field current. For the alternator under load, the saturation curve is assumed to represent the air-gap voltage E_r vs. the net



*Air gap voltages (E_r) for dc traction motor operating at rated power and speed.

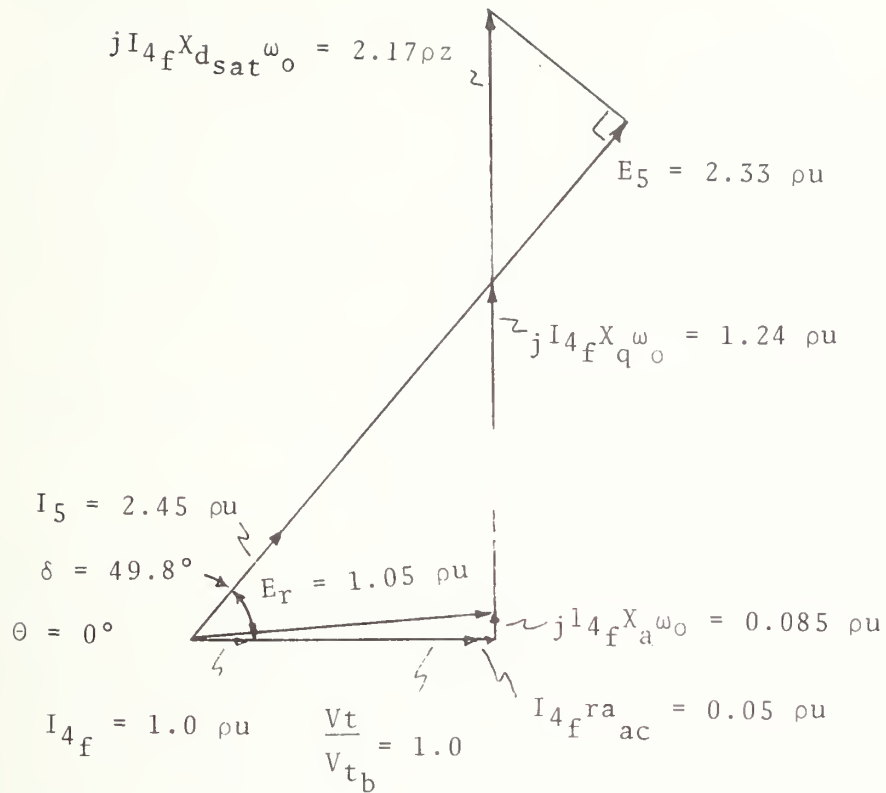
Fig. 10

Saturation Curves for Alternator

direct-axis ampere turns expressed in equivalent field amperes. At no-load condition, of course, the air-gap voltage is identical with the terminal voltage; the net direct-axis ampere turns are merely the field ampere turns.

The air-gap voltage point represents the degree of saturation of the machine. For base operation with $PF = 1.0$, the air-gap voltage is $E_r = 362 \text{ V}$ (Point O). For conditions when the dc traction motor is operating at rated 70 hp and rated 2730 r/min while the alternator is running at $\omega_o = 1.0 \text{ pu}$, the air-gap voltage is $E_r = 265 \text{ V}$ (Point M); i.e., in other words, the alternator is less saturated than it is during base operation. For the same load, but with the alternator running at $\omega_o = 0.5 \text{ pu}$, the alternator is heavily saturated at $E_r = 252 \text{ V}$ (Point N).

Phasor diagrams - The dynamic model of the alternator is expressed as a phasor diagram. It is used to calculate air-gap voltage E_r and the field current I_f at each instant of time during the mission to obtain two of the five loss components. The phasor diagram for the alternator at base conditions is shown in Fig. 11. The air-gap voltage E_r is calculated first to find the degree of saturation; the position of the direct axis, identified with the power angle δ , is calculated next using the quadrature-axis reactance x_q . The magnetizing portion of the direct-axis reactance ($x_d - x_a$) is corrected for



*Alternator base conditions: 345 V (l-n); 75.8 kW; 1.0 PF; 12,000 r/min.

Fig. 11

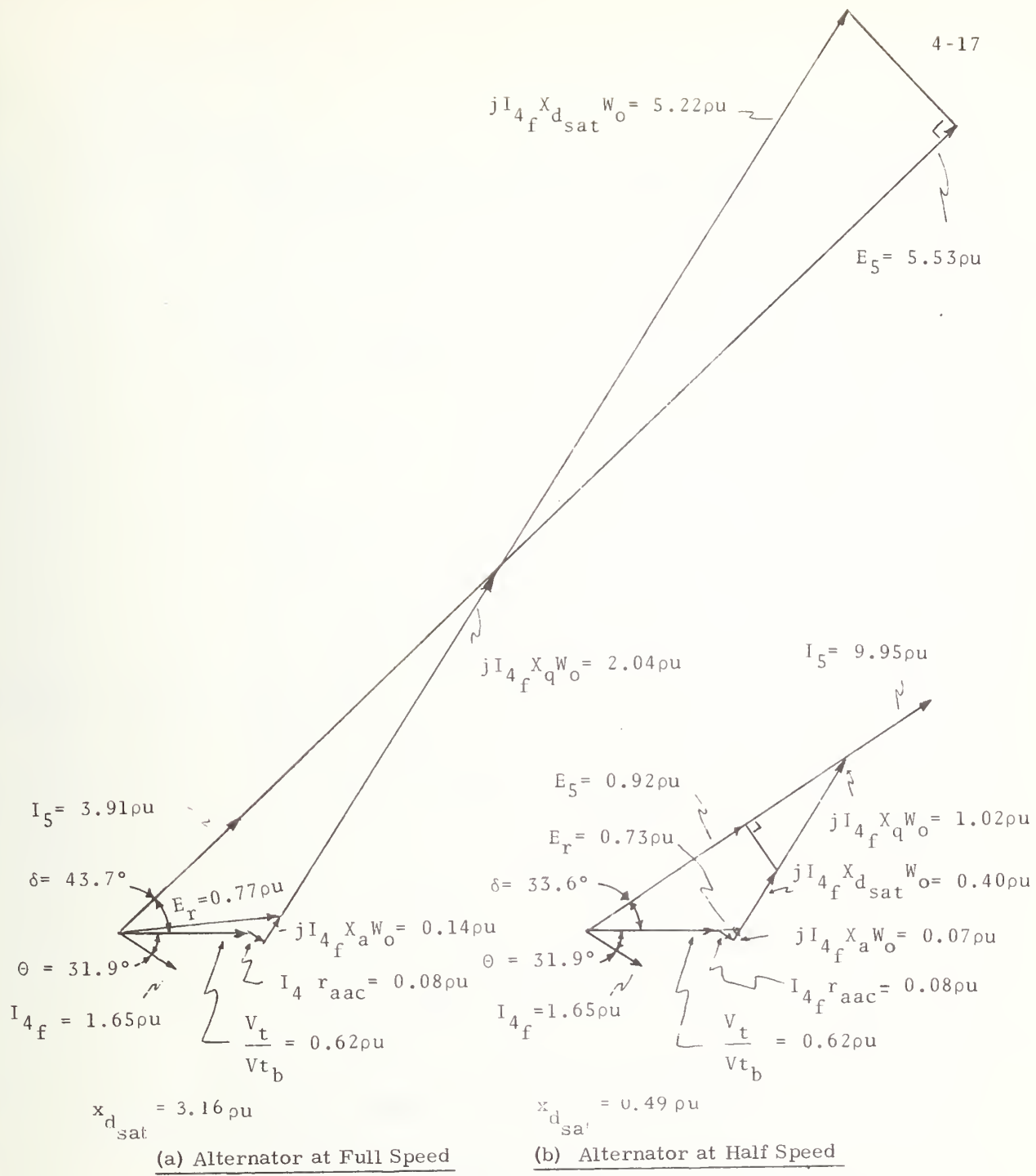
Alternator Phasor Diagram, Traveling Mode:
Generator Operation at Alternator Base Conditions*

saturation using the slope of the Kingsley air-gap line through the air-gap voltage point, as shown in Fig. 10. The diagram is finally completed to find the excitation voltage E_5 . To find the field current in amperes, the per-unit excitation voltage must be corrected for saturation by using the ratio of the slopes of the Kingsley air-gap line relative to the base air-gap line. For example:

$$\begin{aligned}\text{Corrected } E_5 &= E_5 / \text{slope ratio} = 2.33 \text{ pu} / 0.954 = 2.45 \text{ pu} \\ I_5 &= 2.45 \text{ pu} \times 14.3 \text{ A} = 35 \text{ A} ,\end{aligned}$$

The phasor diagrams for the alternator at two points in the traveling mode are shown in Fig. 12. These diagrams correspond to the conditions of the flywheel and alternator at full speed and half speed while the dc traction motor is running at its base conditions. The operating points are also shown on the saturation curves of Fig. 10. The terminal voltage is 0.62 pu or 215 V; the armature current is 1.65 pu or 121 A, at PF = 0.85 lag.

As Fig. 10 shows, at full speed, point M, the alternator is hardly saturated; the field current is 3.91 pu, or 56 A. At half speed, point N, the alternator is heavily saturated. Since the field current is 9.95 pu, or 142 A, both the armature and field losses are extremely high. Over a typical mission, the alternator might have to carry even higher

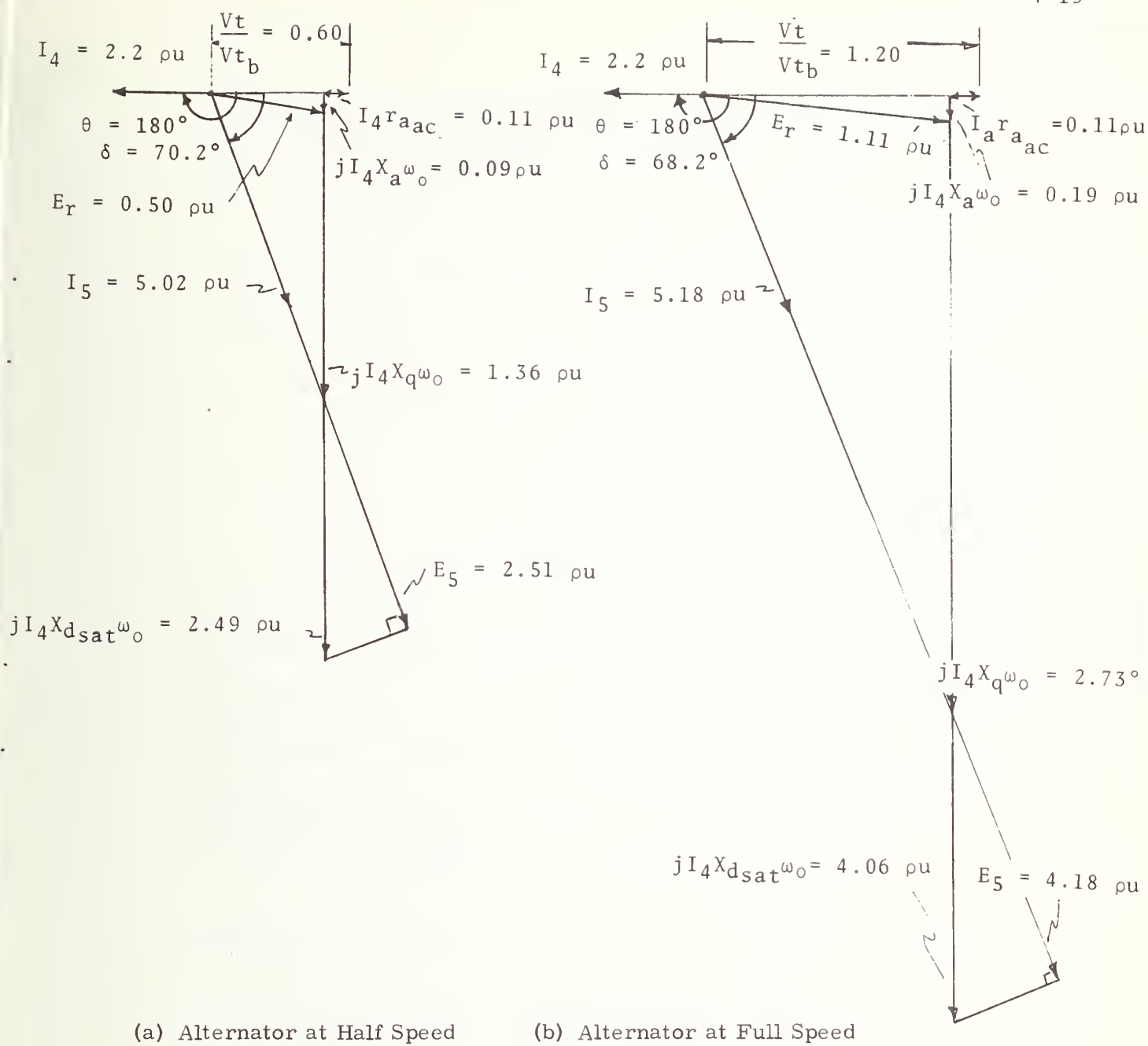


*Alternator Operation: 215 V (l-n); 66.1 kW; 0.85 PF lag; 12,000 and 6,000 r/min.
Fig. 12

Alternator Phasor Diagrams, Traveling Mode:
Generator Operation at DC Traction Motor Base Conditions*

armature currents to support the tractive force requirements of the dc traction motor. If such high armature currents occur when the flywheel has run down to half speed, the alternator field current might be even higher than the 9.95 pu value, and increased losses, proportional to I_5^2 would result.

The phasor diagrams for the alternator operating as a synchronous motor at points in the wayside charging mode are shown in Fig. 13. These diagrams are based on 2.2 pu armature current at PF = 1.0. The terminal voltage increases linearly with speed to a final value of 1.2 pu when the alternator is at rated speed. During the charging period, at half speed, the alternator is not saturated; the field current is 5.02 pu, or 71.8 A. At full speed, the alternator is partially saturated; the field current is 5.18, or 74.0 A. The field current is practically constant during this mode of operation. The alternator operating as a motor could operate at even higher power, and thus, shorten the charging time if the final value of the terminal voltage were raised above 1.2 pu. However, the field current and losses, as well as the temperature rise, would be higher than for the assumed charging condition. The limitation on charging is the pull-out power for the alternator, operating as a synchronous motor.



*Input to Machine: At half speed, 207 V, 100 kW; at full speed, 414 V, 200 kW.

Fig. 13

Alternator Phasor Diagrams, Wayside Charging Mode:

Alternator Operating as a Synchronous Motor*

Power loss model - The five equations for the power loss model are written in terms of the per-unit variables but yield the power loss components in kW. The equations for the armature and field circuit copper losses (A_1 and A_2) are derived from the circuit resistances, including that of the exciter. The equation for the iron loss (A_3) assumes a variation with air-gap voltage, to the 2.0 power. The air-gap voltage is proportional to the product of speed and flux. The friction and windage loss (A_4) is assumed to vary as ω_o^3 . The stray load loss (A_5) has a constant term and a term dependent upon armature current. The five equations in per-unit variables for the baseline alternator yield the following loss components in kW:

$$\begin{aligned}
 A_1 &= 3.94 I_4^2 && - \text{Armature copper loss} \\
 A_2 &= 0.280 + 0.24 I_5^2 && - \text{Exciter and field circuit copper loss} \\
 A_3 &= 1.45 E_r^2 && - \text{Iron loss} \\
 A_4 &= 2.05 \omega_o^3 && - \text{Friction and windage loss} \\
 A_5 &= 0.207 + 1.67 I_4^2 && - \text{Stray load loss} .
 \end{aligned}$$

At the base conditions, the sum of the loss components given by the power-loss equations must equal the known total loss of the alternator. The loss components for the alternator are shown in Table 10.

Table 10
Alternator Loss Components at Base Conditions

A_1	= 3.94 kW	- Armature copper loss
A_2	= 1.63 kW	- Exciter and field circuit copper loss
A_3	= 1.60 kW	- Iron loss
A_4	= 2.04 kW	- Friction and windage loss
A_5	= 0.39 kW	- Stray load loss
P_7	= 9.60 kW	- Total loss

The manufacturer usually supplies the armature and field circuit resistances and the full-load efficiency. Once efficiency is known, the total loss in kW can be calculated. The loss components A_3 , A_4 , and A_5 can be allocated using typical values from a handbook or text on electric machine design.

The alternator losses during the traveling mode, when the dc traction motor is operating at its base condition (2730 r/min and 70 hp), are shown in Table 11 for two conditions: when the alternator is at full speed and at half speed. These operating points correspond to the phasor diagrams in Fig. 12. Because the armature current is 1.65 pu,

both the armature and the field losses are higher than for the base conditions of Table 10. Compared to the base loss of only 9.60 kW, the total loss varies from 19.4 kW at full speed to 37.5 kW at half speed. The relative magnitude of the total loss at full speed and at half speed can be shifted by selecting the base voltage for the alternator. Selecting a base voltage higher than 345 V will reduce the field loss A_2 but raise the armature resistance and thus the armature loss A_1 . Selecting a base voltage lower than 345 V will produce the opposite effects on the loss components A_1 and A_2 .

Table 11

Alternator Loss Components During Traveling Mode*

<u>Loss Component</u>	<u>Alternator</u>	
	Full-speed	Half-speed
A_1	11.6 kW	11.6 kW - Armature copper loss
A_2	4.0 kW	24.0 kW - Exciter and field circuit copper loss
A_3	0.9 kW	0.8 kW - Iron loss
A_4	2.1 kW	0.3 kW - Friction and windage loss
A_5	0.8 kW	0.8 kW - Stray load loss
P_7	19.4 kW	37.5 kW - Total loss

* Constant Load of 78.0 kVA, 66.1 kW, 215 V (1 - n)

The alternator losses during wayside charging are shown in Table 12 for the alternator at half speed and at full speed. Compared to the base losses of only 9.60 kW, the total losses are practically constant, ranging from 27.2 kW to 30.8 kW.

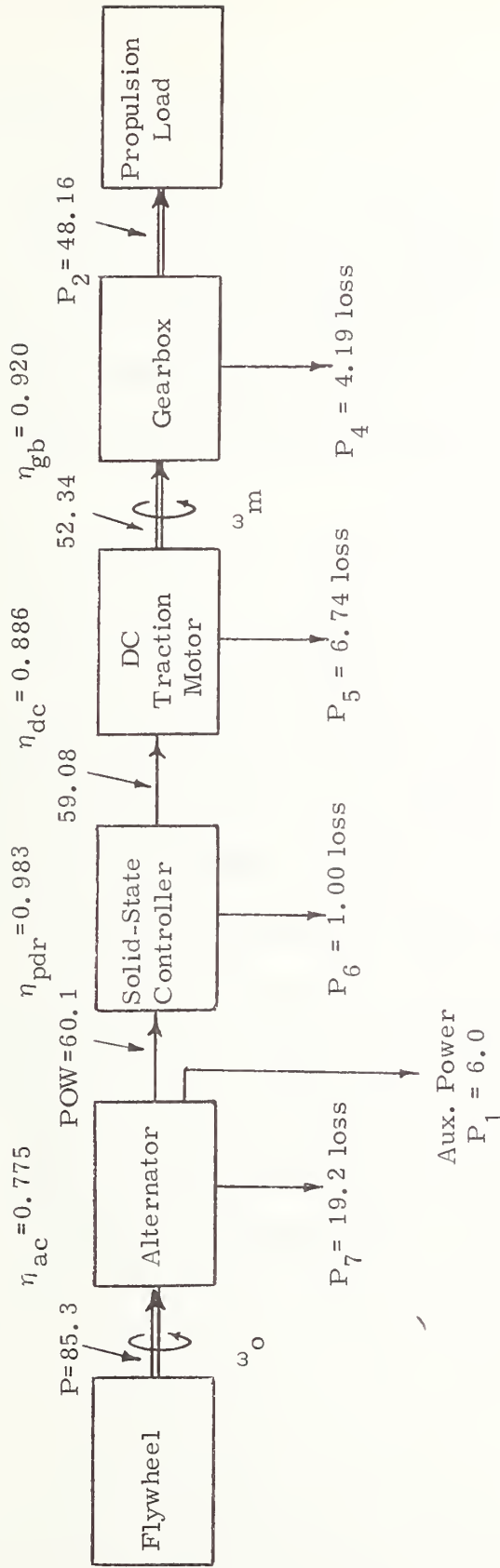
Table 12

Alternator Losses During Wayside Charging Mode*

<u>Loss Component</u>	<u>Alternator</u>	
	<u>Half-speed</u>	<u>Full-speed</u>
A_1	19.1 kW	19.1 kW - Armature copper loss
A_2	6.3 kW	6.7 kW - Exciter and field circuit copper loss
A_3	0.4 kW	1.8 kW - Iron loss
A_4	0.3 kW	2.1 kW - Friction and windage loss
A_5	1.1 kW	1.1 kW - Stray load loss
P_7	27.2 kW	30.8 kW - Total loss

*Armature current 2.2 pu; PF = 1.0 (motoring); terminal voltage proportion to speed, up to 1.2 pu at full speed.

Propulsion System Losses. The combination of the dynamic and power loss models for the energy-storage unit and power-train components will yield both the component and the overall propulsion system power losses at each instant of time during the mission cycle. For example, the component losses when the dc traction motor is running at its base condition and the flywheel is at full speed are shown in Fig. 14. The dc traction motor is delivering 70 hp, or 48 kW, at the drive-wheels. The flywheel must supply 85.3 kW to overcome the alternator and power-train losses and provide the required auxiliary load of 6 kW. The overall propulsion-system efficiency is 62 percent. If the flywheel were running at less than full speed and/or the dc traction motor providing more than its base torque of 135 lb ft, the propulsion-system losses would be even greater than those under base conditions.



Note: Power in kW. Efficiency in pu.

*DC traction motor operating at Base Conditions of 135 lb ft torque and 2730 r/min speed. Flywheel operating at 12,000 r/min ($\omega_o = 1.0$).

Fig. 14

Power and Efficiency of Electric Propulsion

System Components*

Thermal Models

The temperatures of the major components of the drive system at each instant of travel time are calculated by using thermal models. The power losses required for the calculation are obtained from the power loss models. The maximum component temperatures show whether the components have been properly selected to withstand the service conditions of the vehicle.

The insulations of rotating electric machines, i. e. , the alternator and dc traction motor, are assigned maximum allowable hot spot temperatures by the manufacturer. Whenever the operating temperature exceeds the allowable temperature, the service life of the machine is reduced, typically by a factor of two for each 10°C that the limit is exceeded. If temperature excesses are large, e. g. , more than 60°C , complete failure of the component may result. If the machine does not reach its temperature limit, even during heaviest conditions of load, the machine has been selected too conservatively and will be too heavy. One purpose of the simulation is to provide the designer with means for selecting optimal ratings for the major components of the drive system.

Unlike the rotating electric machines, the thyristors in the solid-state controller will burn out if the junction temperature exceeds the allowable value even for a fraction of a second. The temperature rise can be reduced by selecting larger thyristors with greater thermal mass and conductivity and/or selecting thyristor heat sinks with greater thermal mass and higher heat dissipation rates.

Thermal models were not developed for the gearbox nor the flywheel. The gearbox losses are small and its temperature rise is therefore not expected to be large. Furthermore, because the gearbox has a large heat capacity, the effects of overheating would not be drastic. The flywheel does not require a thermal model to calculate the temperature of its bearings. They must be selected to withstand full speed regardless of the mission of the vehicle.

The thermal models use lumped parameters of thermal mass and thermal conductivity to represent the actual distributed parameters of the electric machines and the thyristors of the solid-state controller. The power losses are the independent variables (inputs); the temperatures are the dependent variables (outputs). Since the temperature variation lags in time the power loss inputs, vehicle operation must

be simulated long enough -- i. e. , over several mission cycles -- to allow the temperature variations to reach a steady-state pattern.

Rotating Electric Machines. Similar thermal models are used for the alternator and dc traction motor. The rotor is represented by one thermal mass and the stator by a second thermal mass. Additional lumped elements can be used at the discretion of the modeler; two thermal masses are sufficiently accurate for demonstrating the simulation procedure.

For convenience, the differential equations of the thermal models are obtained from thermal-to-electrical analogs. Thermal capacitance of each mass is the product of that mass and its specific heat. Thermal resistance is a measure of the temperature differential required to obtain a given rate of heat flow. The thermal-to-electrical analog equivalents are given in Table 13.

Table 13
Thermal-to-Electric Analogs

Temperature	T	Voltage	V
Thermal Resistance	$1/Ah$	Resistance	R
Thermal Mass	mC_p	Capacitance	C
Heat Rate	\dot{Q}	Current	I
Thermal Energy	Q	Charge	Q

The electric circuit that represents the analog equations of the thermal model for the dc traction motor is shown in Fig. 15. The current sources are the heat rates, i.e., the power losses, of the rotor and the stator. The temperatures of the rotor, air gap, and stator are the node variables with respect to ground, i.e., the ambient temperature. The same thermal model of Fig. 15, with suitable symbols, represents the equations for the thermal model of the alternator.

The parameters required to construct a thermal model of a rotating electric machine are not provided by the manufacturer. They must be estimated from the weight of the machine, the losses, and the temperature when the machine is operated at rated conditions. The weight must be divided between the rotor and stator; an average specific heat, such as $0.11 \text{ cal/g/}^{\circ}\text{C}$, is used for the copper and iron portions to calculate the thermal masses. The losses must also be divided between the rotor and stator. Thermal resistances are calculated by using the rated temperature, the ambient temperature, and an estimate of the intermediate air-gap temperature. The calculations for the thermal models of the baseline electric machines are given in Appendix A.

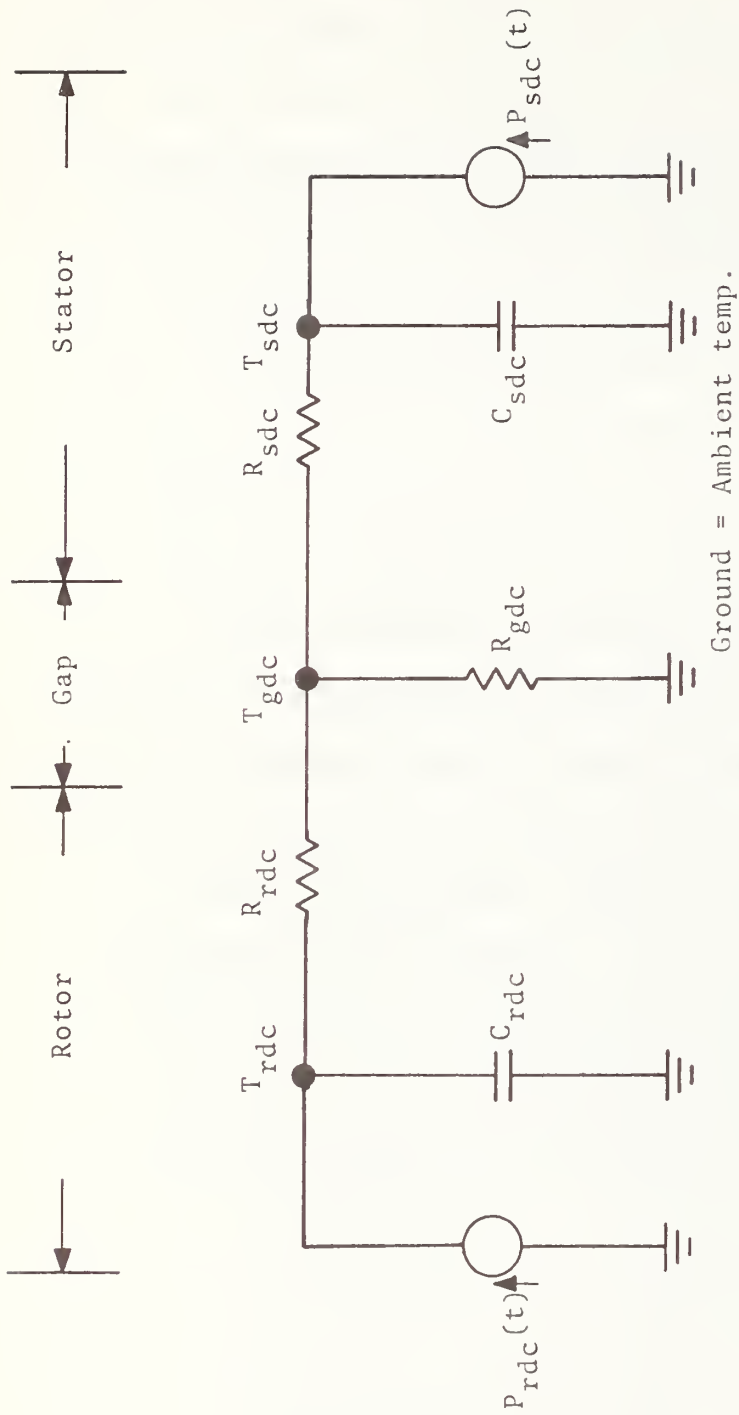


Fig. 15

Thermal Circuit Model for DC Traction Motor

Although the power loss models provide five loss components for the alternator and the dc traction motor, the thermal models require as inputs only the total rotor loss and the total stator loss. These losses are allocated in the thermal models by the two following equations, which incorporate the weighting coefficients R_{di} and S_{di} :

$$P_{rdc} = R_{d1}D_1 + R_{d2}D_2 + R_{d3}D_3 + R_{d4}D_4 + R_{d5}D_5$$

$$P_{sdc} = S_{d1}D_1 + S_{d2}D_2 + S_{d3}D_3 + S_{d4}D_4 + S_{d5}D_5$$

where:

$$R_{di} + S_{di} = 1.0 \text{ for } i = 1, 2, \dots, 5.$$

In the alternator, all of the armature power loss D_1 occurs in the stator; hence, $R_{d1} = 0$ and $S_{d1} = 1.0$. In the dc traction motor, the armature power loss occurs in the series field and interpoles on the stator and in the armature winding on the rotor; the coefficients are thus allocated $R_{d1} = 0.95$ and $S_{d1} = 0.05$. The allocations either are obvious or must be made on a judgmental basis. The allocations for the alternator and dc traction motor are given in Table 14. No matter how the loss components are allocated, the total power loss must be discharged into the total thermal mass of each electric machine. Temperature errors, if any, between the rotor and stator of the two-mass

thermal model will occur only because the power loss components are not accurately assigned to the rotor or the stator.

Table 14
Weighting Coefficients for Thermal Models
of Electric Machines

Mach. Ele- ment	DC Machine					AC Machine				
	D ₁	D ₂	D ₃	D ₄	D ₅	A ₁	A ₂	A ₃	A ₄	A ₅
Rotor	0.95	0	0.6	0.8	1.0	0	1.0	0.2	0.7	0.2
Stator	0.05	1.0	0.4	0.2	0	1.0	0	0.8	0.3	0.8

The flow chart for calculating the temperatures of the dc traction motor is shown in Fig. 16. The flow chart uses the parameters of thermal resistance R_r and R_s , as well as the thermal time constants $R_r C_r$ and $R_s C_s$. The rotor and stator components of the power loss are the inputs; the dc traction motor temperatures are the outputs.

In the dc traction motor, the heat from the power losses is dissipated by convection to the air, which is blown through the air gap by fans at 400 ft³/min. In the alternator, the heat is dissipated by forcing an oil spray to circulate within the machine at a rate of 4 gal/min. The oil is cooled in an external heat exchanger. The numerical values

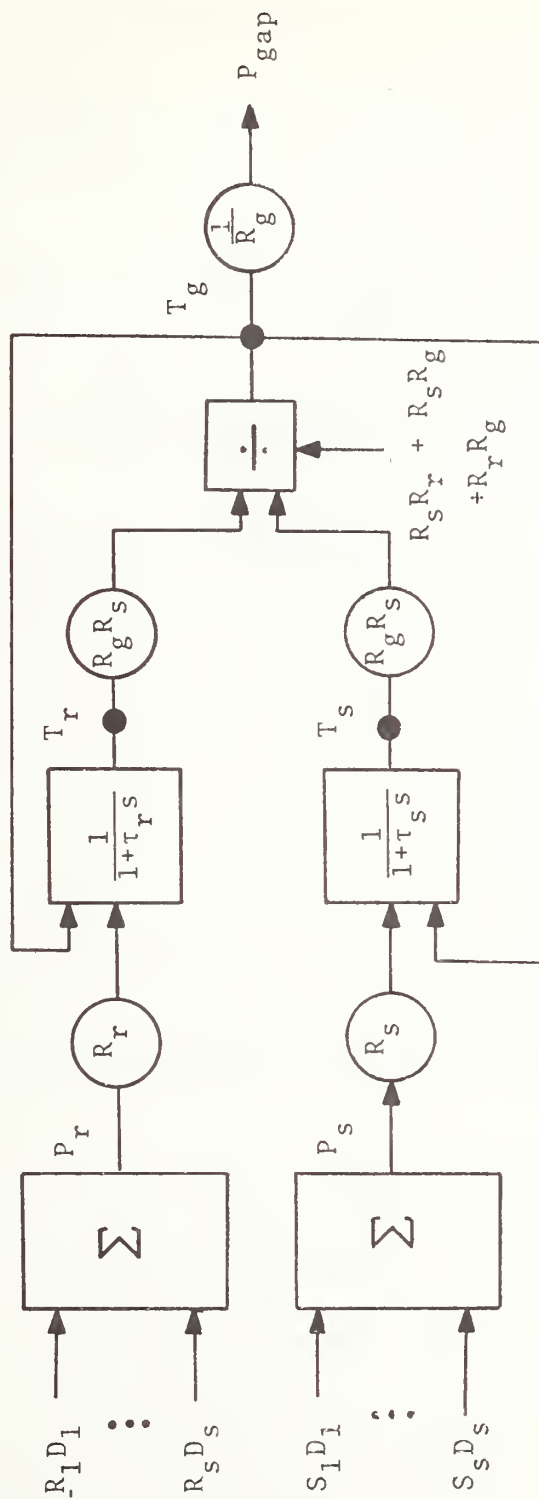


Fig. 16

Flowchart of Thermal Computations for DC Traction Motor

of the parameters for the thermal models of the electric machines are given in Table 15.

Table 15

Thermal Resistances and Time Constants
for Electric Machines

<u>Parameter</u>		<u>DC Traction</u> <u>Motor</u>	<u>Alternator</u>
Rotor-to-gap therm. res. R_r		8.2° C/kW	18.8° C/kW
Stator-to-gap therm. res. R_s		21.6° C/kW	7.4° C/kW
Gap-to-amb. therm. res. R_g		3.0° C/kW	3.0° C/kW
Rotor therm. time constant τ_r		512 s	65 s
Stator therm. time constant τ_s		1127 s	40 s

Solid-State Controller. The six thyristors of the controller are mounted on a common heat sink assembly which is cooled by convection and/or forced air. The thermal model for this component uses two lumped thermal masses: one for the six thyristor junctions; the second for heat sink assembly. The mass of the junctions is negligible compared to the heat sink assembly and can be neglected. The circuit in Fig. 17 represents the analog equations of the controller's thermal model.

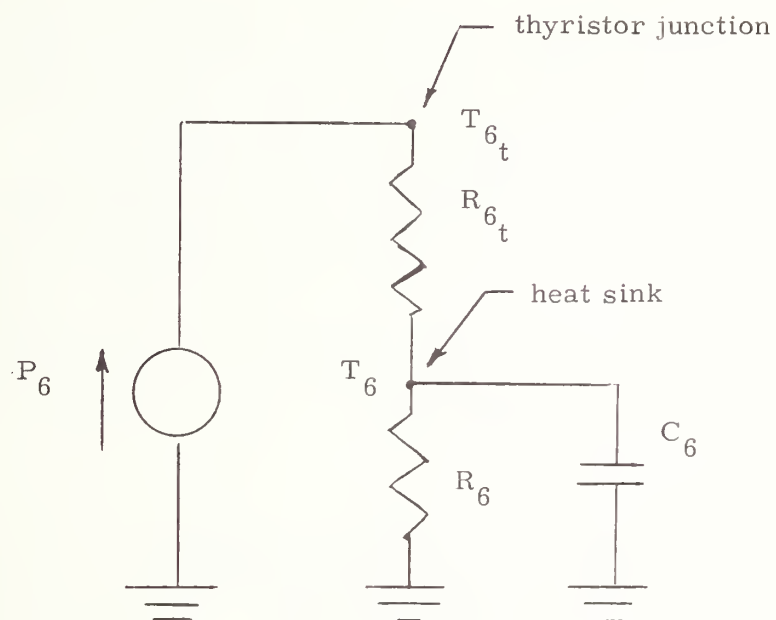


Fig. 17

Thermal Circuit Model for Solid-State Controller

The power loss is calculated as the sum of junction losses of all six thyristors. The junction-to-heat sink thermal resistance represents six thyristors in parallel. Manufacturers provide values of thermal resistance for their thyristors, and data from which thermal resistances and time constants of their heat sinks can be calculated. The parameters for the solid-state controller are given in Table 16.

Table 16

Thermal Resistances and Time Constants
for Solid-State Controller

Junction-to-heat sink resistance	R_{6t}	58.8° C/kW
Heat sink-to-ambient resistance	R_6	19.6° C/kW
Heat sink time constant	T_6	18.4 s

Changing Ratings of Major Components

The simulation of the electric propulsion system is intended for both analysis and design purposes. The numerical values in the models of the simulation are based on the specific components of the baseline system. The simulation provides information on the electrical and mechanical variables, the power losses and the temperatures, as the vehicle carries out its mission. The specific components of the baseline system may have to be changed several times in the models in order to optimize the electric propulsion system. The changes in the components can result in such effects as reduction of energy losses over a mission cycle; change of recharging time; decrease of propulsion system weight; and reduction of component temperatures.

Changes can be made in the electric machines of speed and torque ratings, method of cooling and maximum temperature. Changes can be made in the controller by selecting different thyristors and heat sink assembly. The numerical values in the electric-machine models can be modified either by incorporating the values for the new machines, or by using dimensional-analysis on the baseline values to find the new values. Since machine electrical and thermal parameters vary slowly with changes in power rating, the dimensional-analysis technique to be described in this section is sufficiently accurate for changes of $\pm 50\%$ in power rating from the baseline conditions. For small changes of power rating, the per-unit machine ratings can be left unchanged.

Changes in Electrical Ratings of Electric Machine. The frame of an electric machine determines its torque rating. Its power rating is proportional to how fast the machine is run. Of course, many secondary factors must be considered, e. g. , mechanical strength, losses, ventilation, commutation, and bearings. In this section, we will consider changes in the power ratings of the dc traction motor and the alternator, assuming that their rated speed is not changed.

The power rating P of any rotating electric machine, such as the alternator or dc traction motor, is of the dimensional form:

$$P = \ell^4 J B_m N,$$

where:

ℓ = linear dimension

J = current density

B_m = flux density

N = speed ,

Assume that the machine size is increased or decreased, i. e. , by its linear dimension ℓ , without changing either the configuration, the densities, or the turns. Then, the copper and iron losses are proportional to ℓ^3 , which is the volume of material. The winding resistances both in ohms and in per-unit terms vary as ℓ^{-1} ; the winding inductances

in henries vary as ℓ , and the time constants vary as ℓ^2 . The pu alternator reactances at a given speed and frequency vary as ℓ . The friction and windage loss considered as a surface phenomenon can be assumed to vary as ℓ^2 .

Consider the 70-hp dc traction motor of the baseline system as an example of how the machine parameters vary with the linear dimension ℓ . Assume that the dc traction motor is found to operate with too low a temperature over a mission cycle. To increase the temperature the rating will be reduced to 60 hp and the mission cycle repeated. The parameters will change as follows:

Rating reduction	ℓ^4	$= (60/70)^{1/4} = 0.857$
Linear dimension	ℓ	$= (60/70)^{1/4} = 0.962$
Copper and iron loss (kW)	ℓ^3	$= (0.962)^3 = 0.890$
Resistance (pu)	ℓ^{-1}	$= (0.962)^{-1} = 1.04$
Friction & windage loss (kW)	ℓ^2	$= (0.962)^2 = 0.927$

These parameter changes are small. For a 0.14 pu reduction of power rating, the pu resistance increases by only 0.04 pu; the pu copper and iron losses at the new rating increase by only $(0.890/0.857)-1 = 0.04$ pu, as well.

The assumption of maintaining the same number of turns in the electric machine as its size is changed is merely a convenience. The assumption washes out when the effects are expressed in pu. After its size has been changed the machine can be wound for any combination of voltage and current that meets the new power rating.

Changes in Speed Ratings of Electric Machines. When the speed, current or voltage ratings of an electric machine, such as the alternator or dc traction motor, are changed, with or without a simultaneous change in linear dimension, the change in the parameters is more complicated than for a change of ℓ alone. Under the assumption of the same winding geometry (i.e. number of slots, space factor, and winding design) the voltage and current ratings can both be varied by a ratio k , which does not affect the power rating. The ratio k is defined as the turns ratio or the number of turns of the new machine divided by the number of turns on the original machine. Independent values of the turns ratio k can be assigned to the stator windings and the rotor windings. The parameters are now scaled as follows:

Power rating	$\ell^4 N$
Current rating	$\ell^2 k^{-1}$
Voltage rating	$\ell^2 N k$

Resistance (Ω)	$\ell^{-1} k^2$
Inductance (H)	ℓk^2
Reactance (Ω)	$\ell N k^2$
Base impedance (Ω)	$N k^2$
Resistance (pu)	$(\ell N)^{-1}$
Reactance (pu)	ℓ
Copper loss (kW)	ℓ^3
Copper loss (pu)	$(\ell N)^{-1}$
Iron loss (kW)	$\ell^3 N^2$
Iron loss (pu)	$N \ell^{-1}$
Friction & windage loss (kW)	$\ell^2 N^3$
Friction & windage loss (pu)	$N^2 \ell^{-2}$
Excitation power loss (kW)	ℓ^3
Excitation power loss (pu)	$(\ell N)^{-1}$

Consider the flywheel and alternator of the baseline system as an example of how the machine parameters vary with the linear dimension and the speed. Assume that the flywheel and alternator will be changed: the rated speed will be reduced from 12,000 r/min to 9,000 r/min and the power rating raised from 75 kVA to 100 kVA.

The key parameters will change as follows:

Rating increase	$\ell^4 N$	=	$(100/75)$	= 1.33
Speed ratio	N	=	$(9000/12,000)$	= 0.75
Linear dimension	ℓ	=	$(1.33/0.75)^{1/4}$	= 1.155
Resistance (pu)	$(\ell N)^{-1}$	=	$(1.155 \times 0.75)^{-1}$	= 1.155
Reactance (pu)	ℓ	=	(1.155)	= 1.155
Copper loss (pu)	$(\ell N)^{-1}$	=	$(1.55 \times 0.75)^{-1}$	= 1.155
Iron loss (pu)	$N \ell^{-1}$	=	0.75×1.155^{-1}	= 0.65
Friction & windage				
loss (pu)	$N^2 \ell^{-2}$	=	$0.75^2 \times 1.155^{-2}$	= 0.42 .

Changes in Electrical Rating of Solid-State Controller. The snubber network loss varies directly with the rating of the dc traction motor. The thyristor forward drop power loss varies directly as the rated or base armature current of the dc traction motor, i. e. , the loss coefficient is:

$$R_{2_b} = \frac{3}{1000} I_{a_b} \quad \text{kW.}$$

Changes in Thermal Parameters. The parameters for the thermal models of the machines must be changed as the ratings are altered either by size or by speed, or both. Two parameters are used in the thermal models: thermal resistance and thermal mass. The thermal mass can be combined with the thermal resistance to form an alternative parameter: thermal time constant. The thermal

resistances are defined for the paths extending from the rotor and stator hot spots into the air gap, and from the air gap to ambient-temperature heat sink. The resistances will depend somewhat upon the speed of the rotor as it affects heat transfer in the air gap. For the first-order model, we will assume that the thermal resistances are independent of the speed. The parameters are then as follows:

$$\begin{aligned} \text{Thermal mass} & \sim \ell^3 \\ \text{Thermal resistance} & \ell^{-1} \\ \text{Thermal time constant} & \ell^2 . \end{aligned}$$

For example, for the change of alternator rating from 75 kVA to 100 kVA, and speed from 12,000 r/min to 9000 r/min, in the previous section, the thermal parameters will change as follows:

Linear dimension	ℓ	= 1.155
Speed ratio	N	= 0.75
Thermal mass	$\ell^3 = (1.155)^3$	= 1.542
Thermal resistance	ℓ^{-1}	= 0.867
Thermal time constant	$\ell^2 = (1.155)^2$	= 1.335 .

For the solid-state controller, as the rating of the dc traction motor current (I_{ab}) varies, the thermal parameters are varied as follows:

Thermal mass (C_6)	$\sim I_{ab}^{-1}$
Thermal resistance (R_6 and R_{6t})	$\sim I_{ab}^{-1}$
Thermal time constant (τ_6)	— no change.

5. RESULTS

Sample Run

Using the baseline components, the computer program for the electric propulsion system simulation was run in order to check on several items, namely, the models, the ratings selected for the components, and to validate the simulation. The results were obtained as a print-out and as charts; the charts displayed traces of power, electrical variables, and temperatures, with time as the independent variable. These charts are shown in Figs. 18 through 21.

Mission Profile - The route traversed by the existing Morgantown vehicle was used in the simulation to test the baseline flywheel energy-storage vehicle. The required elevation and velocity profiles were shown in Fig. 4; they are repeated in terms of roadway grade and vehicle speed profiles in Fig. 18. The route has an outbound portion, which is basically uphill, to the Engineering Station (B), and a return inbound portion down the hill to the starting point at Walnut Station (A). The dwell-times between the segments of the route are used for charging the flywheel. The vehicle is assumed to make continuous round-trips, stopping at the terminals only to handle passengers and charge the flywheel. The two profiles represent inputs to the program. The

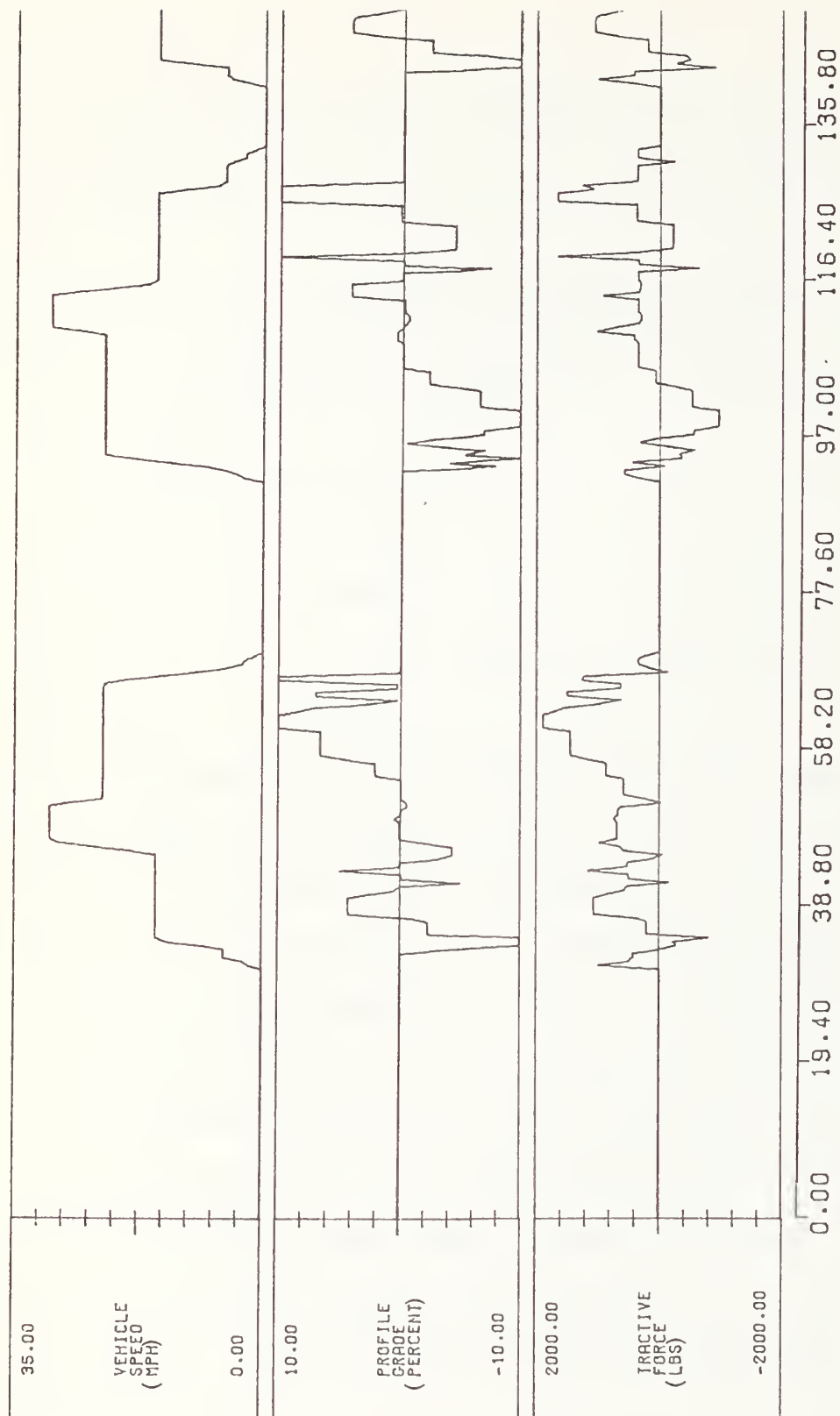


Fig. 18

Vehicle Speed, Roadway Grade Profile and Vehicle
Tractive Force Requirements

(SEC) * 10¹

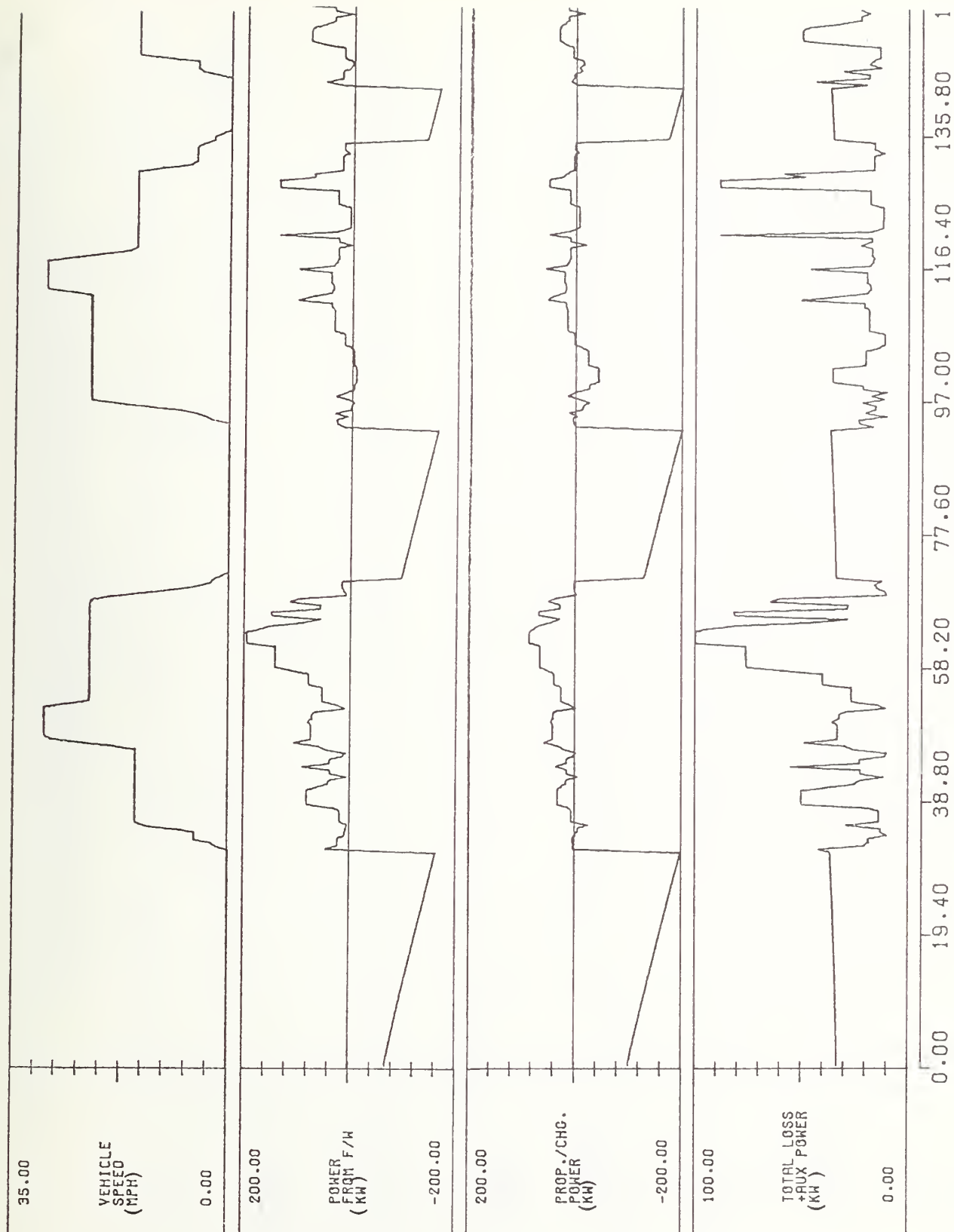
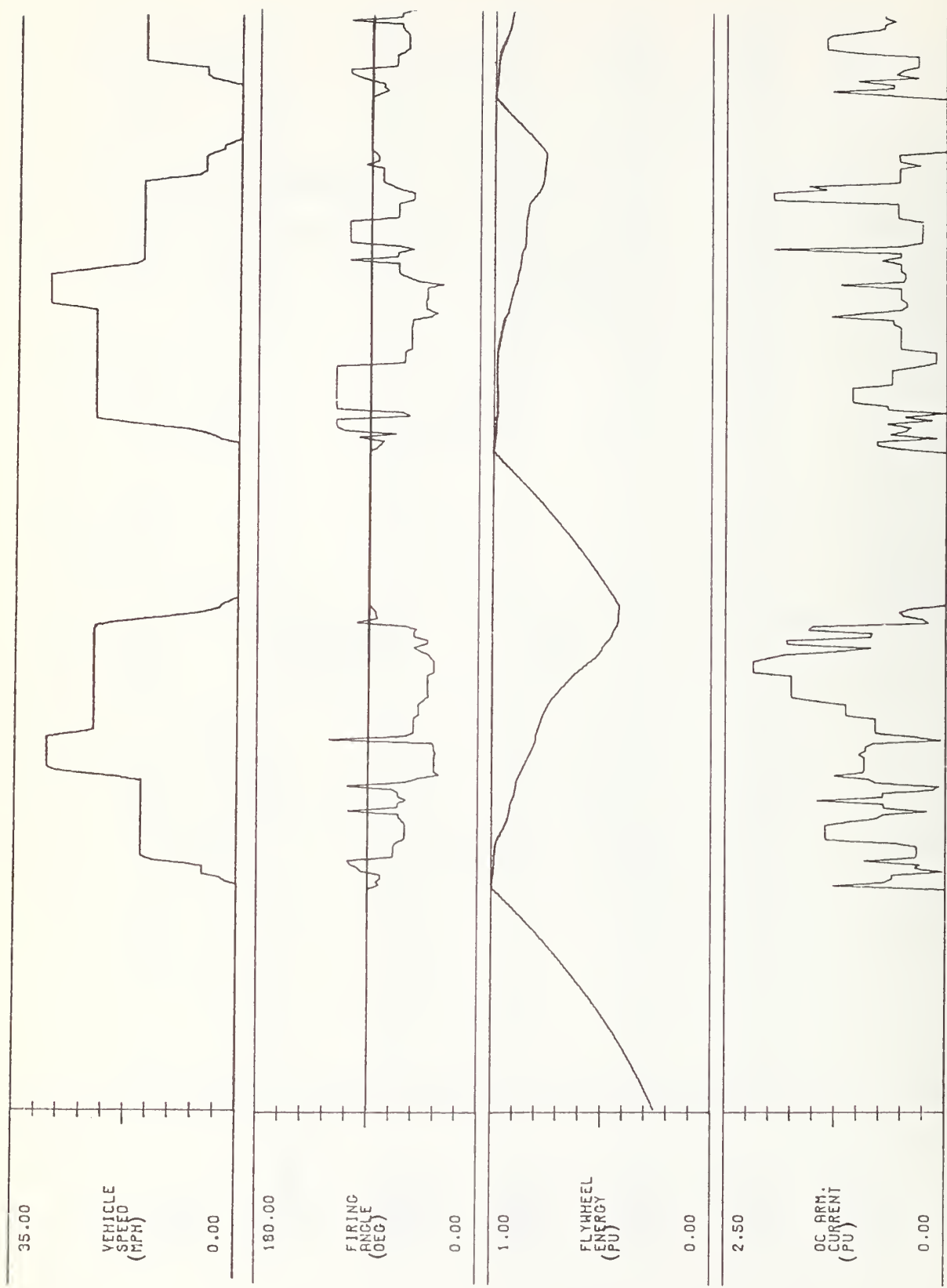


Fig. 19

Power and Loss Performance

(SEC) $\times 10^1$



0.00 19.40 38.80 58.20 77.60 97.00 116.40 135.80 1

Fig. 20

Controller, Flywheel and DC Traction Motor Performance (SEC) *10¹

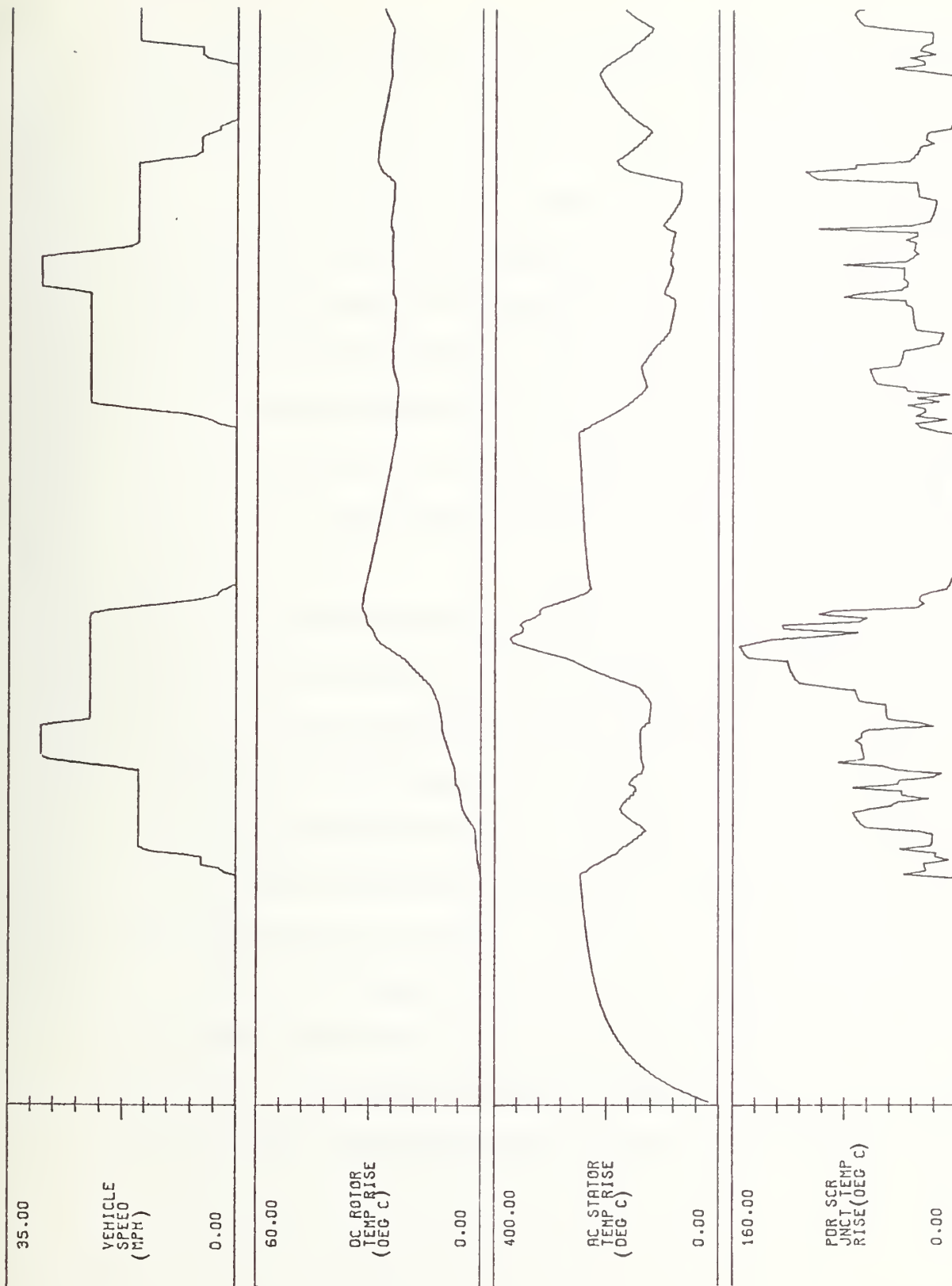


Fig. 21

Electric Machine and Controller Temperatures

vehicle speed is shown as a reference on all of the charts describing vehicle performance.

Tractive Force - For vehicle weight, wind conditions, and tire inflation, the computer calculates the tractive force required to meet the speed and grade profiles. The tractive force is shown in Fig. 18 for the two segments of the route. Negative tractive force obviously means braking. The base tractive force for the 70-hp dc traction motor is 750 lb. At 620 s on the chart, the peak tractive force is 1900 lb; the motor must deliver 2.5 times its base value.

The peak tractive force would be reduced in an actual vehicle, having an on-board speed-control unit. The unit would be designed to control the firing angle of the solid-state controller to coordinate as closely as possible the actual speed of the vehicle with the command speed. Furthermore, the controller would also limit the maximum current that it could deliver to the armature of the traction motor. This limiter would protect the controller and the dc traction motor, as well as limiting vehicle acceleration for the comfort of the passengers. As a consequence of the control actions, the dc traction motor would apply tractive-force peaks less than those shown in Fig. 18. Instead, the vehicle would slow down while negotiating the maximum

grades and require less tractive force. With reduced peak tractive forces and currents, the actual propulsion-system losses would be less than the losses calculated in this simulation.

In the second chart of Fig. 19, the trace is the flywheel power.

Negative values represent the charging power when the alternator operates a synchronous motor; positive values represent the flywheel power delivered to the alternator for propulsion. In the third chart, the negative values represent the wayside inverter charging power during the charging periods. During the traveling periods, the positive values represent propulsion power and the negative values represent braking power at the wheels. The charging power reaches 200 kW when the flywheel reaches full speed of 12,000 r/min. The only regeneration of energy to the flywheel in Fig. 19 occurs at about 1000 s, as the vehicle is descending a 10 percent grade. The braking power at the wheels is 43 kW; only 7 kW reaches the flywheel. Of the remaining 36 kW, 6 kW is auxiliary power and the rest is the loss of the electric propulsion system.

The power losses are shown in the fourth chart of Fig. 19. During the charging period the trace is the sum of the power loss of the alternator operating as a synchronous motor and the auxiliary power.

During the traveling period, the trace is the total power loss of the electric propulsion system and the auxiliary power. The most severe losses are evident when peak tractive force is required on the outbound segment of the route. For example, at 620 s, the flywheel power is 195 kW; the propulsion power is 85 kW; and the sum of the losses and auxiliary power is 110 kW. At this point in the mission, the propulsion system efficiency is only 45 percent. As a matter of fact, the power losses are so high on the outbound segment that the energy efficiency of the electric propulsion system is only 47.4 percent.

The trace of flywheel energy is shown in Fig. 20. During the first charging period, the flywheel is accelerated from half speed, i.e., 25 percent energy, to full speed, i.e., 100 percent energy. At the end of the uphill outbound segment, the flywheel speed has declined to 7,760 r/min, i.e., 42 percent energy. At the end of the downhill inbound segment, the flywheel speed has declined to 10,400 r/min, i.e., 69 percent energy. Note that the 7 kW of power regeneration at about 1000 s produces the only increase of the flywheel energy, during either the outbound or inbound segments of the mission cycle.

Electrical Operation - In Fig. 20, the firing angle of the solid-state controller and the armature current of the dc traction motor

show the state of the electrical system at each interval of travel time. Consider as a reference that, at a firing angle of 90° , the controller applies zero voltage to the dc traction motor. As the angle is shifted toward 0° , the voltage increases and the motor provides tractive force; as the angle shifts toward 180° , the voltage increases negatively and the motor provides regenerative braking force. The regenerative action can be seen during the downhill inbound segment of the mission when the firing angle shifts to 120° . At each interval of travel time, the computer reads out the firing angle which makes the propulsion system meet the speed and tractive-force requirements of the vehicle. As previously noted, in an actual vehicle the control unit would generate the necessary firing angles as the vehicle traversed its route.

The dc armature current trace in Fig. 20 roughly tracks the tractive force shown in Fig. 18. Saturation of the dc traction motor causes the armature current to exceed proportionality to tractive force, while the compounding effect of the series field acts on the armature current in the opposite direction. The peak armature current needed to deliver the peak tractive force is about 2.2 pu at about 620 s. At this current, the armature power loss is about five times its value at rated current. However, since the armature current is less than rated value over most of the route, the average armature power loss is less than the rated value.

Component Temperature - The temperature rise traces of the critical parts of the dc traction motor, the alternator, and the solid-state controller are shown in Fig. 21. The armature of the traction motor reaches a temperature of 32°C near the end of the first uphill outbound segment and 47°C near the end of the second uphill outbound segment. The rated temperature rise of the dc traction motor is 80°C over a 40°C ambient. Since the traction motor armature has a long thermal time constant of 512 s, the temperature does not track the armature current. Furthermore, the dc traction motor tends to cool down during the charging periods, when the vehicle is stationary, with the result that the dc traction motor temperature does not reach the limits set by the manufacturer.

The stator of the alternator has a relatively short thermal time constant of 40 s. The alternator heats up during both the charging and the traveling modes and carries overload currents as well. The chart shows a stator temperature rise of 246°C at the end of the first charging period, 370°C at the end of the first uphill outbound segment, and 355°C at the end of the second uphill outbound segment. The rated temperature rise set by the manufacturer is 160°C over a 40°C ambient. The alternator clearly must be replaced with a larger machine, so as to reduce the power losses and the temperature rise.

Because the junction thermal mass and time constant are negligible, the trace of thyristor junction temperature follows the armature current. The heat sink has a thermal time constant of only 19 s. Its temperature rise reaches a peak of 155°C when peak tractive force is required. The rated temperature of the junction set by the manufacturer is either 125°C or 150°C , depending upon the type of thyristor. For a 40°C ambient, the corresponding rated temperature rise is either 85°C or 110°C , compared to the peak value on the chart of 155°C . The results show that the thyristors must be replaced with larger units and/or the thermal time constant of the heat sink increased to insure that the controller will not fail.

System Redesign. The purpose of testing the baseline electric propulsion system was to demonstrate the procedures for using the simulation. The particular type of propulsion system modeled has been proposed by several companies for application to a flywheel energy-storage vehicle. The solid-state controller and dc traction motor are actually on the existing Morgantown vehicle. The 75-kVA alternator and the flywheel correspond to the energy-storage unit originally selected for the San Francisco MUNI flywheel trolley coach. The test run for the simulation of our particular configuration and components shows that the baseline dc traction motor is conservatively loaded,

but the baseline alternator and solid-state controller are overloaded. In actual operation, they will suffer excessive temperature rises and may be expected to break down as a consequence.

If the baseline system were to be built, one or more of the following steps of redesign would be required to insure that the component temperatures did not exceed the manufacturers' limits:

Select an alternator and a controller for larger power ratings in order to reduce their temperature rises to allowable levels.

Reduce the size and hp rating of the dc traction motor.

Set the base speed lower to correspond to a vehicle speed of 23 mi/h, at which peak torque is required.

Use independent field weakening to reach the maximum vehicle speed of 30 mi/h, at which less than peak torque is required.

Supply the on-board auxiliary load from a battery, which can be charged from wayside equipment each time the flywheel is charged. Maintain the charge on the battery from the alternator; only allow it to charge when it is not heavily loaded with propulsion power.

Control the dc traction motor voltage with a combination of alternator field control and controller firing angle control so as to reflect as high a power factor as possible to the alternator. The reduced armature and field currents will reduce the power losses and temperatures in the alternator field and stator windings.

Increase the flywheel energy storage capacity in order to reduce the speed drop of the alternator over a mission. The alternator field current to support the terminal voltage at large armature current and low speed will be reduced. The temperature rise, consequently, will be reduced, as well.

Increase the alternator terminal voltage during the charging period, so that the voltage at the end of the period is greater than 1.2 pu. For the same current, the power will be greater, the charging period shorter, and the stator temperature rise reduced.

The proposed steps of redesign can be tested with the simulation of the electric propulsion system by making appropriate changes in the component models. The charts of component temperatures will show when the redesign has achieved a viable system.

Extension to Other Systems

The procedure in this report for developing a simulation of an electric propulsion system for a flywheel energy-storage vehicle can be applied to other propulsion systems. The simulation can be used to analyze these other propulsion systems when the components are known, or to select components to meet criteria of temperature or power losses. Simulations are particularly suitable for determining the capacity of the energy-storage equipment required for the vehicle to complete its mission.

In order to develop a simulation for a new electric propulsion system, the models must be formulated in the same sequence as described in this report. The dynamic models, which are basically the equations for the electric machines and other components, will provide all of the dependent electrical and mechanical variables of the propulsion system. The power loss models of the components will then provide the power loss components as a function of the electrical and mechanical variables. Finally, the thermal models will generate the component temperatures, as a function of the same variables.

For each electric propulsion system, the parameters for formulating the models of the components must be obtained from a combination of

manufacturers' data, handbook data of typical components, and electric-machine design texts. Dimensional analysis can be used to find parameters for specific component ratings from available data.

Conclusions

The Flywheel Propulsion Simulation has been developed for use as an engineering tool for evaluation and design of flywheel-electric-drive propulsion systems for short-range vehicles. This simulation makes it possible to evaluate performance of candidate propulsion systems, operating over given mission profiles, defined in terms of velocity and grade profiles. Wayside recharge and regenerative braking are featured, and power losses and equipment temperature rises are computed on a dynamic basis.

The example shown in the sample run (Chapter V and Appendix D) was not intended to be an optimum design, but an illustration of how the simulation can be used in a specific instance.

The procedure described in this report is a powerful tool in analyzing and designing electric propulsion systems. The use of this procedure will help avert design errors, where components are too large or too small, run too hot or too cold, and require expensive and time-consuming modifications after the vehicles are built and tested.

6. CONCLUSIONS

This report has described a digital computer simulation suitable for modeling the electric-drive system associated with a flywheel energy-storage vehicle in which the electrical, mechanical, and thermal operational characteristics of the propulsion system are included. Parameters associated with the route, the vehicle, or the propulsion system components, can be varied and the overall effect of these variations on the performance of the vehicle can be rapidly determined. The particular simulation describes the system more accurately and provides more meaningful data than other previously used simulations, where efficiencies are assigned to each component in the drive train either from estimated average values, or values computed from a multivariable equation. Since the simulation includes thermal models of the electric machines and solid-state controller, component temperatures can be tracked, and also components of different ratings and designs can be evaluated. Furthermore, the simulation method can be applied to electric-drive systems for battery and flywheel energy-storage vehicles, to hybrid vehicles, and to vehicles operating from wayside power.

For the sample run and prototype drive system described in this report, the results indicate that the alternator must be larger (higher rating) to reduce its operating temperatures to acceptable levels. Likewise, the dc traction motor can be smaller, because its operating temperature is less than the allowable level. The rating of the solid-state controller should be increased to reduce its operating temperature.

The results of our preliminary work have shown that the electric-drive system can be optimized for low losses and maximum usage of the flywheel stored energy. The following steps are required. First, the machines should be operated for as little time as possible beyond their ampere ratings. A current limiter should be incorporated into the controller, or larger machines should be used if necessary. Second, the flywheel and alternator of the drive system should not be burdened with supplying the auxiliary power at all times, particularly when the drive system is operating at full capacity. A battery should be used as a supplementary power source for the auxiliary load. Third, a phase-controlled rectifier should not be used to control the speed of the dc traction motor, particularly when the dc motor is required to run at low speed and high torque over a substantial portion of the route. The high current at low power factor drawn from the alternator causes its stator

and field losses to be excessive. To reduce system losses, the dc motor speed should be controlled by the alternator field current; the controller should be operated either full-on, firing angle $\alpha = 0^\circ$, or full regeneration, $\alpha \approx 180^\circ$.

The electric-drive system described in this report is frequently used for studies of flywheel energy-storage vehicles. For this reason, it was selected as a basis for developing the modeling procedure. Other configurations, which are less lossy over a given route, can be studied by the same techniques. Electric-drive systems which are patterned after stationary industrial drives, or after vehicle drives using contact-rail power, will not necessarily be optimum for flywheel energy-storage vehicles. The regenerative braking feature of the system described in this report would probably be more attractive if a true urban route (over five stops per mile) were used to test the drive system, since braking would be done more frequently.

In summary, this electric-drive system simulation can be used to determine suitability of a given system configuration for an intended mission. Also, changes in the ratings of components and different configurations of components can be analyzed in order to optimize the drive system.

REFERENCES

1. "The Oerlikon Electrogyro, Its Development and Application for Omnibus Service," Automobile Engineer, December 1955.
2. Weinstein, C. H. , "R-32 Energy Storage Propulsion System," IEEE Conference Record of IAS Annual Meeting, 1975.
3. San Francisco Municipal Railway Improvement Corporation and U.S. Department of Transportation, "Energy Storage-Propelled Transit Vehicle Application Study," Final Report, April 30, 1975.
4. Reimers, E. , "Hybrid Electric Propulsion Utilizing Reconnectable Motor Windings in Wheels," IEEE Conference Record of IAS Annual Meeting, 1973.
5. Kusko, A. , Raposa, F. L. , King, C. M. , Somuah, C. B. , "Modeling of Electric Drive Systems for KEW (Flywheel) Vehicles," 1976 Intersociety Conference and Exposition on Transportation, Los Angeles CA., July 18, 1976.
6. The Boeing, Co. "Morgantown Personal Rapid Transit, System Operational Description Manual," Report M-PRT-1-1, Seattle WA, March, 1975.
7. LMSC, Inc. , "Proposal for Kinetic Energy Wheel (KEW) Design, Fabrication, and Test," Report LMSC-D083011, Sunnyvale CA, 7 January 1974.
8. Taulbee, J. K. , "Integrated-Drive Generator for Aircraft Accelerates Trend Toward Less Weight and Longer Life," Westinghouse Engineer, January 1971.
9. "Power Pack Thyristor," publication PSI-33(909), Power Semiconductors, Inc. , Devon CT 06480.
10. Randtronics, "Operation and Maintenance Manual for PRT Vehicle Propulsion System 2500," Vol. IV, 1974.

11. Fitzgerald, A.E., Kingsley, C., Kusko, A., "Electric Machinery," McGraw-Hill Book Co., Third Ed., New York NY, 1971.
12. Kingsley, Jr., C., "Saturated Synchronous Reactance," Trans. AIEE, vol. 54, No. 3, pp. 300-305, March 1935.
13. "Standard Handbook for Electrical Engineers," McGraw-Hill Book Co., Tenth Ed., New York NY, 1968.
14. "ASEA Industrial Drive Motors, 5 - 1250 HP," Catalog OK55-1, ASEA Inc., 4 New King St., White Plains NY 10602.
15. "Personal communications" with W. Shilling of Westinghouse Electric Corp., Aerospace Electrical Div., Lima OH.

Part I DYNAMIC AND POWER LOSS MODELS

The dynamic and power loss mathematical models are the sets of equations that describe the flywheel energy-storage vehicle's drive system in both its traveling and wayside charging modes of operation. For convenience, the equations are divided into sections corresponding to the components or functions which they describe. A pictorial diagram of the major system components is shown in Fig. 3. The input constants for the baseline drive system are given in Appendix B. The parameters for the equations are listed in Appendix C. The prime objective of the calculations using the dynamic models is to determine the flywheel power at each instant of time as the vehicle travels on its route. Hence, the calculations start from the tractive force and power required by the vehicle drive wheels, and are carried back through the dynamic models of the propulsion-system components to the flywheel. The equations are presented in this same order of calculation.

A. Propulsion Requirements

The input variables from the mission profile are:

Vehicle velocity	$V(t)$	ft/s
Roadway grade	$G(t)$	rad
Wind velocity	$V_w(t)$	mi/h

The tractive force components are:

Eq.

$$\text{Inertia force} \quad F_i = \frac{W}{g} \left(\frac{\Delta V}{\Delta t} \right) \text{MF} \quad \text{lb.} \quad 1$$

$$\text{Grade force} \quad F_g = W G \quad \text{lb.} \quad 2$$

$$\text{Tire friction force} \quad F_t = \mu W (1 + C_c V) \quad \text{lb.} \quad 3$$

Aerodynamic drag force

$$F_w = \frac{1}{2} \rho (V + V_w)^2 \text{SGN}(V + V_w) C_d A \quad \text{lb.} \quad 4$$

The total tractive force and traction power at the drive-wheels are:

$$\text{Total tractive force} \quad F = F_i + F_g + F_t + F_w \quad \text{lb.} \quad 5$$

$$\text{Total traction power} \quad P_2 = 1.36 \times 10^{-3} F \cdot V \quad \text{kW} \quad 6$$

If F and P_2 are negative, the dc traction motor must shift into the regenerative braking mode.

B. Gearbox (Transmission)

The vehicle speed and tractive force, when the dc traction motor is operating at its base speed of 2730 r/min and 70.17 hp, are given by:

Eq.

$$\text{Vehicle speed} \quad V_b = \frac{2\pi N_b R}{60 \gamma} = 47.18 \quad \text{ft/s} \quad 1$$

$$\text{Tractive force} \quad F_b = \frac{5252 (\text{hp}_b)}{N_b} \frac{\gamma \eta_{gb}}{R} = 751 \quad \text{lb} \quad 2$$

The gearbox losses for an assumed efficiency η_{gb} are:

$$\text{Motoring} \quad P_4 = \left(\frac{1}{\eta_{gb}} - 1 \right) P_2 \quad \text{kW} \quad 3$$

$$\text{Braking} \quad P_4 = \left(1 - \eta_{gb} \right) \left| P_2 \right| \quad \text{kW} \quad 4$$

C. DC Traction Motor

The normalized vehicle speed and tractive force are,

$$\text{Vehicle speed, normalized} \quad V_o = \frac{V}{\sigma V_b} \quad \text{pu} \quad 1$$

$$\text{Tractive force, normalized} \quad 2$$

$$(\text{motoring}) \quad F_o = \frac{F}{F_b} \quad \text{pu}$$

$$(\text{braking}) \quad F_o = \frac{F}{F_b} \eta_{gb}^2 \quad \text{pu} .$$

The equations for the armature current needed to develop the required tractive force must take into account the series field, saturation, and field weakening control above the base speed of the dc traction motor.

Ampere turns, ratio of series-to-total, at dc traction motor base conditions for λ series-to-shunt field turns and σ field weakening.

$$C_l = \frac{\lambda \sigma I_{ab}}{I_{f_{dc_b}} + \lambda \sigma I_{ab}} \quad \text{pu} . \quad 3$$

Armature current parameter

$$SQ = \frac{1}{2} \left[- \left(\frac{1 - C_l}{C_l} \right) + B_{dc} |F_o| \right] \quad \text{pu} . \quad 4$$

Armature current normalized

$$I_o = SQ + \sqrt{SQ^2 + \frac{F_o}{C_l} \left[A_{dc} + B_{dc} (1 - C_l) \right]} \quad \text{pu} . \quad 5$$

When the dc traction motor runs over its base speed σV_b and $\sigma < 1$, the shunt field is assumed to be weakened. The normalized armature and shunt field currents are:

Armature current, normalized

$$I_o = \frac{E_{bb}}{V_{dc_b}} \frac{V_o}{\sigma} F_o \quad \text{pu} \quad \text{Eq. 6}$$

$$I_{f_r} = \frac{1}{1 - C_l} \left[\frac{\frac{A_{dc}}{\frac{E_{bb}}{V_{dc_b}} \frac{V_o}{\sigma}} - B_{dc}}{-C_l I_o} \right] \quad \text{pu.}$$

The normalized ampere turns for shunt and series fields are given by:

$$\text{Full field} \quad I_{f_{dc}} = (1 - C_l) + C_l I_o \quad \text{pu} \quad 7$$

$$\text{Field weakened} \quad I_{f_{dc}} = (1 - C_l) I_{f_r} + C_l I_o \quad \text{pu.}$$

The shunt and series fields of the dc traction motor are reversed when the motor transfers from the motoring to the braking mode. The voltage equations are the following:

$$\begin{aligned} \text{Discriminant} \quad \text{SGN } F &= +1 \text{ FOR } F \geq 0 \quad (\text{motoring}) \\ \text{SGN } F &= -1 \text{ FOR } F < 0 \quad (\text{braking}) \end{aligned} \quad 8$$

Flux-conductor product

$$\Phi_{dc} = \frac{SGN F}{\sigma} \left[\frac{|I_{f_{dc}}|}{A_{dc} + B_{dc} |I_{f_{dc}}|} \right] \text{ pu} . \quad \text{Eq. 9}$$

$$\text{Back emf base} \quad E_{bb} = V_{dc_b} (1 - \Psi) - 2.0 \quad V , \quad 10$$

Back emf normalized

$$E_4 = \left(\frac{E_{bb}}{V_{dc_b}} \right) V_0 \Phi_{dc} \quad \text{pu} . \quad 11$$

Terminal voltage normalized

$$E_o = \frac{V_{dc}}{V_{dc_b}} = E_4 + \Psi I_o + \frac{2}{V_{dc_b}} \quad \text{pu} . \quad 12$$

When the base speed at which field weakening is used is reduced to σV_b and a smaller traction motor is used, the motor parameters change to:

Armature resistance

$$R_{a_{dc}}^l = \frac{R_{a_{dc}}}{\sigma} . \quad 13$$

Armature current, base

$$I_{a_b}^l = \sigma I_{a_b} , \quad 14$$

The five loss components and the efficiency for the dc traction motor are given in the following equations:

Armature copper loss, 120°C

Eq.

$$D_1 = 1.39 \times 10^{-3} (I_{a_b}^1 I_o)^2 R_{a_{dc}}^1 \text{ kW} \quad 15$$

Shunt field loss $D_2 = 10^{-3} I_{f_{dc}} V_{f_{dc}} \text{ kW} \quad 16$

Friction, windage and core loss

$$D_3 = D_{3_b} V_o^{2.5} \text{ kW} \quad 17$$

Stray load loss $D_4 = \frac{0.01}{\eta_{gb}} \cdot P_2 \text{ (motoring)} \text{ kW} \quad 18$

$$D_4 = 0.01 \cdot \eta_{gb} \cdot |P_2| \text{ (braking)} \text{ kW} \quad 18$$

Brush loss $D_5 = 10^{-3} \cdot 2 (I_{a_b}^1 I_o) \text{ kW} \quad 19$

Total loss $P_5 = D_1 + D_2 + D_3 + D_4 + D_5 \text{ kW} \quad 20$

DC traction motor efficiency

$$\eta_{dc} = \frac{1}{1 + \frac{P_5 \eta_{gb}}{P_2}} \text{ (motoring)} \text{ pu} \quad 21$$

$$\eta_{dc} = \frac{1}{1 + \frac{P_5}{\eta_{gb} |P_2|}} \text{ (braking)}$$

D. Solid-State Controller

The controller losses and efficiency are:

$$\text{Snubber loss} \quad R_1 = 10^{-5} \left(V_{dc_b} \mid E_o \right) \left(I_{a_b}^1 \mid I_o^1 \right) \text{ kW} . \quad \text{Eq. 1}$$

$$\text{Thyristor loss} \quad R_2 = \sigma R_{2_b} I_o \text{ kW} . \quad 2$$

Total controller loss

$$P_6 = R_1 + R_2 \text{ kW} . \quad 3$$

Controller efficiency

$$\eta_{p_{dr}} = \frac{1}{1 + \frac{P_6}{100 R_1}} \quad (\text{motoring}) \quad \text{pu} \quad 4$$

$$\eta_{p_{dr}} = 1 - \frac{P_6}{100 R_1} \quad (\text{braking}) \quad \text{pu} .$$

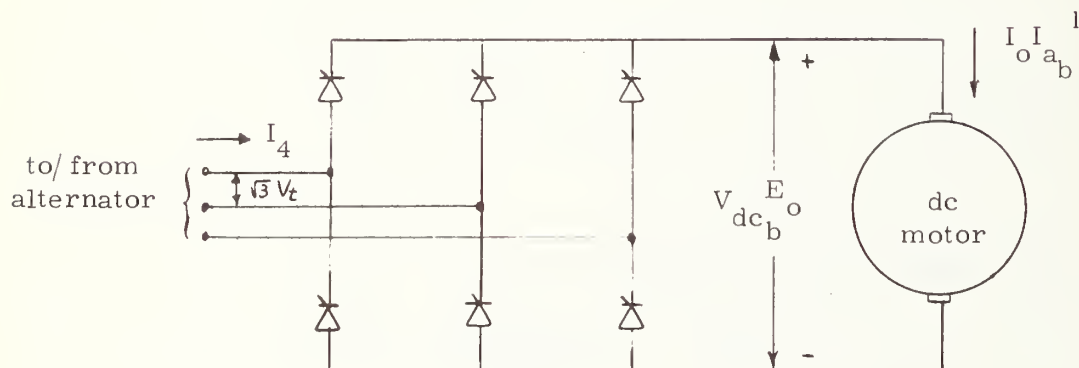


Fig. A-1 Circuit Diagram for Solid-State Controller

E. Alternator

The alternator power, reactive power, and kVA are given in the following sequence of equations:

Power to controller

Eq.

$$P_{pdr} = P_2 + P_4 + P_5 + P_6 - D_2 \quad \text{kW} \quad 1$$

Alternator power output

$$POW = P_{pdr} + P_1 \quad \text{kW} \quad 2$$

Reactive power to controller. (fundamental component)

$$Q_{pdr} = \sqrt{\left[\frac{3}{10^3} \left(\frac{\sqrt{6}}{\pi} \right) V_t I_{ab}^1 I_o \right]^2 - P_{pdr}^2} \quad \text{rkVa} \quad 3$$

Auxiliary load reactive power

$$Q_1 = P_1 \tan \theta_1 \quad \text{rkVa} \quad 4$$

Alternator reactive (fundamental component) power output

$$Q = Q_{pdr} + Q_1 \quad \text{rkVa} \quad 5$$

Alternator kVA output, (fundamental component)

$$S_1 = \sqrt{POW^2 + Q^2} \quad \text{kVA} \quad \text{Eq. 6}$$

Alternator power factor

$$\cos \theta = \frac{POW}{S_1} \quad \text{pu} \quad 7$$

Alternator (harmonic components) reactive power output

$$Q_h = 3 \times 10^{-3} (0.242) V_t I_{a_b}^1 I_o \quad \text{rkVa} \quad 8$$

Alternator total kVA output,

$$S = \sqrt{S_1^2 + Q_h^2} \quad \text{kVA} \quad 9$$

The alternator base and normalized voltage and current in terms of the rewind factor RWF are given in the following equations:

Alternator base voltage (1-n)

$$V_{t_b} = V_{t_{b_o}} (\text{RWF}) \quad \text{V} \quad 10$$

Alternator base armature current

$$I_{4_b} = \frac{10^3 S_b}{3 V_{t_b}} \quad \text{A} \quad 11$$

Alternator normalized armature current

Eq.

$$I_4 = \frac{10^3 S}{3 V_t I_{4b}} \quad \text{pu} \quad 12$$

Alternator normalized fundamental current

$$I_{4f} = \left(\frac{S_1}{S} \right) I_4 \quad \text{pu} \quad 13$$

The following equations describe the phasor diagram model, such as shown in Fig. . The equations are used to calculate the excitation voltage E_5 , taking into account saturation.

Alternator power angle

$$\tan \delta = \frac{I_{4f} \left[X_q \omega_o \cos \theta - R_{a_{ac}} \sin \theta \right]}{\frac{V_t}{V_{t_b}} + I_{4f} \left[X_q \omega_o \sin \theta + R_{a_{ac}} \cos \theta \right]} \quad \text{pu} \quad 14$$

Alternator air-gap voltage

$$E_r = \sqrt{\left(\frac{V_t}{V_{t_b}} + I_{4f} \left[X_a \omega_o \sin \theta + R_{a_{ac}} \cos \theta \right] \right)^2 + \left(I_{4f} \left[X_a \omega_o \cos \theta - R_{a_{ac}} \sin \theta \right] \right)^2} \quad \text{pu} \quad 15$$

Field current for E_r

$$I_{f_{ac_r}} = \frac{A_{ac} E_r}{\omega_o - B_{ac} E_r} \quad \text{pu} \quad \text{Eq. 16}$$

Slope of air-gap line at ω_o

$$K_{ag_r} = \omega_o K_{ag} \quad \text{pu} \quad 17$$

Slope of Kingsley air-gap line (cannot exceed K_{ag_r})

$$\text{slope } B = \frac{E_r}{I_{f_{ac_r}}} \quad \text{pu} \quad 18$$

$$\text{Ratio of slopes } K_{fact} = \frac{K_{ag_r}}{\text{slope } B} \quad \text{pu} \quad 19$$

Kingsley saturated synchronous reactance

$$X_{d_{sat}} = X_a + \frac{X_d - X_a}{K_{fact}} \quad \text{pu} \quad 20$$

Excitation voltage

$$E_5 = \frac{V_t}{V_{t_b}} \cos \delta + I_{4_f} \left[R_{a_{ac}} \cos (\delta + \theta) + X_{d_{sat}} \omega_o \sin (\delta + \theta) \right] \quad \text{pu} \quad 21$$

Alternator field current

$$I_5 = \frac{E_5}{\text{slope } B} \quad \text{pu} \quad 22$$

$$I_5 = I_5 (\text{pu}) \cdot I_{5_b} \quad \text{A}$$

The firing angle of the controller thyristors needed to provide the required dc traction motor armature voltage is given in the following equations:

Commutation voltage drop Eq.

$$E_x = \frac{3}{\pi} I_{a_b} I_o X_d'' Z_b \omega_o \quad V \quad 23$$

Controller firing angle

$$\cos \alpha = \frac{V_{dc_b} \frac{E_o + E_x + 3.0}{2.34 V_t}}{\quad} \quad \text{pu} \quad 24$$

The loss components and efficiency of the alternator are given in the following equations:

Armature copper loss

$$A_1 = A_{1_b} I_4^2 \quad \text{kW} \quad 25$$

Exciter and field loss

$$A_2 = A_{2_{b_0}} + A_{2_{b_1}} I_5^2 \quad \text{kW} \quad 26$$

Core loss

$$A_3 = A_{3_b} \left(\frac{E_r}{E_{r_o}} \right)^2 \quad \text{kW} \quad 27$$

Friction and windage loss

Eq.

$$A_4 = A_{4_b} \cdot \omega_o^3 \quad \text{kW} \quad 28$$

Stray load loss

$$A_5 = A_{5_{b0}} + A_{5_{b1}} \left(\frac{I_4}{RWF} \right)^2 \quad \text{kW} \quad 29$$

Total alternator loss

$$P_7 = A_1 + A_2 + A_3 + A_4 + A_5 \quad \text{kW} \quad 30$$

Alternator efficiency

$$\eta_{ac} = \frac{1}{1 + \frac{P_7}{POW}} \quad (\text{traveling}) \quad \text{pu} \quad 31$$

$$\eta_{ac} = 1 - \frac{P_7}{|POW|} \quad (\text{charging}) \quad \text{pu}$$

F. Flywheel

In the traveling mode, the flywheel supplies the net power for propulsion, losses, and auxiliary load. The equations for calculating the flywheel acceleration and angular speed are as follows:

Total drive system loss Eq.

$$P_3 = P_4 + P_5 + P_6 + P_7 \quad \text{kW} \quad 1$$

Total flywheel power

$$P = P_1 + P_2 + P_3 - P_{in} \quad \text{kW} \quad 2$$

Flywheel integration constant

$$K_1 = \frac{550}{0.746 I_b \omega_{f \max_b}^2} = 1.5562 \times 10^{-5} \text{ kW}^{-1} \text{ s}^{-1} \quad 3$$

for $\begin{cases} I_b = 30 \text{ lb-ft-s}^2 \\ \omega_{f \max_b} = 400\pi \text{ rad/s} \end{cases}$

Flywheel inertia coefficient

$$K_2 = \frac{I_b}{I} \quad \text{pu} \quad 4$$

Flywheel maximum speed coefficient

$$K_3 = \left(\frac{\omega_{f \max_b}}{\omega_{f \max}} \right)^2 \quad \text{pu} \quad 5$$

Flywheel acceleration

Eq.

$$\dot{\omega}_f = -K_1 K_2 K_3 \omega_{f_{\max}} \left(\frac{P}{\omega_o} \right) \quad \text{rad/s}^2 \quad 6$$

Flywheel angular speed

$$\omega_o = \omega_{oi} + \sum \left(\frac{\dot{\omega}_f}{\omega_{f_{\max}}} \right) \Delta t = \left(\frac{\omega_f}{\omega_{f_{\max}}} \right) \text{ pu} \quad 7$$

Part II THERMAL MODELS

The thermal models are the equations that provide the component temperature rises in terms of the component losses calculated from the power loss models of Part I.

G. DC Traction Motor

Loss power to rotor

Eq.

$$P_{r_{dc}} = R_{d_1} D_1 + R_{d_2} D_2 + R_{d_3} D_3 + R_{d_4} D_4 + R_{d_5} D_5 \quad \text{kW} \quad 1$$

Loss power to stator

$$P_{s_{dc}} = S_{d_1} D_1 + S_{d_2} D_2 + S_{d_3} D_3 + S_{d_4} D_4 + S_{d_5} D_5 \quad \text{kW} \quad 2$$

Constraint

$$R_{d_i} + S_{d_i} = 1.0 \text{ for } i = 1, 2, \dots, 5 \quad 3$$

Rate of rotor temperature rise

$$T_{r_{dc}} = \frac{T_{g_{dc}} - T_{r_{dc}} + P_{r_{dc}} R_{r_{dc}}}{\tau_{r_{dc}}} \quad ^\circ\text{C/s} \quad 4$$

Rate of stator temperature rise

$$T_{s_{dc}} = \frac{T_{g_{dc}} - T_{s_{dc}} + P_{s_{dc}} R_{s_{dc}}}{\tau_{s_{dc}}} \quad \text{Eq. } 5 \quad ^\circ\text{C/s}$$

Air-gap temperature rise

$$T_{g_{dc}} = \frac{R_{g_{dc}} R_{s_{dc}} T_{r_{dc}} + R_{g_{dc}} R_{r_{dc}} T_{s_{dc}}}{R_{r_{dc}} R_{s_{dc}} + R_{r_{ac}} R_{g_{dc}} + R_{s_{dc}} R_{g_{dc}}} \quad ^\circ\text{C} \quad 6$$

Loss power to air gap

$$P_{dc_{out}} = \frac{T_{g_{dc}}}{R_{g_{dc}}} \quad \text{kW} \quad 7$$

Rotor time constant

$$\tau_{r_{dc}} = R_{r_{dc}} C_{r_{dc}} \quad \text{s} \quad 8$$

Stator time constant

$$\tau_{s_{dc}} = R_{s_{dc}} C_{s_{dc}} \quad \text{s} \quad 9$$

H. Alternator

Loss power to rotor

Eq.

$$P_{r_{ac}} = R_{a_1} A_1 + R_{a_2} A_2 + R_{a_3} A_3 + R_{a_4} A_4 + R_{a_5} A_5$$

kW . 1

Loss power to stator

$$P_{s_{ac}} = S_{a_1} A_1 + S_{a_2} A_2 + S_{a_3} A_3 + S_{a_4} A_4 + S_{a_5} A_5$$

kW . 2

Constraint

$$R_{a_i} + S_{a_i} = 1.0 \text{ for } i = 1, 2, \dots, 5$$

3

Rate of rotor temperature rise

$$\dot{T}_{r_{ac}} = \frac{T_{g_{ac}} - T_{r_{ac}} + P_{r_{ac}} R_{r_{ac}}}{\tau_{r_{ac}}} \quad ^\circ\text{C/s} . \quad 4$$

Rate of stator temperature

$$\dot{T}_{s_{ac}} = \frac{T_{g_{ac}} - T_{s_{ac}} + P_{s_{ac}} R_{s_{ac}}}{\tau_{s_{ac}}} \quad ^\circ\text{C/s} . \quad 5$$

Air-gap temperature rise

$$T_{g_{ac}} = \frac{R_{g_{ac}} R_{s_{ac}} T_{r_{ac}} + R_{g_{ac}} R_{r_{ac}} T_{s_{ac}}}{R_{r_{ac}} R_{s_{ac}} + R_{r_{ac}} R_{g_{ac}} + R_{s_{ac}} R_{g_{ac}}} \quad ^\circ\text{C} \quad \text{Eq. 6}$$

Loss power to air gap

$$P_{ac_{out}} = \frac{T_{g_{ac}}}{R_{g_{ac}}} \quad \text{kW} \quad 7$$

Rotor time constant

$$\tau_{r_{ac}} = R_{r_{ac}} C_{r_{ac}} \quad \text{s} \quad 8$$

Stator time constant

$$\tau_{s_{ac}} = R_{s_{ac}} C_{s_{ac}} \quad \text{s} \quad 9$$

I. Solid-State Controller

Rate of heat sink temperature rise

Eq.

$$T_6 = \frac{P_6 R_6 - T_6}{\tau_6} \quad ^\circ\text{C/s} \quad 1$$

Loss power to ambient air

$$P_{6\text{out}} = \frac{T_6}{R_6} \quad \text{kW} \quad 2$$

Heat sink time constant

$$\tau_6 = R_6 C_6 \quad \text{s} \quad 3$$

Thyristor junction temperature rise

$$T_{6t} = T_6 + P_6 R_{6t} \quad ^\circ\text{C} \quad 4$$

Part III WAYSIDE CHARGING MODE

The auxiliary power (P_1) is set to zero. The tractive power (P_2) and wind force (V_w) are also zero. The vehicle transmission losses (P_4), dc traction motor losses (P_5), and controller losses (P_6) are all zero. The equations representing the inputs to the alternator (operating as a synchronous motor) as it accelerates the flywheel from initial speed to full speed are:

Terminal voltage

$$V_t = V_{t_{c_{max}}} \cdot \omega_o \quad \text{Eq. 1}$$

Power input

$$P_{in_w} = K_{p_{in}} \cdot P_{in_{max}} \cdot \omega_o \quad \text{kW} \quad 2$$

kVA input

$$S = \frac{P_{in_w}}{|\cos \theta|} \quad \text{kVA} \quad 3$$

Armature current

$$I_4 = \frac{10^3 S}{3 V_t I_{4_b}} \quad \text{pu} \quad 4$$

The other alternator parameters and the alternator losses in the charging mode are computed by using the same equations as those used in the traveling mode, with two exceptions:

$$I_{4_f} = I_4 \quad (\text{No harmonics in wayside power})$$

$$\eta_{ac} = \frac{(P_{in_w} - P_7)}{P_{in_w}} \quad (\text{Alternator efficiency during charging})$$

where P_7 is the total alternator (motor) loss in the charging mode.

Flywheel acceleration and angular velocity are found from,

$$\begin{array}{l} \text{Acceleration} \\ \ddot{\omega}_f = -K_1 K_2 K_3 \left(\frac{P_7 - P_{in_w}}{\omega_0} \right), \omega_{f_{\max}} \end{array} \quad \begin{array}{l} \text{Eq.} \\ \text{rad/s}^2 \quad 5 \end{array}$$

Angular velocity,

$$\omega_0 = \omega_{0_i} + \sum_{\Delta t=1}^n \left(\frac{\dot{\omega}_f}{\omega_{f_{\max}}} \right) \Delta t \quad \text{rad/s} \quad 6$$

Part I CONSTANTS FOR A COMPUTER SIMULATION RUN

<u>Symbol</u> (Program)	<u>Symbol</u> (Equations)	<u>Definition</u>	<u>Nom.</u> <u>Value</u>	<u>Units</u>
WT, VMASS	W	Weight of vehicle with load	12,238	lb
VAREA	A	Projected area of vehicle	53.	ft ²
A A	μ	Rolling coefficient of friction	0.0230	--
B B	C_c	Coulomb coefficient of friction	0.000175	h/ mi
C C	C_d	Aerodynamic drag coefficient	0.610	--
WIND	V_w	Wind velocity	30.	mi/ h
I	I	Flywheel moment of inertia	45.	slug-ft
ALIM	\dot{V}_{\max}	Acceleration limit (abs.)	1.0	mi/ h/ s
F B	F_b	Base value, tractive force	751	lb
V B	V_b	Base value, vehicle velocity	47.18	ft/ s
IAB	I_{a_b}	Base value, dc motor armature current	140.	A
$W\phi$	ω_o	Speed of energy storage unit (initial)	0.5	pu
NGB	η_{gb}	Efficiency of gearbox	0.92	--
VDCB	V_{dc_b}	Base value of dc motor terminal voltage	420.	V
VTRUN	$V_{t_{\text{run}}}$	Const. terminal voltage (l-n) of alt.-traveling	215.	V
K1	$10^5 K_1$	Integration constant	1.55626	kW ⁻¹ s ⁻¹
RGDC	$R_{g_{dc}}$	DC motor thermal res., gap to ambient	2.97	°C/ kW
RADC	$R_{a_{dc}}$	DC motor arm. circuit res. at 20°C	0.150	ohms
D3B	D_{3_b}	DC motor, friction, windage, & core losses at base conditions	1.556	kW

(continued)

<u>Symbol</u> (Program)	<u>Symbol</u> (Equations)	<u>Definition</u>	<u>Nom.</u> <u>Value</u>	<u>Units</u>
AAC	A_{ac}	AC machine, saturation curve, Frolich coefficient	0.3584	pu
BAC	B_{ac}	AC machine, saturation curve, Frolich coefficient	0.6417	pu
ADC	A_{dc}	DC motor, saturation curve, Frolich coefficient	0.50	pu
BDC	B_{dc}	DC motor, saturation curve, Frolich coefficient	0.50	pu
PSI	Ψ	IR drop/ dc motor base term. voltage	0.05	pu
R2B	R_{2b}	SCR loss coefficient, controller	0.412	kW
A1B	A_{1b}	AC machine, armature Cu loss at base cond	3.938	kW
A2B ϕ	A_{2bo}	AC machine, exciter and field Cu loss, const	0.28	kW
A2B1	A_{2b1}	AC machine, and field Cu loss, coefficient	0.2394	kW
A3B	A_{3b}	AC machine, core loss, coefficient	1.601	kW
A4B	A_{4b}	AC machine, friction & windage loss at maximum speed	2.045	kW
A5B ϕ	A_{5bo}	AC machine, stray load loss, constant	0.207	kW
A5B1	A_{5b1}	AC machine, stray load loss, coefficient	1.671	kW
P1	P_1	Real power to auxiliary load	6.0	kW
T81	θ_1	Power factor angle, auxiliary load	0.64350	rad.

(continued)

<u>Symbol</u> (Program)	<u>Symbol</u> (Equations)	<u>Definition</u>	<u>Nom.</u> Value	<u>Units</u>
XQ	X_q	AC machine, q-axis synchronous reactance	1.24	pu
RAAC	$R_{a_{ac}}$	AC machine, armature resistance	0.0495	pu
X2 ϕ	X_d	AC machine, armature reactance	0.145	pu
XD	X_d	AC machine, d-axis unsaturated synchronous reactance	3.40	pu
WFMAX	$\omega_{f_{max}}$	Maximum speed, flywheel & alternator	12,000.	r/min
LAMBDA	λ	Series/shunt field turns	0.04034	--
RRDC	$R_{r_{dc}}$	DC motor, thermal resistance, rotor-to-gap	8.17	°C/kW
RSDC	$R_{s_{dc}}$	DC motor, thermal resistance, stator - to-gap	21.6	°C/kW
RCRDC	$\tau_{r_{dc}}$	DC motor, rotor thermal time constant	512.	s
RCSDC	$\tau_{s_{dc}}$	DC motor, stator thermal time constant	1127.	s
RD1	R_{d_1}	Thermal weighting coefficient, $-D_1$, loss to dc motor rotor	0.95	--
RD2	R_{d_2}	Thermal weighting coefficient, $-D_2$, loss to dc motor rotor	0.	--
RD3	R_{d_3}	Thermal weighting coefficient, D_3 , loss to dc motor rotor	0.6	--
RD4	R_{d_4}	Thermal weighting coefficient, D_4 , loss to dc motor rotor	0.8	--

(continued)

<u>Symbol</u>	<u>Symbol</u>		<u>Nom.</u>	
<u>(Program)</u>	<u>(Equations)</u>	<u>Definition</u>	<u>Value</u>	<u>Units</u>
RD5	R_{d_5}	Thermal weighting coefficient, D_5 , loss to dc motor rotor	1.0	--
SD1	S_{d_1}	Thermal weighting coefficient, D_1 , loss to dc motor stator	0.05	--
SD2	S_{d_2}	Thermal weighting coefficient - D_2 , loss to dc motor stator	1.0	--
SD3	S_{d_3}	Thermal weighting coefficient, D_3 loss to dc motor stator	0.4	--
SD4	S_{d_4}	Thermal weighting coefficient, D_4 , loss to dc motor stator	0.2	--
SD5	S_{d_5}	Thermal weighting coefficient, D_5 loss to dc motor stator	0.	--
R6	R_6	Thermal resistance of controller heat sink to ambient	19.6	°C/kW
TAU6	τ_6	Controller heat sink, thermal time const.	18.4	s
SIGMA	σ	Field weakening factor new/old motor base speed	1.0	--
I FDCB	$I_{f_{dc,b}}$	Base value, shunt field current	12.0	A
TB	T_b	Base output torque, dc motor	135.0	lb·ft

(continued)

<u>Symbol</u> (Program)	<u>Symbol</u> (Equations)	<u>Definition</u>	<u>Nom.</u> Value	<u>Units</u>
NB	N_b	Base speed, dc motor	2730	r/ min
HPB	HP_b	Base horsepower, dc motor	70.17	hp
VFDC	$V_{f_{dc}}$	Shunt field voltage, dc motor	24.0	V
RWF	RWF	Rewind factor, ac machine, new/ old term. -volt	3.0	--
ER ϕ	E_{r_o}	Air gap voltage at base condition	1.05	pu
RRAC	$R_{r_{ac}}$	AC machine thermal resistance, rotor- to-gap	18.8	$^{\circ}\text{C}/\text{kW}$
RSAC	$R_{s_{ac}}$	AC machine, thermal resistance, stator- to-gap	7.42	$^{\circ}\text{C}/\text{kW}$
RGAC	$R_{g_{ac}}$	AC machine, thermal resistance, gap-to-amb.	3.03	$^{\circ}\text{C}/\text{kW}$
RCRAC	$\tau_{r_{ac}}$	AC machine, rotor thermal time constant	64.9	s
RCSAC	$\tau_{s_{ac}}$	AC machine, stator thermal time constant	39.5	s
SB	S_b	Base kVA output of alternator	75.8	kVA
VTB ϕ	$V_{t_{bo}}$	AC machine, base term. voltage (l-n) before rewind	115.0	V
KAG	K_{ag}	Slope of air gap line	1.519	pu
XA	X_a	AC machine, armature leakage reactance	0.085	pu

(continued)

<u>Symbol</u>	<u>Symbol</u>		<u>Nom.</u>	
<u>(Program)</u>	<u>(Equations)</u>	<u>Definition</u>	<u>Value</u>	<u>Units</u>
I5B	I_{5b}	AC machine, field current, base condition	14.26	A
RA1	R_{a1}	Thermal weighting coefficient- A_1 loss to ac machine rotor	0.	--
RA2	R_{a2}	Thermal weighting coefficient- A_2 loss to ac machine rotor	1.0	--
RA3	R_{a3}	Thermal weighting coefficient- A_3 loss to ac machine rotor	0.2	
RA4	R_{a4}	Thermal weighting coefficient- A_4 loss to ac machine rotor	0.7	--
RA5	R_{a5}	Thermal weighting coefficient, A_5 loss to ac machine rotor	0.2	--
SA1	S_{a1}	Thermal weighting coefficient, A_1 loss to ac machine stator	1.0	--
SA2	S_{a2}	Thermal weighting coefficient, A_2 loss to ac machine stator	0.	--
SA3	S_{a3}	Thermal weighting coefficient, A_3 loss to ac machine stator	0.8	--
SA4	S_{a4}	Thermal weighting coefficient, A_4 loss to ac stator	0.3	--

(concluded)

<u>Symbol</u>	<u>Symbol</u>		<u>Nom.</u>	
<u>(Program)</u>	<u>(Equations)</u>	<u>Definition</u>	<u>Value</u>	<u>Units</u>
SA5	S_{a_5}	Thermal weighting coefficient, A_5 loss to ac machine stator	0.8	--
KPIN	$K_{P_{in}}$	Input power gain factor, - charging mode	1.0	--
R6T	R_{6_t}	Thermal resistance, controller SCR to heat sink	58.8	°C/ kW
VTCMAX	$V_{t_{c_{max}}}$	AC machine, terminal voltage (max), charging mode	414.0	V
PIN MAX	$P_{in_{max}}$	Maximum input power, ac machine, charging mode	200.0	kW
MF	MF	Mass factor due to rotary inertia	1.08	--
ZB	Z_b	Base impedance of alternator	4.70	Ω

Part II OTHER CONSTANTS

<u>Symbol</u>	<u>Symbol</u>		<u>Nom.</u>	
<u>(Program)</u>	<u>(Equations)</u>	<u>Definition</u>	<u>Value</u>	<u>Units</u>
EBB	E_{bb}	DC motor, back emf at base condition	397.	V
	g	Gravitation constant	32.17	ft/s ²
	I_b	Nominal flywheel moment of inertia	30.	slug-ft ²
	R	Drive wheel radius	1.1833	ft
	γ	Gear ratio (motor speed/ wheel speed)	7.17	--
	ρ	Air density (sea level)	2.378×10^{-3}	slugs/ft ³
	$\omega_{f \max_b}$	Nominal flywheel maximum speed	400π	rad/s
	ω_{o_i}	Initial value of flywheel speed	0.5	pu
MTRIP		Number of round trips for a run	1.5	-

PARAMETERS FOR COMPUTER PROGRAM

<u>Symbol</u> (Program)	<u>Symbol</u> (Equations)	<u>Definition</u>	<u>Units</u>
A1	A_1	AC machine, armature cu loss, 200°C	kW
A2	A_2	AC machine, exciter and field cu loss	kW
A3	A_3	AC machine, core loss	kW
A4	A_4	AC machine, friction and windage loss	kW
A5	A_5	AC machine, stray load loss	kW
C1	C_1	(Series/ total) amp-turns at dc motor base	--
D1	D_1	Armature circuit cu loss at 120°C	kW
D2	D_2	DC motor, shunt field cu loss	kW
D3	D_3	DC motor, friction, windage, and core losses	kW
D4	D_4	DC motor, stray load loss	kW
D5	D_5	DC motor, brush commutation loss	kW
E4	E_4	DC motor, back-emf	pu
E5	E_0	DC motor, terminal voltage	pu
ER	E_r	AC machine, air gap voltage	pu
E5	E_5	AC machine, excitation voltage	pu
EX	E_x	Controller, commutation voltage drop	V
R FORCE	F_i	Vehicle, inertia force	lb
	F_g	Vehicle, gravity (grade) force	lb
	F_t	Vehicle, tire friction force	lb
	F_w	Vehicle, aerodynamic force (incl. wind)	lb
FT	F	Vehicle, required tractive force	lb
$F\phi$	F_0	Tractive force/dc motor base tract. force	pu
GRADE	G	Grade of roadway (profile)	rad
IAB	I_a^1	DC motor, base armature current (with field weak.)	A
I_0	I_0^b	DC motor, armature current	pu

(continued)

<u>Symbol</u> (Program)	<u>Symbol</u> (Equations)	<u>Definition</u>	<u>Units</u>
IFR	I_{f_r}	DC motor, shunt field current with field weak	pu
IFDC	$I_{f_{dc}}$	DC motor, total field current	pu
IFACR	$I_{f_{ac_r}}$	AC machine, field current for air gap voltage (E_r)	pu
I4B	I_{4_b}	AC machine, armature current after rewind	A
I4	I_4	AC machine, armature current (per phase)	pu
I4F	I_{4_f}	Fundamental component of I_4	pu
I5	I_5	AC machine, required field current	pu
KAGR	K_{ag_r}	Slope of air gap line, reduced speed	pu
K2	K_2	Flywheel, moment of inertia coefficient	pu
K3	K_3	Flywheel, maximum speed coefficient	pu
KFACT	K_{fact}	Ratio of slopes of air-gap lines, Kingsley Method	pu
PINW	P_{in_w}	Charging power, ac motor	kW
PRDC	$P_{r_{dc}}$	Loss power, dc motor rotor	kW
PSDC	$P_{s_{dc}}$	Loss power, dc motor stator	kW
PRAC	$P_{r_{ac}}$	Loss power, ac machine rotor	kW
PSAC	$P_{s_{ac}}$	Loss power, ac machine stator	kW
PDC OUT	$P_{dc_{out}}$	DC motor, rate of cooling by forced air	kW
PAC OUT	$P_{ac_{out}}$	AC machine, rate of cooling by forced oil	kW
P	P	Total power from flywheel	kW

(continued)

<u>Symbol</u> (Program)	<u>Symbol</u> (Equations)	<u>Definition</u>	<u>Units</u>
P2	P_2	Propulsion power at wheels	kW
P3	P_3	Total losses of propulsion system	kW
P4	P_4	Transmission losses	kW
P5	P_5	Total dc motor loss	kW
P6	P_6	Total controller loss	kW
P7	P_7	Total ac machine loss	kW
PPDR	P_{pdr}	Power, alternator to controller	kW
POW	POW	Total alternator power	kW
QPDR	Q_{pdr}	Fundamental alternator reactive power	kvar
Q	Q	Total alternator fundamental reactive power	kvar
Q1	Q_1	Reactive power, auxiliary load	kvar
QH	Q_h	Reactive power, alternator - higher freq. comp.	kvar
RADC	$R_{a_{dc}}$	DC motor, armature circuit res. at 20° C w/ field weak Ω	
R1	R_1	Controller, snubber losses	kW
R2	R_2	Controller, SCR losses	kW
S	S	Total kVA output of alternator	kVA
S1	S_1	Fundamental mode of total alternator output	kVA
SQ1	SQ	DC motor, armature current parameter	---
SLOPEB	Slope B	AC machine air gap voltage/corres. field current	pu

(continued)

Symbol (Program)	Symbol (Equations)	Definition	Units
TRDC	T_{rac}	Temperature rise, dc motor rotor	$^{\circ}\text{C}$
TSDC	T_{sdc}	Temperature rise, dc motor stator	$^{\circ}\text{C}$
TGDC	T_{gdc}	Temperature rise, dc motor air gap	$^{\circ}\text{C}$
TRAC	T_{rac}	Temperature rise, ac machine rotor	$^{\circ}\text{C}$
TSAC	T_{sac}	Temperature rise, ac machine stator	$^{\circ}\text{C}$
TGAC	T_{gac}	Temperature rise, ac machine cooling oil	$^{\circ}\text{C}$
T6	T_6	Temperature rise, controller, heat sink (fins)	$^{\circ}\text{C}$
T6T	T_{6t}	Temperature rise, controller, SCR junction	$^{\circ}\text{C}$
TIME	t	Time from start of a run	s
DELTAT	Δt	Computation step size	s
VMPH - VMPHY	ΔV	Change in vehicle velocity over Δt	mi/h
V	V	Vehicle velocity (from profile)	ft/s
V_{ϕ}	V_o	Vehicle velocity/ vehicle vel. at dc motor base speed pu	
H WIND	V_w	Wind speed (headwind is positive)	mi/h
	V_{dc}	Terminal voltage, dc motor	V
VT	V_t	Terminal voltage, ac machine ($l-n$)	V
VTB	V_{tb}	Base ac machine term. voltage ($l-n$) after rewind	V
XDSAT	X_{dsat}	Direct axis saturated synchronous reactance	pu

(concluded)

Symbol (<u>Program</u>)	Symbol (<u>Equations</u>)	<u>Definition</u>	<u>Units</u>
A	α	Firing angle for controller	deg
D	δ	Power angle for ac machine	deg
NGB	η_{gb}	Gearbox efficiency	deg
NDC	η_{dc}	DC motor efficiency	
NPD	η_{pdr}	Controller efficiency	
NAC	η_{ac}	AC machine efficiency	
PHIDC	Φ_{dc}	Total dc flux - conductor product	pu
T8	θ	AC machine power factor angle	deg
$W\phi$	ω_o	Flywheel and alternator speed/maximum speed	pu

APPENDIX D. TABULAR OUTPUTS FOR SAMPLE RUN (ONE-ROUND TRIP)
Part I DYNAMICS AND POWER LOSS OUTPUTS (FOR Ø3.DAT)

FFFFFFFFFFF	000000000	RRRRRRRRR	000000000	333333333
FFFFFFFFFFF	000000000	RRRRRRRRR	000000000	333333333
FFFFFFFFFFF	000000000	RRRRRRRRR	000000000	333333333
FFF	000	RRR	000	333
FFF	000	RRR	000	333
FFF	000	RRR	000	333
FFF	000	RRR	000000	333
FFF	000	RRR	000	333
FFF	000	RRR	000000	333
FFF	000	RRR	000	333
FFFFFFFFF	000	RRRRRRRRR	000	333
FFFFFFFFF	000	RRRRRRRRR	000	333
FFFFFFFFF	000	RRRRRRRRR	000	333
FFF	000	RRR	000000	333
FFF	000	RRR	000000	333
FFF	000	RRR	000000	333
FFF	000	RRR	000	333
FFF	000	RRR	000	333
FFF	000	RRR	000	333
FFF	000000000	RRR	000000000	333333333
FFF	000000000	RRR	000000000	333333333
FFF	000000000	RRR	000000000	333333333

```

LPT3PL Version 6(344)      Running on LPT000
*START* user CLARE [4177,117] Job FOR03 Seq. 779 Date 28-Jun-76 18:54:49 Monitor TSC DECSYSTEM-10 602-1 *START*
Request created: 28-Jun-76 18:50:54
File: DSR00:FOR03[4177,117] Created: 28-Jun-76 18:32:00 Printed: 28-Jun-76 18:55:13
QUEUE Switches: /FILE:ASCII /COPIES:2 /SPACING:1 /LWI:614 /FORMS: STD.
File will be deleted after printing

```

VEHICLE :

HOEING 21 PASSENGER BUS
 EQUIV. WT. = 13222. LBS
 TIRE RADIUS = 14.2 INCHES
 GEAR RATIO = 7.17
 GEARBOX EFF. = .9200
 TIRE FRICTION : ROLLING COEFF. = 0.023000 LBF/LBM
 COULOMB COEFF. = 0.000175 LBF/LAM/MPH
 AERO. DRAG : FRONTAL AREA = 53.00 SQ.-FT.
 DRAG COEFF. = 0.61
 WIND VELOCITY : 30.0 MPH (RETARDING)-OUTBOUND LEG
 -30.0 MPH (AIDING) -RETURN LEG

PROFILE :

MORGANTOWN ROADWAY
 OUTBOUND DISTANCE : WALNUT TO ENGINEERING = 2.065 MI.
 RETURN DISTANCE : ENGINEERING TO WALNUT = 2.065 MI.
 VELOCITY PROFILE : SHOWN ON PLOT , MAX. SPEED = 30.0 MPH
 MINIMUM WAIT TIME AT EACH STOP = 30. SEC.
 (LONGER WAIT TIME ALLOWED TO RECHARGE FLYWHEEL)

FLYWHEEL :

INITIAL SPEED = 6000. RPM
 MOMENT OF INERTIA = 45.0 SLUG-FT.-SQ.
 INITIAL KINETIC ENERGY = 3.347 KW.-HR.

D.C. MOTOR/GEN. :

NEMA FRAME SIZE 324A, MGF. BY ASEA, WT. = 550. LBM
 COMPOUND-WOUND, 4 POLES, FORCED-AIR COOLED
 FIELD WEAKENING CONFIGURATION IS NOT USED - CONST. SHUNT FIELD
 BASE TORQUE = 135.00 LBF-FT
 BASE SPEED = 2730. RPM
 BASE H.P. = 70.17 H.P.
 RATED ARMATURE VOLTAGE = 420. VOLTS
 RATED ARMATURE CURRENT = 140. AMPS
 ARMATURE RESISTANCE (20 DEG C) = 0.05 PU = 0.150000 OHMS
 SHUNT FIELD VOLTAGE = 24.0 VOLTS
 SHUNT FIELD CURRENT = 12.0 AMPS
 RATIO OF (SERIES/SHUNT) TURNS FOR FIELD = 0.040340
 RATIO OF (SERIES/TOTAL) AMP-TURNS AT BASE COND. = 0.32
 SAT. CURVE PROEGLICH EQ. COEFF. : ADC = 0.500 PU
 BDC = 0.500 PU

LOSS COMPONENTS AT BASE CONDITION (NO FIELD WEAKENING)

ARM. & SERIES FLD. CU LOSS = 0.0782 PU = 4.095 KW
 SHUNT FIELD CU LOSS = 0.0055 PU = 0.288 KW
 FRICT., WINDAGE, & CORE LOSS = 0.0297 PU = 1.556 KW
 STRAY LOAD LOSS = 0.0100 PU = 0.522 KW
 BRUSH COMMUTATION LOSS = 0.0053 PU = 0.280 KW

TOTAL DC LOSS

= 0.1287 PU = 6.741 KW

EFFICIENCY AT BASE CONDITION

= 0.8860

(continued)

(continued)

PDR : 3-PHASE CONTROLLED BRIDGE
 SNUBBER LOSSES = 1.4% OF OUTPUT
 RATED AT 140. AMPS D.C.
 EFFICIENCY AT BASE CONDITIONS = 0.9830

A.C. MOTOR/GEN. : BRUSHLESS-AIRCRAFT TYPE, MGF. BY WESTINGHOUSE, WT. = 42. LBM
 SYNCHRONOUS, 3-PHASE, 4 POLES, OIL COOLED
 POWER RATING = 75.8 KVA
 BASE SPEED = 12000. RPM, MIN. SPEED = 6000. RPM
 REWIND FACTOR = 3.00
 BASE TERMINAL VOLTAGE = 345. VOLTS (LINE-NEUTRAL)
 OUTPUT-TERMINAL VOLTAGE-CONST. AT 215. V (LINE-NEUTRAL)
 BASE CURRENT = 73.2 AMPS/PHASE
 BASE FIELD CURRENT = 14.26 AMPS
 AIR GAP VOLTAGE BEFORE REWIND = 1.05 PU

ARMATURE CONSTANTS (PER PHASE) :
 RESISTANCE (200 DEG. C.) = 0.0495 PU = 0.2412 OHMS
 DIRECT AXIS (UNSAT.) REACT = 3.4000 PU = 16.560 OHMS
 QUADRAURE AXIS REACT. = 1.2400 PU = 6.0300 OHMS
 ARM. LEAKAGE FLUX REACT. = 0.0850 PU = 0.4140 OHMS
 SUBTRANSIENT REACT. = 0.1450 PU = 1.2170 OHMS

SAT. CURVE FROELICH-EO. COEFF. : AAC = 0.3584 PU
 BAC = 0.6417 PU
 SLOPE OF AIR GAP LINE : KAG = 1.5190 PU

LOSS COMPONENTS AT BASE CONDITION (NO FIELD WEAKENING)
 ARM. CU LOSS = 0.0520 PU = 3.938 KW
 EXCITER AND FLD. CU LOSS = 0.0215 PU = 1.633 KW
 CORE LOSS = 0.0211 PU = 1.601 KW
 FRICT. & WINDAGE LOSS = 0.0270 PU = 2.045 KW
 STRAY LOAD LOSS = 0.0052 PU = 0.393 KW
 TOTAL AC LOSS = 0.1268 PU = 9.610 KW

EFFICIENCY AT BASE CONDITION = 0.8875

WAYSIDE RECHARGE : TERMINAL VOLTAGE PROPORTIONAL TO FLYWHEEL/MOTOR SPEED
 INPUT POWER PROPORTIONAL TO FLYWHEEL/MOTOR SPEED
 AT FULL SPEED, TERMINAL VOLTAGE IS 20% OVER RATED VALUE (414 VOLTS)
 AT FULL SPEED, INPUT POWER = 2.61 TIMES RATED (OUTPUT) POWER FOR KPIN = 1.0
 ARMATURE CURRENT HELD CONSTANT DURING RECHARGE
 POWER FACTOR HELD CONSTANT DURING RECHARGE
 AUX. LOAD SUPPLIED FROM WAYSIDE POWER DURING RECHARGE

CHARGING MODE DATA : (Station A, Initial)

TIME	W0	WFDOT	PINW	VT	I4	I5	E5	NAC	A1	A2	A3	A4	A5	P7	DELTA	THETA
IN	IN	RAD/	IN	IN	IN	IN	IN	IN	IN	IN	IN	IN	IN	IN	IN	IN
SEC	SEC	SEC	KW	VOLTS	PU	PU	PU		KW	KW	KW	KW	KW	KW	DEG	DEG
5.	5070	1.75	101.1	209.3	2.199	5.026	2.530	0.732	19.0	6.3	0.4	0.3	1.1	27.1	-70.1	180.0
10.	5140	1.76	102.5	212.2	2.199	5.029	2.553	0.735	19.0	6.3	0.4	0.3	1.1	27.1	-70.1	180.0
15.	5210	1.78	103.9	215.1	2.199	5.032	2.576	0.739	19.0	6.3	0.4	0.3	1.1	27.2	-70.0	180.0
20.	5281	1.79	105.3	218.0	2.199	5.035	2.600	0.742	19.0	6.3	0.4	0.3	1.1	27.2	-70.0	180.0
25.	5352	1.80	106.8	221.0	2.199	5.037	2.623	0.745	19.0	6.4	0.4	0.3	1.1	27.2	-69.9	180.0
30.	5424	1.81	108.2	224.0	2.199	5.040	2.647	0.748	19.0	6.4	0.4	0.3	1.1	27.3	-69.9	180.0
35.	5496	1.82	109.6	226.9	2.199	5.043	2.671	0.751	19.0	6.4	0.5	0.3	1.1	27.3	-69.8	180.0
40.	5569	1.82	111.1	229.9	2.199	5.046	2.695	0.754	19.0	6.4	0.5	0.4	1.1	27.3	-69.8	180.0
45.	5641	1.83	112.5	232.9	2.199	5.049	2.719	0.757	19.0	6.4	0.5	0.4	1.1	27.4	-69.7	180.0
50.	5715	1.84	114.0	236.0	2.199	5.052	2.743	0.760	19.0	6.4	0.5	0.4	1.1	27.4	-69.7	180.0
55.	5788	1.85	115.5	239.0	2.199	5.055	2.768	0.762	19.0	6.4	0.5	0.4	1.1	27.4	-69.7	180.0
60.	5862	1.86	116.9	242.1	2.199	5.057	2.792	0.765	19.0	6.4	0.5	0.4	1.1	27.5	-69.6	180.0
65.	5936	1.87	118.4	245.1	2.199	5.060	2.817	0.768	19.0	6.4	0.5	0.4	1.1	27.5	-69.6	180.0
70.	6011	1.88	119.9	248.2	2.199	5.063	2.842	0.770	19.0	6.4	0.6	0.4	1.1	27.6	-69.5	180.0
75.	6086	1.89	121.4	251.3	2.199	5.066	2.867	0.773	19.0	6.4	0.6	0.5	1.1	27.6	-69.5	180.0
80.	6161	1.89	122.9	254.4	2.199	5.068	2.892	0.775	19.0	6.4	0.6	0.5	1.1	27.6	-69.4	180.0
85.	6237	1.90	124.4	257.6	2.199	5.071	2.917	0.778	19.0	6.4	0.6	0.5	1.1	27.7	-69.4	180.0
90.	6312	1.91	125.9	260.7	2.199	5.074	2.942	0.780	19.0	6.4	0.6	0.5	1.1	27.7	-69.4	180.0
95.	6389	1.92	127.5	263.9	2.199	5.076	2.968	0.782	19.0	6.4	0.6	0.5	1.1	27.8	-69.3	180.0
100.	6465	1.92	129.0	267.0	2.199	5.079	2.993	0.784	19.0	6.5	0.7	0.5	1.1	27.8	-69.3	180.0
105.	6542	1.93	130.5	270.2	2.199	5.081	3.018	0.787	19.0	6.5	0.7	0.6	1.1	27.9	-69.3	180.0
110.	6619	1.94	132.1	273.4	2.199	5.084	3.044	0.789	19.0	6.5	0.7	0.6	1.1	27.9	-69.2	180.0
115.	6696	1.95	133.6	276.6	2.199	5.086	3.070	0.791	19.0	6.5	0.7	0.6	1.1	27.9	-69.2	180.0
120.	6774	1.95	135.2	279.8	2.199	5.089	3.096	0.793	19.0	6.5	0.7	0.6	1.1	28.0	-69.1	180.0
125.	6851	1.96	136.7	283.0	2.199	5.091	3.122	0.795	19.0	6.5	0.8	0.7	1.1	28.0	-69.1	180.0
130.	6929	1.96	138.3	286.2	2.199	5.094	3.148	0.797	19.0	6.5	0.8	0.7	1.1	28.1	-69.1	180.0
135.	7008	1.97	139.8	289.5	2.199	5.096	3.174	0.799	19.0	6.5	0.8	0.7	1.1	28.1	-69.0	180.0
140.	7086	1.98	141.4	292.7	2.199	5.099	3.200	0.801	19.0	6.5	0.8	0.7	1.1	28.2	-69.0	180.0
145.	7165	1.98	143.0	296.0	2.199	5.101	3.226	0.802	19.0	6.5	0.8	0.7	1.1	28.2	-69.0	180.0
150.	7244	1.99	144.6	299.3	2.199	5.104	3.253	0.804	19.0	6.5	0.9	0.8	1.1	28.3	-69.0	180.0
155.	7323	1.99	146.2	302.5	2.199	5.106	3.279	0.806	19.0	6.5	0.9	0.8	1.1	28.3	-68.9	180.0
160.	7403	2.00	147.7	305.8	2.199	5.108	3.305	0.808	19.0	6.5	0.9	0.8	1.1	28.4	-68.9	180.0
165.	7483	2.01	149.3	309.1	2.199	5.111	3.332	0.809	19.0	6.5	0.9	0.9	1.1	28.5	-68.9	180.0
170.	7563	2.01	150.9	312.4	2.199	5.113	3.359	0.811	19.0	6.5	1.0	0.9	1.1	28.5	-68.8	180.0
175.	7643	2.02	152.5	315.7	2.199	5.115	3.385	0.813	19.0	6.5	1.0	0.9	1.1	28.6	-68.8	180.0
180.	7723	2.02	154.1	319.1	2.199	5.117	3.412	0.814	19.0	6.5	1.0	0.9	1.1	28.6	-68.8	180.0
185.	7804	2.03	155.8	322.4	2.199	5.120	3.439	0.816	19.0	6.6	1.0	1.0	1.1	28.7	-68.8	180.0
190.	7884	2.03	157.4	325.7	2.199	5.122	3.466	0.817	19.0	6.6	1.0	1.0	1.1	28.7	-68.7	180.0
195.	7965	2.04	159.0	329.1	2.199	5.124	3.493	0.819	19.0	6.6	1.1	1.0	1.1	28.8	-68.7	180.0
200.	8047	2.04	160.6	332.5	2.199	5.126	3.520	0.820	19.0	6.6	1.1	1.1	1.1	28.9	-68.7	180.0
205.	8128	2.05	162.2	335.8	2.199	5.128	3.547	0.822	19.0	6.6	1.1	1.1	1.1	28.9	-68.7	180.0
210.	8209	2.05	163.9	339.2	2.199	5.130	3.575	0.823	19.0	6.6	1.1	1.1	1.1	29.0	-68.6	180.0
215.	8291	2.06	165.5	342.6	2.199	5.133	3.602	0.824	19.0	6.6	1.2	1.2	1.1	29.1	-68.6	180.0
220.	8373	2.06	167.1	346.0	2.199	5.135	3.629	0.826	19.0	6.6	1.2	1.2	1.1	29.1	-68.6	180.0
225.	8455	2.06	168.8	349.4	2.199	5.137	3.657	0.827	19.0	6.6	1.2	1.2	1.1	29.2	-68.6	180.0
230.	8537	2.07	170.4	352.8	2.199	5.139	3.684	0.828	19.0	6.6	1.2	1.3	1.1	29.3	-68.5	180.0
235.	8620	2.07	172.1	356.2	2.199	5.141	3.712	0.830	19.0	6.6	1.3	1.3	1.1	29.3	-68.5	180.0
240.	8702	2.08	173.7	359.6	2.199	5.143	3.739	0.831	19.0	6.6	1.3	1.3	1.1	29.4	-68.5	180.0
245.	8785	2.08	175.4	363.0	2.199	5.145	3.767	0.832	19.0	6.6	1.3	1.4	1.1	29.5	-68.5	180.0
250.	8868	2.08	177.0	366.4	2.199	5.147	3.795	0.833	19.0	6.6	1.4	1.4	1.1	29.5	-68.4	180.0

(continued)

TIME IN SEC	W0	WFDOT RAD/SEC	PINW IN KW	VT IN VOLTS	I4 IN PU	I5 IN PU	F5 IN PU	NAC	A1 IN KW	A2 IN KW	A3 IN KW	A4 IN KW	A5 IN KW	P7 IN KW	DELTA		THETA	
															IN	DEG	IN	DEG
255.	.8951	2.09	178.7	369.9	2.199	5.149	3.822	0.834	19.0	6.6	1.4	1.5	1.1	29.6	-68.4	180.0		
260.	.9034	2.09	180.3	373.3	2.199	5.150	3.850	0.835	19.0	6.6	1.4	1.5	1.1	29.7	-68.4	180.0		
265.	.9117	2.10	182.0	376.8	2.199	5.152	3.878	0.836	19.0	6.6	1.4	1.5	1.1	29.8	-68.4	180.0		
270.	.9201	2.10	183.7	380.2	2.199	5.154	3.906	0.838	19.0	6.6	1.5	1.6	1.1	29.8	-68.4	180.0		
275.	.9284	2.10	185.4	383.7	2.199	5.156	3.934	0.839	19.0	6.6	1.5	1.6	1.1	29.9	-68.3	180.0		
280.	.9368	2.11	187.0	387.1	2.199	5.158	3.962	0.840	19.0	6.6	1.5	1.7	1.1	30.0	-68.3	180.0		
285.	.9452	2.11	188.7	390.6	2.199	5.160	3.990	0.841	19.0	6.7	1.6	1.7	1.1	30.1	-68.3	180.0		
290.	.9536	2.11	190.4	394.1	2.199	5.162	4.018	0.842	19.0	6.7	1.6	1.8	1.1	30.2	-68.3	180.0		
295.	.9620	2.12	192.1	397.6	2.199	5.163	4.046	0.843	19.0	6.7	1.6	1.8	1.1	30.2	-68.3	180.0		
300.	.9704	2.12	193.7	401.1	2.199	5.165	4.074	0.843	19.0	6.7	1.7	1.9	1.1	30.3	-68.3	180.0		
305.	.9789	2.12	195.4	404.5	2.199	5.167	4.102	0.844	19.0	6.7	1.7	1.9	1.1	30.4	-68.2	180.0		
310.	.9873	2.12	197.1	408.0	2.199	5.169	4.131	0.845	19.0	6.7	1.7	2.0	1.1	30.5	-68.2	180.0		
315.	.9958	2.13	198.8	411.5	2.199	5.170	4.159	0.846	19.0	6.7	1.8	2.0	1.1	30.6	-68.2	180.0		

TRAVELING MODE DATA : (Outbound Leg)

D-6

TIME IN SEC	VEL IN MPH	PROP. FORCE LBS	W0	F/W POWER K.W.	PROP. POWER K.W.	THETA IN DEG	D.C. LOSS K.W.	A.C. LOSS K.W.	E0	I0	D IN DEG	E5	15	NAC	NDC	PDR LOSS K.W.	A IN DEG	E2TOT IN KW-HR	E3TOT IN KW-HR	I4
320.	2.0	996.	0.9990	45.80	3.96	79.1	7.33	27.55	0.13	1.27	6.9	6.64	4.98	0.395	0.370	0.62	80.6	0.00	0.02	2.10
325.	2.7	481.	0.9978	22.50	2.60	77.8	2.39	10.96	0.11	0.68	6.9	4.33	2.93	0.507	0.542	0.32	82.7	0.00	0.04	1.17
330.	5.4	420.	0.9958	22.82	4.55	74.3	2.00	9.56	0.18	0.60	9.0	3.99	2.68	0.576	0.712	0.31	79.5	0.01	0.07	1.05
335.	5.4	420.	0.9946	22.81	4.55	74.3	2.00	9.55	0.18	0.60	8.9	3.98	2.68	0.576	0.712	0.31	79.5	0.02	0.09	1.05
340.	5.4	420.	0.9936	9.50	-0.21	47.6	0.32	3.37	-0.12	0.03	10.4	1.14	0.76	0.635	0.000	0.01	95.6	0.03	0.11	0.18
345.	8.4	271.	0.9930	8.51	-4.56	84.7	0.97	5.55	-0.20	0.35	1.7	2.68	1.78	0.325	0.768	0.18	98.4	0.02	0.12	0.63
350.	13.4	226.	0.9926	6.49	-6.04	87.0	0.95	4.92	-0.33	0.29	0.3	2.38	1.58	0.206	0.829	0.18	104.7	0.01	0.13	0.54
355.	15.0	814.	0.9923	4.69	-24.29	99.7	4.53	15.91	-0.38	0.93	-8.9	5.32	3.67	0.000	0.797	0.59	106.2	-0.02	0.16	1.51
360.	15.0	213.	0.9919	19.79	6.35	61.6	1.10	5.57	0.41	0.32	14.4	2.64	1.75	0.714	0.862	0.21	69.0	-0.02	0.17	0.64
365.	15.0	213.	0.9908	19.78	6.35	61.6	1.10	5.57	0.41	0.32	14.4	2.64	1.75	0.714	0.862	0.21	69.0	-0.01	0.18	0.64
370.	15.0	213.	0.9898	19.77	6.35	61.6	1.10	5.56	0.41	0.32	14.4	2.64	1.75	0.715	0.862	0.21	69.0	-0.01	0.19	0.64
375.	15.0	213.	0.9888	19.77	6.35	61.6	1.10	5.56	0.41	0.32	14.4	2.63	1.75	0.715	0.862	0.21	69.0	0.00	0.20	0.64
380.	15.0	385.	0.9876	29.77	11.47	63.1	2.06	8.87	0.44	0.55	16.1	3.74	2.54	0.699	0.858	0.37	66.8	0.01	0.21	1.00
385.	15.0	1076.	0.9842	81.94	32.10	60.5	8.81	31.25	0.54	1.36	22.1	6.66	5.31	0.617	0.798	0.99	59.6	0.05	0.26	2.26
390.	15.0	1078.	0.9798	82.15	32.18	60.5	8.84	31.34	0.54	1.36	22.1	6.62	5.32	0.617	0.798	0.99	59.6	0.09	0.32	2.26
395.	15.0	1078.	0.9755	82.14	32.18	60.5	8.84	31.33	0.54	1.36	22.0	6.57	5.33	0.617	0.798	0.99	59.6	0.14	0.38	2.26
400.	15.0	1078.	0.9711	82.12	32.18	60.5	8.84	31.31	0.54	1.36	22.0	6.52	5.33	0.617	0.798	0.99	59.6	0.18	0.44	2.26
405.	15.0	1077.	0.9667	82.00	32.14	60.5	8.83	31.24	0.54	1.36	22.0	6.46	5.33	0.618	0.798	0.99	59.6	0.23	0.50	2.26
410.	15.0	949.	0.9628	62.91	25.32	61.8	6.16	22.45	0.51	1.11	20.1	5.66	4.47	0.642	0.817	0.79	61.8	0.27	0.55	1.87
415.	15.0	563.	0.9601	41.47	16.80	63.0	3.40	13.27	0.47	0.78	17.6	4.47	3.33	0.678	0.843	0.53	64.8	0.30	0.59	1.35
420.	15.0	506.	0.9581	37.55	15.10	63.1	2.94	11.71	0.46	0.71	17.1	4.19	3.09	0.686	0.848	0.48	65.4	0.32	0.61	1.24
425.	15.0	155.	0.9564	6.66	-4.62	82.6	0.79	3.99	-0.36	0.20	2.1	1.90	1.31	0.374	0.814	0.13	106.8	0.33	0.63	0.40
430.	15.0	506.	0.9557	37.54	15.10	63.1	2.94	11.70	0.46	0.71	17.1	4.17	3.09	0.686	0.848	0.48	65.4	0.33	0.63	0.40
435.	15.0	506.	0.9536	37.53	15.10	63.1	2.94	11.69	0.46	0.71	17.1	4.16	3.09	0.686	0.848	0.48	65.5	0.35	0.67	1.24
440.	15.0	1167.	0.9507	89.86	34.82	60.0	9.98	34.97	0.55	1.46	22.6	6.52	5.68	0.600	0.791	1.07	58.9	0.38	0.70	2.41
445.	15.0	506.	0.9459	37.49	15.10	63.1	2.94	11.65	0.46	0.71	17.0	4.10	3.10	0.687	0.848	0.48	65.5	0.42	0.77	1.24
450.	15.0	506.	0.9439	37.48	15.10	63.1	2.94	11.65	0.46	0.71	17.0	4.09	3.10	0.687	0.848	0.48	65.5	0.44	0.80	1.24
455.	15.0	84.	0.9424	13.12	2.52	55.5	0.66	3.64	0.38	0.13	12.5	1.64	1.14	0.716	0.806	0.09	70.8	0.46	0.81	0.35
460.	15.0	56.	0.9419	8.32	-1.66	63.6	0.58	3.22	-0.36	0.08	7.1	1.32	0.92	0.599	0.621	0.05	106.8	0.45	0.82	0.23
465.	19.0	588.	0.9398	48.55	22.21	57.5	3.85	13.95	0.59	0.81	21.7	4.41	3.44	0.711	0.863	0.61	58.4	0.48	0.84	1.40
470.	24.0	642.	0.9367	60.35	30.63	49.7	4.73	15.58	0.74	0.87	28.0	4.58	3.64	0.741	0.876	0.74	49.1	0.51	0.87	1.51
475.	29.0	988.	0.9323	105.68	57.00	36.2	9.01	27.49	0.95	1.26	41.4	5.72	4.91	0.739	0.873	1.23	32.0	0.57	0.91	2.13
480.	30.0	686.	0.9277	73.98	40.91	38.4	5.80	16.83	0.92	0.92	36.9	4.63	3.76	0.772	0.885	0.88	36.1	0.64	0.96	1.59
485.	30.0	686.	0.9236	73.97	40.91	38.4	5.80	16.82	0.92	0.92	36.9	4.59	3.76	0.772	0.885	0.88	36.1	0.69	0.99	1.59
490.	30.0	686.	0.9194	73.95	40.91	38.4	5.80	16.80	0.92	0.92	36.8	4.55	3.77	0.772	0.885	0.88	36.1	0.75	1.03	1.59
495.	30.0	686.	0.9152	73.93	40.91	38.4	5.80	16.79	0.92	0.92	36.8	4.52	3.77	0.772	0.885	0.88	36.1	0.81	1.07	1.59
500.	30.0	686.	0.9110	73.92	40.91	38.4	5.80	16.77	0.92	0.92	36.7	4.48	3.77	0.772	0.885	0.88	36.1	0.86	1.11	1.59
505.	30.0	737.	0.9066	79.48	43.99	37.7	6.31	18.41	0.93	0.98	37.8	4.62	3.98	0.768	0.883	0.95	35.0	0.92	1.15	1.69
510.	30.0	671.	0.9023	72.33	40.05	38.6	5.65	16.29	0.92	0.91	36.3	4.35	3.73	0.774	0.885	0.86	36.5	0.98	1.19	1.57
515.	30.0	671.	0.8981	72.32	40.05	38.6	5.65	16.27	0.92	0.91	36.2	4.31	3.73	0.774	0.885	0.86	36.5	1.04	1.22	1.57
520.	30.0	605.	0.8941	65.32	36.10	39.6	5.03	14.26	0.90	0.83	34.7	4.04	3.47	0.781	0.886	0.78	38.0	1.09	1.26	1.45
525.	27.0	34.	0.8923	8.58	-1.82	55.0	1.33	2.88	-0.64	0.05	8.3	1.16	0.86	0.652	0.204	0.04	122.0	1.11	1.27	0.20
530.	22.4	246.	0.8916	25.60	10.97	53.6	1.70	5.69	0.61	0.37	18.8	2.48	1.97	0.775	0.875	0.28	58.2	1.11	1.28	0.72
535.	22.4	583.	0.8885	52.70	26.04	52.6	4.07	13.67	0.68	0.80	24.8	3.97	3.46	0.739	0.874	0.65	52.9	1.15	1.31	1.40
540.	22.4	583.	0.8855	52.69	26.04	52.6	4.07	13.66	0.68	0.80	24.7	3.95	3.47	0.739	0.874	0.65	52.9	1.18	1.34	1.40
545.	22.4	583.	0.8824	52.68	26.04	52.6	4.07	13.65	0.68	0.80	24.7	3.93	3.47	0.739	0.874	0.65	52.9	1.22	1.37	1.40
550.	22.4	583.	0.8793	52.67	26.04	52.6	4.07	13.64	0.68	0.80	24.7	3.90	3.48	0.739	0.874	0.65	52.9	1.25	1.39	1.40
555.	22.4	583.	0.8762	52.66	26.04	52.6	4.07	13.64	0.68	0.80	24.6	3.88	3.48	0.740	0.874	0.65	52.9	1.29	1.42	1.40
560.	22.4	868.	0.8721	78.92	38.73	50.2	6.90	22.97	0.73	1.13	28.6	4.75	4.62	0.708	0.859	0.95	48.9	1.34	1.46	1.91
565.	22.4	868.	0.8674	78.91	38.73	50.2	6.90	22.96	0.73	1.13	28.5	4.70	4.63	0.708	0.859	0.95	48.9	1.39	1.51	1.91

(continued)

D-7

TIME IN SEC	VEL IN MPH	PROP. FORCE LBS	W0	F/W POWER K.W.	PROP. POWER K.W.	THETA IN DEG	D.C. LOSS K.W.	A.C. LOSS K.W.	E0	I0	D IN DEG	E5	I5	NAC	NDC	PDR LOSS K.W.	A IN DEG	E2TOT IN K.W.-HR	E3TOT IN K.W.-HR	I4
570.	22.4	868.	0.4627	78.91	38.73	50.2	6.90	22.95	0.73	1.13	28.5	4.65	4.64	0.708	0.859	0.95	49.0	1.44	1.56	1.91
575.	22.4	868.	0.4579	78.90	38.73	50.2	6.90	22.95	0.73	1.13	28.4	4.60	4.64	0.708	0.859	0.95	49.0	1.50	1.61	1.91
580.	22.4	868.	0.4519	117.23	53.30	47.3	10.92	36.08	0.79	1.48	32.4	5.27	5.88	0.678	0.841	1.30	44.7	1.56	1.67	2.46
585.	22.4	1455.	0.8438	141.10	64.97	44.9	14.66	48.25	0.82	1.75	35.3	5.58	6.84	0.657	0.828	1.57	41.5	1.65	1.76	2.88
590.	22.4	1455.	0.8351	141.12	64.97	44.9	14.66	48.28	0.82	1.75	35.2	5.45	6.86	0.657	0.828	1.57	41.5	1.74	1.86	2.88
595.	22.4	1455.	0.8263	141.16	64.97	44.9	14.66	48.31	0.82	1.75	35.1	5.32	6.88	0.657	0.828	1.57	41.6	1.83	1.95	2.88
600.	22.4	1455.	0.8174	141.19	64.97	44.9	14.66	48.35	0.82	1.75	35.0	5.19	6.91	0.657	0.828	1.57	41.6	1.92	2.05	2.88
605.	22.4	1455.	0.8084	141.24	64.97	44.9	14.66	48.40	0.82	1.75	34.9	5.05	6.93	0.657	0.828	1.57	41.7	2.01	2.15	2.88
610.	22.4	1455.	0.7993	141.29	64.97	44.9	14.66	48.45	0.82	1.75	34.8	4.92	6.96	0.656	0.828	1.57	41.7	2.10	2.25	2.88
615.	22.4	1455.	0.7901	141.35	64.97	44.9	14.66	48.51	0.82	1.75	34.7	4.78	6.99	0.656	0.828	1.57	41.8	2.19	2.34	2.88
620.	22.4	1403.	0.7794	195.27	84.96	40.8	22.02	72.97	0.88	2.19	39.4	4.90	8.64	0.626	0.807	2.03	36.4	2.29	2.46	3.56
625.	22.4	1403.	0.7663	195.50	84.96	40.8	22.02	73.10	0.88	2.19	39.3	4.67	8.71	0.626	0.807	2.03	36.5	2.41	2.61	3.56
630.	22.4	1403.	0.7529	195.78	84.96	40.8	22.02	73.38	0.88	2.19	39.1	4.43	8.79	0.625	0.807	2.03	36.6	2.53	2.75	3.56
635.	22.4	1403.	0.7393	196.12	84.96	40.8	22.02	73.72	0.88	2.19	39.0	4.18	8.88	0.624	0.807	2.03	36.7	2.65	2.90	3.56
640.	22.4	1708.	0.7258	171.87	76.15	42.6	18.63	62.64	0.85	2.00	36.7	3.91	8.23	0.635	0.816	1.83	39.2	2.76	3.04	3.27
645.	22.4	1508.	0.7151	148.43	67.32	44.4	15.47	52.16	0.83	1.80	34.4	3.68	7.55	0.648	0.826	1.62	41.6	2.86	3.14	2.90
650.	22.4	940.	0.7071	86.48	41.97	49.6	7.73	26.09	0.75	1.21	27.6	3.14	5.35	0.697	0.855	1.03	48.5	2.93	3.22	2.04
655.	22.4	623.	0.7014	56.18	27.81	52.3	4.42	14.83	0.69	0.85	23.1	2.61	4.04	0.735	0.872	0.70	52.7	2.98	3.26	1.47
660.	22.4	1508.	0.6925	148.99	67.32	44.4	15.47	52.73	0.83	1.80	34.1	3.33	7.73	0.645	0.826	1.62	41.7	3.06	3.34	2.96
665.	22.4	1508.	0.6812	149.35	67.32	44.4	15.47	53.09	0.83	1.80	34.0	3.16	7.83	0.644	0.826	1.62	41.8	3.15	3.45	2.96
670.	22.4	623.	0.6735	56.34	27.81	52.3	4.42	14.99	0.69	0.85	22.7	2.39	4.16	0.733	0.872	0.70	52.8	3.22	3.52	1.47
675.	22.1	611.	0.6694	54.89	26.92	52.8	4.29	14.66	0.68	0.84	22.1	2.34	4.14	0.732	0.872	0.68	53.5	3.25	3.54	1.45
680.	19.4	1768.	0.5630	113.62	48.93	52.1	11.66	41.48	0.70	1.56	26.6	2.87	7.07	0.634	0.820	1.28	51.0	3.31	3.60	2.58
685.	14.4	1718.	0.5549	94.88	34.88	60.7	10.61	39.26	0.54	1.51	19.7	2.81	6.98	0.585	0.781	1.10	60.6	3.36	3.68	2.49
690.	9.4	149.	0.6505	7.29	-2.78	78.0	0.60	3.14	-0.22	0.20	2.9	1.20	1.84	0.551	0.766	0.11	100.0	3.38	3.72	0.40
695.	5.0	168.	0.6498	12.46	-1.66	69.7	0.67	3.86	0.14	-0.26	6.6	1.34	2.11	0.683	0.731	0.13	82.4	3.38	3.73	0.52
700.	2.8	331.	0.6487	16.56	1.87	76.3	1.41	6.89	0.10	0.48	5.3	1.75	2.94	0.577	0.590	0.23	83.9	3.38	3.74	0.87
705.	2.5	363.	0.6474	17.39	1.80	77.1	1.59	7.60	0.10	0.53	5.1	1.81	3.10	0.556	0.551	0.25	84.2	3.39	3.75	0.93
710.	1.1	250.	0.6463	12.97	0.56	76.4	0.97	5.21	0.05	0.37	4.7	1.54	2.54	0.589	0.386	0.17	86.6	3.39	3.76	0.69

CHARGING MODE DATA : (Station B)

TIME	W0	WFOOT	PLMW	VT	I4	I5	NAC	A1	A2	A3	A4	A5	P7	DELTA	THETA
IN		RAD/	IN	IN	IN	IN	IN	IN	IN	IN	IN	IN	IN	IN	IN
SEC		SEC-SQ	KW	VOLTS	PU	PU	PU	KW	KW	KW	KW	KW	KW	DEG	DEG
715.	.6505	1.93	129.8	268.7	2.199	5.080	3.006	0.786	19.0	6.5	0.7	0.6	1.1	27.8	-69.3
720.	.6582	1.93	131.3	271.8	2.199	5.083	3.032	0.788	19.0	6.5	0.7	0.6	1.1	27.9	-69.2
725.	.6659	1.94	132.9	275.0	2.199	5.085	3.057	0.790	19.0	6.5	0.7	0.6	1.1	27.9	-69.2
730.	.6736	1.95	134.4	278.2	2.199	5.088	3.083	0.792	19.0	6.5	0.7	0.6	1.1	28.0	-69.2
735.	.6814	1.96	136.0	281.5	2.199	5.090	3.109	0.794	19.0	6.5	0.7	0.6	1.1	28.0	-69.1
740.	.6892	1.97	137.5	284.7	2.199	5.093	3.135	0.796	19.0	6.5	0.8	0.7	1.1	28.1	-69.1
745.	.6970	1.97	139.1	287.9	2.199	5.095	3.161	0.798	19.0	6.5	0.8	0.7	1.1	28.1	-69.1
750.	.7048	1.97	140.7	291.2	2.199	5.098	3.187	0.800	19.0	6.5	0.8	0.7	1.1	28.2	-69.0
755.	.7127	1.98	142.2	294.4	2.199	5.100	3.214	0.802	19.0	6.5	0.8	0.7	1.1	28.2	-69.0
760.	.7206	1.99	143.8	297.7	2.199	5.102	3.240	0.803	19.0	6.5	0.9	0.8	1.1	28.3	-69.0
765.	.7285	1.99	145.4	301.0	2.199	5.105	3.266	0.805	19.0	6.5	0.9	0.8	1.1	28.3	-68.9
770.	.7365	2.00	147.0	304.2	2.199	5.107	3.293	0.807	19.0	6.5	0.9	0.8	1.1	28.4	-68.9
775.	.7444	2.00	148.6	307.5	2.199	5.110	3.319	0.809	19.0	6.5	0.9	0.8	1.1	28.4	-68.9
780.	.7524	2.01	150.2	310.8	2.199	5.112	3.346	0.810	19.0	6.5	0.9	0.9	1.1	28.5	-68.9
785.	.7604	2.01	151.8	314.2	2.199	5.114	3.373	0.812	19.0	6.5	1.0	0.9	1.1	28.5	-68.8
790.	.7684	2.02	153.4	317.5	2.199	5.116	3.399	0.814	19.0	6.5	1.0	0.9	1.1	28.6	-68.8
795.	.7765	2.02	155.0	320.8	2.199	5.119	3.426	0.815	19.0	6.6	1.0	1.0	1.1	28.7	-68.8
800.	.7846	2.03	156.6	324.1	2.199	5.121	3.453	0.817	19.0	6.6	1.0	1.0	1.1	28.7	-68.7
805.	.7926	2.03	158.2	327.5	2.199	5.123	3.480	0.818	19.0	6.6	1.1	1.0	1.1	28.8	-68.7
810.	.8008	2.04	159.8	330.8	2.199	5.125	3.507	0.820	19.0	6.6	1.1	1.0	1.1	28.8	-68.7
815.	.8089	2.04	161.5	334.2	2.199	5.127	3.534	0.821	19.0	6.6	1.1	1.1	1.1	28.9	-68.7
820.	.8170	2.05	163.1	337.6	2.199	5.129	3.561	0.822	19.0	6.6	1.1	1.1	1.1	29.0	-68.6
825.	.8252	2.05	164.7	340.9	2.199	5.132	3.589	0.824	19.0	6.6	1.2	1.1	1.1	29.0	-68.6
830.	.8334	2.06	166.3	344.3	2.199	5.134	3.616	0.825	19.0	6.6	1.2	1.2	1.1	29.1	-68.6
835.	.8416	2.06	168.0	347.7	2.199	5.136	3.643	0.826	19.0	6.6	1.2	1.2	1.1	29.2	-68.6
840.	.8498	2.07	169.6	351.1	2.199	5.138	3.671	0.828	19.0	6.6	1.2	1.2	1.1	29.2	-68.5
845.	.8580	2.07	171.3	354.5	2.199	5.140	3.698	0.829	19.0	6.6	1.3	1.3	1.1	29.3	-68.5
850.	.8662	2.07	172.9	357.9	2.199	5.142	3.726	0.830	19.0	6.6	1.3	1.3	1.1	29.4	-68.5
855.	.8745	2.08	174.6	361.4	2.199	5.144	3.754	0.831	19.0	6.6	1.3	1.4	1.1	29.4	-68.5
860.	.8828	2.08	176.2	364.8	2.199	5.146	3.781	0.833	19.0	6.6	1.3	1.4	1.1	29.5	-68.5
865.	.8911	2.09	177.9	368.2	2.199	5.148	3.809	0.834	19.0	6.6	1.4	1.4	1.1	29.6	-68.4
870.	.8994	2.09	179.5	371.7	2.199	5.150	3.837	0.835	19.0	6.6	1.4	1.5	1.1	29.7	-68.4
875.	.9077	2.09	181.2	375.1	2.199	5.151	3.865	0.836	19.0	6.6	1.4	1.5	1.1	29.7	-68.4
880.	.9161	2.10	182.9	378.6	2.199	5.153	3.892	0.837	19.0	6.6	1.5	1.6	1.1	29.8	-68.4
885.	.9244	2.10	184.5	382.0	2.199	5.155	3.920	0.838	19.0	6.6	1.5	1.6	1.1	29.9	-68.4
890.	.9328	2.10	186.2	385.5	2.199	5.157	3.948	0.839	19.0	6.6	1.5	1.7	1.1	30.0	-68.3
895.	.9412	2.11	187.9	388.9	2.199	5.159	3.976	0.840	19.0	6.7	1.6	1.7	1.1	30.0	-68.3
900.	.9495	2.11	189.6	392.4	2.199	5.161	4.004	0.841	19.0	6.7	1.6	1.7	1.1	30.1	-68.3
905.	.9580	2.11	191.3	395.9	2.199	5.162	4.032	0.842	19.0	6.7	1.6	1.8	1.1	30.2	-68.3
910.	.9664	2.12	192.9	399.4	2.199	5.164	4.061	0.843	19.0	6.7	1.6	1.8	1.1	30.3	-68.3
915.	.9748	2.12	194.6	402.9	2.199	5.166	4.089	0.844	19.0	6.7	1.7	1.9	1.1	30.4	-68.2
920.	.9832	2.12	196.3	406.4	2.199	5.169	4.117	0.845	19.0	6.7	1.7	1.9	1.1	30.5	-68.2
925.	.9917	2.13	198.0	409.9	2.199	5.169	4.145	0.846	19.0	6.7	1.7	2.0	1.1	30.5	-68.2
930.	1.0000	2.13	199.7	413.4	2.199	5.171	4.174	0.847	19.0	6.7	1.8	2.0	1.1	30.6	-68.2

TRAVELING MODE DATA : (Return Leg)

TIME IN SEC	VEL IN MPH	PROP. FORCE LBS	W0	F/W POWER K.W.	PROP. POWER K.W.	THETA IN DEG	D.C. LOSS K.W.	A.C. LOSS K.W.	E0	I0	D IN DEG	E5	I5	NAC	NDC	PDR LOSS K.W.	A IN DEG	E2TOT IN KW-HR	I4 IN KW-HR	
935.	2.7	372.	0.9983	18.51	2.01	76.9	1.65	8.42	0.11	0.54	7.0	3.72	2.45	0.538	0.570	0.26	83.4	3.39	3.79	0.95
940.	3.7	575.	0.9970	27.66	4.28	76.9	3.14	13.48	0.15	0.79	7.8	4.82	3.33	0.508	0.597	0.40	80.7	3.40	3.81	1.35
945.	5.4	771.	0.9955	29.72	6.18	74.9	3.14	13.44	0.20	0.79	9.3	4.79	3.32	0.543	0.682	0.42	78.4	3.40	3.84	1.35
950.	8.4	79.	0.9950	8.95	-1.32	67.3	0.43	3.67	-0.20	0.11	7.1	1.51	1.00	0.576	0.645	0.06	98.9	3.40	3.85	0.28
955.	13.4	452.	0.9937	32.46	12.08	65.1	2.45	10.46	0.41	0.64	15.5	4.15	2.83	0.675	0.842	0.42	68.2	3.41	3.86	1.13
960.	18.4	359.	0.9931	2.48	-13.18	97.3	1.75	6.56	-0.46	0.45	-5.7	3.09	2.05	0.000	0.856	0.31	111.3	3.40	3.88	0.76
965.	22.4	320.	0.9929	0.90	-14.28	99.8	1.83	5.91	-0.56	0.40	-6.9	2.83	1.88	0.000	0.861	0.30	116.8	3.39	3.89	0.68
970.	22.4	564.	0.9923	-3.54	-25.18	106.1	3.19	9.92	-0.58	0.67	-12.5	4.13	2.74	0.278	0.862	0.51	117.2	3.39	3.90	1.09
975.	22.4	122.	0.9924	6.11	-5.43	82.7	1.12	3.87	-0.54	0.16	2.0	1.71	1.14	0.336	0.775	0.12	116.3	3.36	3.92	0.33
980.	22.4	321.	0.9907	31.66	14.33	53.8	2.12	7.59	0.63	0.47	21.4	3.36	2.24	0.758	0.880	0.37	56.8	3.38	3.93	0.88
985.	22.4	4.	0.9900	10.44	0.17	37.3	0.02	3.33	0.54	0.01	12.7	1.08	0.72	0.672	0.166	0.00	62.8	3.38	3.94	0.18
990.	22.4	564.	0.9900	-3.55	-25.18	106.1	3.19	9.91	-0.58	0.67	-12.4	4.13	2.74	0.279	0.862	0.51	117.2	3.35	3.96	1.09
995.	22.4	564.	0.9902	-3.55	-25.18	106.1	3.19	9.91	-0.58	0.67	-12.4	4.13	2.74	0.279	0.862	0.51	117.2	3.32	3.98	1.09
1000.	22.4	959.	0.9906	-7.07	-42.82	110.2	6.30	19.20	-0.61	1.07	-17.2	5.88	4.06	0.277	0.840	0.82	117.5	3.26	4.02	1.71
1005.	22.4	959.	0.9910	-7.07	-42.82	110.2	6.30	19.21	-0.61	1.07	-17.2	5.88	4.06	0.277	0.840	0.82	117.5	3.20	4.06	1.71
1010.	22.4	959.	0.9913	-7.07	-42.82	110.2	6.30	19.21	-0.61	1.07	-17.2	5.89	4.06	0.277	0.840	0.82	117.5	3.14	4.10	1.71
1015.	22.4	959.	0.9917	-7.07	-42.82	110.2	6.30	19.21	-0.61	1.07	-17.2	5.89	4.06	0.277	0.840	0.82	117.5	3.08	4.14	1.71
1020.	22.4	959.	0.9921	-7.07	-42.82	110.2	6.30	19.21	-0.61	1.07	-17.2	5.89	4.06	0.277	0.840	0.82	117.5	3.02	4.19	1.71
1025.	22.4	511.	0.9923	-2.74	-22.82	105.2	2.86	8.93	-0.58	0.62	-11.5	3.86	2.56	0.253	0.864	0.46	117.1	2.98	4.22	1.01
1030.	22.4	511.	0.9925	-2.74	-22.82	105.2	2.86	8.93	-0.58	0.62	-11.5	3.86	2.56	0.253	0.864	0.46	117.1	2.95	4.24	1.01
1035.	22.4	511.	0.9926	-2.74	-22.82	105.2	2.86	8.93	-0.58	0.62	-11.5	3.86	2.56	0.253	0.864	0.46	117.1	2.91	4.25	1.01
1040.	22.4	511.	0.9928	-2.74	-22.82	105.2	2.86	8.93	-0.58	0.62	-11.5	3.86	2.56	0.253	0.864	0.46	117.1	2.88	4.27	1.01
1045.	22.4	511.	0.9929	-2.74	-22.82	105.2	2.86	8.93	-0.58	0.62	-11.5	3.86	2.56	0.253	0.864	0.46	117.1	2.85	4.29	1.01
1050.	22.4	250.	0.9929	2.56	-11.16	96.3	1.53	5.05	-0.56	0.32	-4.4	2.44	1.62	0.000	0.851	0.24	116.6	2.83	4.31	0.56
1055.	22.4	77.	0.9925	14.72	3.42	48.1	1.05	3.86	0.56	0.12	15.6	1.62	1.07	0.732	0.779	0.09	61.3	2.82	4.32	0.34
1060.	22.4	77.	0.9917	14.71	3.42	48.1	1.05	3.86	0.56	0.12	15.6	1.62	1.07	0.733	0.779	0.09	61.3	2.83	4.32	0.34
1065.	22.4	77.	0.9909	14.71	3.42	48.1	1.05	3.85	0.56	0.12	15.6	1.62	1.07	0.733	0.779	0.09	61.3	2.83	4.33	0.34
1070.	22.4	77.	0.9902	14.70	3.42	48.1	1.05	3.85	0.56	0.12	15.6	1.62	1.08	0.733	0.779	0.09	61.3	2.84	4.34	0.34
1075.	22.4	361.	0.9884	34.70	16.10	53.8	2.36	8.42	0.64	0.52	22.1	3.58	2.42	0.755	0.881	0.41	56.2	2.86	4.35	0.96
1080.	22.4	361.	0.9866	34.69	16.10	53.8	2.36	8.41	0.64	0.52	22.1	3.57	2.42	0.756	0.881	0.41	56.2	2.88	4.37	0.96
1085.	22.4	361.	0.9848	34.68	16.10	53.8	2.36	8.40	0.64	0.52	22.1	3.56	2.42	0.756	0.881	0.41	56.2	2.90	4.39	0.96
1090.	22.4	361.	0.9830	34.67	16.10	53.8	2.36	8.39	0.64	0.52	22.0	3.55	2.42	0.756	0.881	0.41	56.2	2.93	4.41	0.96
1095.	22.4	361.	0.9811	34.66	16.10	53.8	2.36	8.38	0.64	0.52	22.0	3.54	2.42	0.756	0.881	0.41	56.2	2.95	4.42	0.96
1100.	22.4	361.	0.9793	34.65	16.10	53.8	2.36	8.37	0.64	0.52	22.0	3.53	2.43	0.756	0.881	0.41	56.2	2.97	4.44	0.96
1105.	22.4	361.	0.9775	34.64	16.10	53.8	2.36	8.36	0.64	0.52	22.0	3.52	2.43	0.757	0.881	0.41	56.2	2.99	4.46	0.96
1110.	22.4	427.	0.9755	39.88	19.06	53.5	2.82	9.87	0.65	0.61	23.1	3.87	2.72	0.751	0.880	0.48	55.1	3.02	4.48	1.10
1115.	22.4	427.	0.9734	39.87	19.06	53.5	2.82	9.86	0.65	0.61	23.1	3.86	2.72	0.751	0.880	0.48	55.1	3.04	4.50	1.10
1120.	25.4	1034.	0.9694	102.75	52.31	43.1	9.16	29.54	0.85	1.31	36.2	6.31	5.10	0.712	0.861	1.20	39.8	3.10	4.54	2.20
1125.	30.0	711.	0.9639	76.88	42.44	38.0	6.95	17.79	0.93	0.95	37.9	5.05	3.83	0.768	0.884	0.91	35.3	3.17	4.60	1.64
1130.	30.0	340.	0.9616	39.35	20.32	42.7	2.97	7.85	0.83	0.50	28.8	3.27	2.30	0.799	0.882	0.45	43.9	3.20	4.62	0.93
1135.	30.0	307.	0.9597	36.27	18.35	42.9	2.76	7.16	0.82	0.45	27.7	3.07	2.16	0.801	0.878	0.41	44.7	3.23	4.64	0.86
1140.	30.0	307.	0.9577	36.26	18.35	42.9	2.76	7.15	0.82	0.45	27.7	3.06	2.16	0.801	0.878	0.41	44.7	3.25	4.65	0.86
1145.	30.0	359.	0.9557	41.06	21.42	42.5	3.09	8.21	0.84	0.52	29.2	3.34	2.39	0.799	0.883	0.47	43.5	3.28	4.67	0.97
1150.	30.0	359.	0.9534	41.05	21.42	42.5	3.09	8.20	0.84	0.52	29.2	3.33	2.39	0.799	0.883	0.47	43.5	3.31	4.69	0.97
1155.	30.0	359.	0.9512	41.04	21.42	42.5	3.09	8.19	0.84	0.52	29.1	3.31	2.39	0.799	0.883	0.47	43.5	3.34	4.71	0.97
1160.	30.0	359.	0.9490	41.03	21.42	42.5	3.09	8.18	0.84	0.52	29.1	3.30	2.39	0.799	0.883	0.47	43.5	3.37	4.73	0.97
1165.	30.0	935.	0.9451	101.84	55.82	34.6	8.50	25.48	0.97	1.21	42.4	5.69	4.69	0.749	0.877	1.19	30.3	3.42	4.76	2.04
1170.	26.0	325.	0.9424	34.52	16.79	48.9	2.44	7.43	0.72	0.48	24.1	3.12	2.27	0.783	0.882	0.40	51.2	3.46	4.79	0.89
1175.	21.0	318.	0.9406	30.08	13.30	55.7	1.99	7.28	0.59	0.47	19.6	3.10	2.27	0.756	0.879	0.35	59.1	3.48	4.80	0.87
1180.	16.0	316.	0.9391	26.13	10.07	61.7	1.68	7.18	0.45	0.46	15.8	3.10	2.27	0.722	0.867	0.32	66.3	3.49	4.82	0.86

(continued)

TIME IN	VEL IN	PROP. FORCE	W0	F/W POWER	PROP. POWER	THETA IN	D.C. LOSS	A.C. LOSS	E0	I0	D IN	E5	I5	NAC	NDC	PDR LOSS	A IN	E2TOT IN	E3TOT IN	I4 IN
SEC	MPH	LBS		K.W.	K.W.	DEG	K.W.	K.W.			DEG					K.W.	DEG	KW-HR	KW-HR	KW-HR
1185.	15.0	357.	0.9365	27.84	10.67	63.1	1.88	8.02	0.43	0.52	15.5	3.31	2.46	0.709	0.860	0.35	67.2	3.52	4.85	0.94
1190.	15.0	357.	0.9349	27.84	10.67	63.1	1.88	8.01	0.43	0.52	15.5	3.30	2.46	0.709	0.860	0.35	67.2	3.53	4.87	0.94
1195.	15.0	357.	0.9334	27.83	10.67	63.1	1.88	8.01	0.43	0.52	15.5	3.29	2.46	0.709	0.860	0.35	67.2	3.55	4.88	0.94
1200.	15.0	633.	0.9326	3.67	-18.90	98.3	3.18	11.40	-0.38	0.75	-7.4	4.13	3.11	0.000	0.817	0.47	106.5	3.54	4.90	1.23
1205.	15.0	357.	0.9315	27.82	10.67	63.1	1.88	8.00	0.43	0.52	15.4	3.28	2.46	0.709	0.860	0.35	67.2	3.55	4.91	0.94
1210.	15.0	357.	0.9300	27.82	10.67	63.1	1.88	7.99	0.43	0.52	15.4	3.27	2.47	0.710	0.860	0.35	67.2	3.56	4.93	0.94
1215.	15.0	1677.	0.9255	138.57	50.05	57.1	17.49	59.56	0.60	1.97	26.0	7.21	7.54	0.571	0.757	1.51	54.6	3.60	4.99	3.22
1220.	15.0	357.	0.9222	27.78	10.67	63.1	1.88	7.96	0.43	0.52	15.4	3.23	2.47	0.710	0.860	0.35	67.2	3.63	5.03	0.94
1225.	15.0	214.	0.9215	5.66	-6.37	87.6	0.97	4.38	-0.36	0.28	-0.0	2.16	1.56	0.184	0.835	0.17	106.8	3.63	5.04	0.51
1230.	15.0	214.	0.9212	5.66	-6.37	87.6	0.97	4.38	-0.36	0.28	-0.0	2.15	1.56	0.184	0.835	0.17	106.8	3.63	5.05	0.51
1235.	15.0	214.	0.9209	5.66	-6.37	87.6	0.97	4.38	-0.36	0.28	-0.0	2.15	1.56	0.184	0.835	0.17	106.8	3.62	5.06	0.51
1240.	15.0	211.	0.9205	5.69	-6.30	87.4	0.96	4.35	-0.36	0.27	0.1	2.14	1.55	0.195	0.834	0.17	106.8	3.61	5.07	0.51
1245.	15.0	211.	0.9202	5.69	-6.30	87.4	0.96	4.35	-0.36	0.27	0.1	2.14	1.55	0.195	0.834	0.17	106.8	3.60	5.07	0.51
1250.	15.0	211.	0.9199	5.69	-6.30	87.4	0.96	4.35	-0.36	0.27	0.1	2.14	1.55	0.195	0.834	0.17	106.8	3.59	5.08	0.51
1255.	15.0	211.	0.9196	5.69	-6.30	87.4	0.96	4.35	-0.36	0.27	0.1	2.14	1.55	0.195	0.834	0.17	106.8	3.58	5.09	0.51
1260.	15.0	386.	0.9184	29.57	11.53	63.2	2.07	8.59	0.44	0.56	15.6	3.36	2.61	0.707	0.858	0.37	66.9	3.59	5.10	1.00
1265.	15.0	386.	0.9167	29.56	11.53	63.2	2.07	8.58	0.44	0.56	15.6	3.35	2.61	0.707	0.858	0.37	66.9	3.61	5.12	1.00
1270.	15.0	386.	0.9150	29.56	11.53	63.2	2.07	8.58	0.44	0.56	15.6	3.34	2.61	0.707	0.858	0.37	66.9	3.62	5.14	1.00
1275.	15.0	386.	0.9133	29.55	11.53	63.2	2.07	8.57	0.44	0.56	15.6	3.33	2.61	0.707	0.858	0.37	66.9	3.64	5.15	1.00
1280.	15.0	386.	0.9117	29.54	11.53	63.2	2.07	8.56	0.44	0.56	15.6	3.32	2.61	0.707	0.858	0.37	66.9	3.65	5.17	1.00
1285.	15.0	1677.	0.9044	138.99	50.05	57.1	17.49	59.58	0.60	1.97	25.9	6.87	7.58	0.570	0.757	1.51	54.7	3.72	5.27	3.22
1290.	15.0	1677.	0.8964	139.01	50.05	57.1	17.49	59.60	0.60	1.97	25.8	6.74	7.59	0.570	0.757	1.51	54.7	3.79	5.39	3.22
1295.	15.0	1677.	0.8884	139.03	50.05	57.1	17.49	59.62	0.60	1.97	25.8	6.61	7.61	0.570	0.757	1.51	54.8	3.86	5.50	3.22
1300.	11.0	1077.	0.8832	72.01	23.56	66.5	8.60	30.91	0.41	1.36	16.6	5.49	5.45	0.569	0.749	0.89	66.6	3.90	5.58	2.25
1305.	6.3	1272.	0.8792	74.34	15.97	72.5	10.94	39.13	0.28	1.56	12.1	5.91	6.18	0.472	0.613	0.91	72.8	3.93	5.64	2.56
1310.	5.4	367.	0.8761	20.06	3.97	73.9	1.65	7.82	0.18	0.53	8.3	3.04	2.55	0.604	0.723	0.27	80.1	3.94	5.69	0.95
1315.	5.4	367.	0.8749	20.06	3.97	73.9	1.65	7.82	0.18	0.53	8.3	3.03	2.55	0.605	0.723	0.27	80.1	3.95	5.70	0.95
1320.	5.4	367.	0.8737	20.05	3.97	73.9	1.65	7.81	0.18	0.53	8.3	3.02	2.56	0.605	0.723	0.27	80.1	3.95	5.71	0.95
1325.	5.4	367.	0.8725	20.05	3.97	73.9	1.65	7.81	0.18	0.53	8.3	3.02	2.56	0.605	0.723	0.27	80.1	3.96	5.73	0.95
1330.	5.4	367.	0.8713	20.05	3.97	73.9	1.65	7.81	0.18	0.53	8.3	3.01	2.56	0.605	0.723	0.27	80.1	3.96	5.74	0.95
1335.	4.4	234.	0.8703	9.57	-2.07	79.6	0.78	4.56	-0.09	0.30	3.8	2.14	1.74	0.509	0.592	0.14	93.6	3.97	5.76	0.57
1340.	2.7	372.	0.8694	17.95	2.01	76.9	1.65	7.86	0.11	0.54	6.4	3.02	2.58	0.555	0.570	0.26	83.6	3.97	5.77	0.95
1345.	2.7	372.	0.8683	17.95	2.01	76.9	1.65	7.86	0.11	0.54	6.4	3.02	2.58	0.555	0.570	0.26	83.6	3.97	5.78	0.95
1350.	1.4	375.	0.8675	16.89	1.01	78.4	1.66	7.89	0.07	0.54	5.5	3.03	2.59	0.525	0.400	0.25	85.3	3.97	5.79	0.95

CHARGING MODE DATA : (Station A, Final)

TIME	W0	WFOOT	PINW	VT	I4	I5	E5	NAC	A1	A2	A3	A4	A5	P7	DELTA	THETA
IN		RAD/	IN	IN	IN	IN	IN		IN	IN	IN	IN	IN	IN	IN	IN
SEC		SEC-SQ	KW	VOLTS	PU	PU	PU		KW	KW	KW	KW	KW	KW	DEG	DEG
1355.	.8740	2.08	174.5	361.1	2.199	5.144	3.752	0.831	19.0	6.6	1.3	1.4	1.1	29.4	-68.5	180.0
1360.	.8823	2.08	176.1	364.6	2.199	5.146	3.779	0.832	19.0	6.6	1.3	1.4	1.1	29.5	-68.5	180.0
1365.	.8906	2.09	177.8	368.0	2.199	5.148	3.807	0.834	19.0	6.6	1.4	1.4	1.1	29.6	-68.4	180.0
1370.	.8989	2.09	179.4	371.4	2.199	5.149	3.835	0.835	19.0	6.6	1.4	1.5	1.1	29.6	-68.4	180.0
1375.	.9072	2.09	181.1	374.9	2.199	5.151	3.863	0.836	19.0	6.6	1.4	1.5	1.1	29.7	-68.4	180.0
1380.	.9155	2.10	182.8	378.3	2.199	5.153	3.891	0.837	19.0	6.6	1.5	1.6	1.1	29.8	-68.4	180.0
1385.	.9239	2.10	184.4	381.8	2.199	5.155	3.919	0.838	19.0	6.6	1.5	1.6	1.1	29.9	-68.4	180.0
1390.	.9322	2.10	186.1	385.3	2.199	5.157	3.947	0.839	19.0	6.6	1.5	1.6	1.1	30.0	-68.3	180.0
1395.	.9406	2.11	187.8	388.7	2.199	5.159	3.975	0.840	19.0	6.7	1.5	1.7	1.1	30.0	-68.3	180.0
1400.	.9490	2.11	189.5	392.2	2.199	5.161	4.003	0.841	19.0	6.7	1.6	1.7	1.1	30.1	-68.3	180.0
1405.	.9574	2.11	191.1	395.7	2.199	5.162	4.031	0.842	19.0	6.7	1.6	1.8	1.1	30.2	-68.3	180.0
1410.	.9658	2.12	192.8	399.2	2.199	5.164	4.059	0.843	19.0	6.7	1.6	1.8	1.1	30.3	-68.3	180.0
1415.	.9743	2.12	194.5	402.7	2.199	5.166	4.087	0.844	19.0	6.7	1.7	1.9	1.1	30.4	-68.2	180.0
1420.	.9827	2.12	196.2	406.1	2.199	5.168	4.115	0.845	19.0	6.7	1.7	1.9	1.1	30.5	-68.2	180.0
1425.	.9912	2.13	197.9	409.6	2.199	5.169	4.144	0.846	19.0	6.7	1.7	2.0	1.1	30.5	-68.2	180.0
1430.	.9996	2.13	199.6	413.1	2.199	5.171	4.172	0.847	19.0	6.7	1.8	2.0	1.1	30.6	-68.2	180.0

PART II - THERMAL OUTPUTS (FOR 26. DAT)

[illegible][illegible]

```

LPTSPL VERSION 6(344) RUNNING ON LPT001
*START* USER CLANKE [4177,117] JOB FDR26 SEQ. 778 DATE 28-JUN-76 18:54:24 MONITOR TSC DECSYSTEM-10 602-1 *START*
REQUEST CREATED: 28-JUN-76 18:50:54
FILE: DSK801FDR26.DAT[4177,117] CREATED: 28-JUN-76 18:32:00 <057> PRINTED: 28-JUN-76 18:54:41
QUEUE SWITCHES: /PRINT:ARROW /FILE:FOR /CODES:1 /SPACING:1 /LIMIT:1346 /FORMS: 510,

```

FLYWHEEL VEHICLE PROPULSION SYSTEM
THERMAL MODEL

THERMAL INPUT WEIGHTING FACTORS FOR D.C. MACHINE:

RD1= 0.95 RD2= 0.00 RD3= 0.60 RD4= 0.80 RD5= 1.00
SD1= 0.05 SD2= 1.00 SD3= 0.40 SD4= 0.20 SD5= 0.00

THERMAL INPUT WEIGHTING FACTORS FOR A.C. MACHINE:

RA1= 0.00 RA2= 1.00 RA3= 0.20 RA4= 0.70 RA5= 0.20
SA1= 1.00 SA2= 0.00 SA3= 0.80 SA4= 0.30 SA5= 0.80

	D.C. MACH.	A.C. MACH.	
ROTOR THERMAL RES.=	8.17	18.80	DEG C/KW
STATOR THERMAL RES.=	21.60	7.42	DEG C/KW
GAP THERMAL RES.=	2.97	3.03	DEG C/KW
ROTOR TIME CONST. =	512.00	64.90	SECONDS
STATOR TIME CONST. =	1127.00	39.50	SECONDS

SCR THERMAL RESISTANCE=	58.80	DEG C/KW
HEAT SINK THERMAL RES.=	19.60	DEG C/KW
HEAT SINK TIME CONST.=	18.40	DEG C/KW

NOTE:

- (1) FOR COMPUTING THERMAL INPUTS FROM COPPER LOSSES:
 - (A) TRACTION MOTOR RESISTANCE ASSUMED CONSTANT AT 120 DEG. C. VALUE
 - (B) SYNCHRONOUS MOTOR RESISTANCE ASSUMED CONSTANT AT 200 DEG. C. VALUE
- (2) ALL SOLUTION TEMPERATURES ARE IN DEG. C. ABOVE AMBIENT TEMP.

(continued)

CHARGING MODE DATA : (Station A,Initial)

D-14

[illegible]

(continued)

TIME IN	DC		UC		DC		DC		DC		PDR		PDR		AC		AC		AC		AC		AC	
	LOSS	KW	LOSS	KW	STATOR	GAP	ROTOR	TEMP	STATOR	TEMP	COOLING	SCR	COOLING	TEMP	LOSS	KW	ROTOR	LOSS	STATOR	COOLING	GAP	TEMP	ROTOR	TEMP
SEC					DEG C	DEG C	DEG C	DEG C	DEG C	DEG C	KW	DEG C	KW	DEG C			DEG C	KW	DEG C	KW	DEG C	DEG C	DEG C	DEG C
255.	0.00	0.00	0.00	0.00	0.00	0.00	0.00	0.00	0.00	0.00	0.00	0.00	0.00	0.00	29.62	8.15	21.47	27.81	218.7	237.8	84.3			
260.	0.00	0.00	0.00	0.00	0.00	0.00	0.00	0.00	0.00	0.00	0.00	0.00	0.00	0.00	29.69	8.18	21.51	27.92	220.2	238.5	84.7			
265.	0.00	0.00	0.00	0.00	0.00	0.00	0.00	0.00	0.00	0.00	0.00	0.00	0.00	0.00	29.77	8.22	21.54	28.03	221.6	239.2	85.0			
270.	0.00	0.00	0.00	0.00	0.00	0.00	0.00	0.00	0.00	0.00	0.00	0.00	0.00	0.00	29.84	8.26	21.58	28.14	223.0	239.9	85.3			
275.	0.00	0.00	0.00	0.00	0.00	0.00	0.00	0.00	0.00	0.00	0.00	0.00	0.00	0.00	29.92	8.31	21.61	28.24	224.3	240.6	85.6			
280.	0.00	0.00	0.00	0.00	0.00	0.00	0.00	0.00	0.00	0.00	0.00	0.00	0.00	0.00	30.00	8.35	21.65	28.35	225.7	241.3	86.0			
285.	0.00	0.00	0.00	0.00	0.00	0.00	0.00	0.00	0.00	0.00	0.00	0.00	0.00	0.00	30.08	8.39	21.69	28.45	227.0	242.0	86.3			
290.	0.00	0.00	0.00	0.00	0.00	0.00	0.00	0.00	0.00	0.00	0.00	0.00	0.00	0.00	30.16	8.43	21.73	28.55	228.3	242.7	86.6			
295.	0.00	0.00	0.00	0.00	0.00	0.00	0.00	0.00	0.00	0.00	0.00	0.00	0.00	0.00	30.24	8.48	21.77	28.66	229.6	243.3	86.9			
300.	0.00	0.00	0.00	0.00	0.00	0.00	0.00	0.00	0.00	0.00	0.00	0.00	0.00	0.00	30.33	8.52	21.81	28.75	230.9	244.0	87.2			
305.	0.00	0.00	0.00	0.00	0.00	0.00	0.00	0.00	0.00	0.00	0.00	0.00	0.00	0.00	30.41	8.57	21.85	28.85	232.2	244.6	87.5			
310.	0.00	0.00	0.00	0.00	0.00	0.00	0.00	0.00	0.00	0.00	0.00	0.00	0.00	0.00	30.50	8.61	21.89	28.95	233.5	245.2	87.8			
315.	0.00	0.00	0.00	0.00	0.00	0.00	0.00	0.00	0.00	0.00	0.00	0.00	0.00	0.00	30.59	8.66	21.93	29.05	234.7	245.9	88.1			

TRAVELING MODE DATA : (Outbound Leg)

[illegible]

(continued)

TIME IN SEC	DC LOSS		DC ROTOR LOSS		DC STATOR LOSS		DC GAP LOSS		DC ROTOR TEMP		DC STATOR TEMP		DC GAP TEMP		PDR COOLING		PDR TEMP		AC LOSS		AC ROTOR TEMP		AC STATOR TEMP		AC GAP TEMP	
	KW	DEG C	KW	DEG C	KW	DEG C	KW	DEG C	KW	DEG C	KW	DEG C	KW	DEG C	KW	DEG C	KW	DEG C	KW	DEG C	KW	DEG C	KW	DEG C	KW	DEG C
570.	6.90	6.02	6.02	12.7	1.13	3.4	3.4	3.4	0.95	0.80	71.8	22.95	6.70	16.25	16.21	145.4	132.5	49.4								
575.	6.90	6.02	6.02	13.1	1.17	3.5	3.5	3.5	0.95	0.84	72.6	22.95	6.70	16.24	16.69	147.6	137.1	50.8								
580.	10.92	9.82	9.82	13.6	1.21	3.6	3.6	3.6	1.30	0.92	94.2	36.08	9.92	26.17	17.49	152.6	146.6	53.8								
585.	14.66	13.35	13.35	14.5	1.28	3.7	3.9	3.9	1.57	1.06	112.9	48.25	12.91	35.35	19.23	162.2	164.9	59.6								
590.	14.66	13.35	13.35	15.5	1.36	3.8	4.1	4.1	1.57	1.18	115.3	48.28	12.95	35.33	21.27	172.9	184.2	65.6								
595.	14.66	13.35	13.35	16.4	1.44	4.0	4.3	4.3	1.57	1.28	117.2	48.31	13.00	35.32	23.16	183.3	201.6	71.3								
600.	14.66	13.35	13.35	17.3	1.52	4.1	4.6	4.6	1.57	1.35	118.6	48.35	13.05	35.30	24.91	193.4	217.7	76.5								
605.	14.66	13.35	13.35	18.3	1.61	4.2	4.8	4.8	1.57	1.42	119.6	48.40	13.11	35.29	26.54	203.2	232.5	81.3								
610.	14.66	13.35	13.35	19.2	1.69	4.4	5.1	5.1	1.57	1.44	120.4	48.45	13.17	35.27	28.04	212.7	246.0	85.8								
615.	14.66	13.35	13.35	20.1	1.76	4.5	5.3	5.3	1.57	1.47	121.0	48.51	13.25	35.26	29.44	221.9	258.4	90.0								
620.	22.02	20.32	20.32	21.3	1.85	4.6	5.6	5.6	2.03	1.54	149.6	72.87	19.59	53.28	31.08	234.4	276.4	96.0								
625.	22.02	20.32	20.32	22.7	1.98	4.8	5.9	5.9	2.03	1.66	151.9	73.10	19.84	53.26	33.98	252.0	302.7	104.6								
630.	22.02	20.32	20.32	24.2	2.10	5.0	6.3	6.3	2.03	1.75	153.7	73.38	20.14	53.24	36.68	269.4	326.8	112.7								
635.	22.02	20.32	20.32	25.6	2.22	5.1	6.7	6.7	2.03	1.82	155.0	73.72	20.49	53.22	39.19	286.5	348.0	120.2								
640.	18.63	17.11	17.11	27.0	2.35	5.3	7.0	7.0	1.83	1.86	143.8	62.64	17.72	44.91	41.54	302.5	367.7	126.7								
645.	15.47	14.11	14.11	27.9	2.43	5.4	7.3	7.3	1.62	1.80	130.7	52.16	15.03	37.13	42.34	310.4	372.0	128.7								
650.	7.73	6.80	6.80	28.5	2.49	5.5	7.4	7.4	1.03	1.67	93.3	26.09	6.00	18.09	42.18	311.8	365.2	127.0								
655.	4.42	3.67	3.67	28.8	2.52	5.6	7.5	7.5	0.70	1.49	70.0	14.83	4.96	9.87	40.89	307.8	352.2	122.7								
660.	15.47	14.11	14.11	29.4	2.56	5.8	7.7	7.7	1.62	1.46	123.9	52.73	15.62	37.11	40.26	310.9	348.1	122.5								
665.	15.47	14.11	14.11	30.3	2.64	5.9	7.9	7.9	1.62	1.50	124.7	53.09	15.99	37.09	41.07	319.2	354.2	124.9								
670.	4.42	3.67	3.67	30.8	2.69	6.0	8.0	8.0	0.70	1.41	68.5	14.99	5.15	9.85	40.95	318.9	346.5	122.9								
675.	4.29	3.56	3.56	30.8	2.70	6.1	8.0	8.0	0.68	1.22	63.9	14.66	5.08	9.158	37.77	310.9	327.3	117.1								
680.	11.66	10.59	10.59	31.2	2.72	6.2	8.1	8.1	1.28	1.17	98.4	41.48	13.15	28.33	37.77	308.8	318.5	114.6								
685.	10.61	9.70	9.70	31.7	2.77	6.3	8.3	8.3	1.10	1.17	87.3	39.26	12.81	26.45	37.91	312.5	318.2	114.9								
690.	0.60	0.27	0.33	32.0	2.80	6.3	8.3	8.3	0.11	1.03	26.5	3.14	1.65	1.99	37.39	309.1	307.7	111.8								
695.	0.67	0.35	0.31	31.7	2.79	6.4	8.3	8.3	0.13	0.81	23.4	3.86	1.91	1.95	35.00	296.7	285.3	104.7								
700.	1.41	1.07	0.34	31.6	2.77	6.4	8.2	8.2	0.23	0.65	26.3	6.89	2.94	3.95	32.86	285.4	265.7	98.4								
705.	1.59	1.24	0.35	31.4	2.77	6.5	8.2	8.2	0.25	0.55	25.4	7.60	3.18	4.42	31.08	275.6	249.2	93.1								
710.	0.97	0.66	0.32	31.3	2.75	6.5	8.2	8.2	0.17	0.46	18.7	5.21	2.40	2.82	29.31	265.1	232.6	87.8								

CHARGING MODE DATA : (Station B)

[illegible]

TRAVELING MODE DATA - (Return Leg)

TIME IN SEC	DC LOSS KW	DC ROTOR LOSS KW	DC STATOR LOSS KW	DC GAP COOLING KW	DC ROTOR TEMP DEG C	DC STATOR TEMP DEG C	DC GAP TEMP DEG C	PDR LOSS KW	PDR COOLING KW	PLR SCR TEMP DEG C	AC LOSS KW	AC ROTOR LOSS KW	AC STATOR LOSS KW	AC GAP COOLING KW	AC ROTOR TEMP DEG C	AC STATOR TEMP DEG C	AC GAP TEMP DEG C
935.	1.65	1.30	0.35	2.08	23.0	6.7	6.2	0.26	0.10	17.0	8.42	3.37	5.05	29.10	239.8	240.7	87.3
940.	3.14	2.71	0.43	2.08	23.0	6.7	6.2	0.42	0.16	20.5	13.48	4.62	8.86	27.79	234.1	228.7	83.5
945.	3.14	2.70	0.44	2.08	23.0	6.7	6.2	2.42	0.22	28.9	13.44	4.61	8.83	26.76	229.3	215.0	80.5
950.	0.43	0.12	0.31	2.08	22.9	6.8	6.2	0.06	0.20	7.2	3.67	2.10	1.58	25.41	221.7	204.8	76.0
955.	2.45	1.99	0.47	2.07	22.8	6.8	6.2	0.42	0.22	28.9	10.46	3.84	6.62	24.12	215.2	192.4	72.4
960.	1.75	1.24	0.51	2.07	22.8	6.8	6.1	0.32	0.24	12.2	6.56	2.89	3.67	22.94	208.5	162.1	68.8
965.	1.63	1.23	0.60	2.06	22.7	6.9	6.1	0.22	0.25	12.2	5.91	2.71	3.19	21.72	201.6	172.8	65.1
970.	3.19	2.51	0.68	2.06	22.6	6.9	6.1	2.51	0.24	34.5	9.92	3.71	6.22	20.57	195.0	162.8	61.9
975.	1.12	0.57	0.56	2.06	22.6	7.0	6.1	0.12	0.28	12.5	3.87	2.16	1.71	19.84	189.8	153.5	59.4
980.	2.12	1.50	0.62	2.06	22.6	7.1	6.1	0.37	0.30	27.6	7.59	3.29	4.51	18.95	184.3	146.1	56.9
985.	0.92	0.38	0.54	2.05	22.5	7.1	6.1	0.00	0.25	5.1	3.33	1.95	1.37	17.98	177.7	136.8	53.8
990.	3.19	2.51	0.68	2.05	22.5	7.2	6.1	0.51	0.29	35.6	9.91	3.70	6.21	17.22	173.0	131.1	51.9
995.	3.19	2.51	0.68	2.06	22.5	7.2	6.1	0.51	0.34	30.6	9.91	3.70	6.21	16.73	169.1	127.1	50.4
1000.	6.30	5.44	0.95	2.08	22.8	7.3	6.2	0.82	0.42	57.3	19.20	5.92	13.28	16.74	168.2	129.1	50.9
1005.	6.30	5.44	0.95	2.10	23.0	7.4	6.3	0.82	0.54	59.0	19.21	5.93	13.28	16.94	167.8	131.5	51.5
1010.	6.30	5.44	0.95	2.12	23.3	7.5	6.3	0.82	0.61	60.4	19.21	5.93	13.28	17.13	167.4	133.8	52.0
1015.	6.30	5.44	0.95	2.15	23.6	7.5	6.4	0.82	0.66	61.4	19.21	5.93	13.28	17.30	167.1	135.0	52.5
1020.	6.30	5.44	0.95	2.17	23.8	7.6	6.5	0.82	0.70	62.2	19.21	5.93	13.28	17.45	166.9	137.7	53.0
1025.	2.86	2.20	0.66	2.19	24.2	7.7	6.5	0.46	0.69	40.8	8.93	3.47	5.47	17.35	164.9	135.6	52.2
1030.	2.86	2.20	0.66	2.19	24.0	7.7	6.5	0.46	0.63	39.7	8.93	3.47	5.47	16.72	161.3	130.4	50.5
1035.	2.86	2.20	0.66	2.19	24.0	7.8	6.5	0.46	0.59	38.9	8.93	3.47	5.47	16.23	157.8	125.5	48.9
1040.	2.86	2.20	0.66	2.20	24.0	7.9	6.5	0.46	0.50	38.3	8.93	3.47	5.47	15.73	154.5	121.1	47.4
1045.	2.86	2.20	0.66	2.20	24.0	7.9	6.5	0.46	0.54	37.8	8.93	3.47	5.47	15.27	151.3	117.1	46.0
1050.	1.53	0.95	0.58	2.20	23.9	8.0	6.5	0.24	0.45	23.6	5.05	2.49	2.56	14.75	147.6	111.9	44.3
1055.	1.05	0.50	0.55	2.19	23.8	8.0	6.5	0.09	0.39	13.0	3.86	2.13	1.74	14.21	142.7	105.1	42.0
1060.	1.05	0.50	0.55	2.18	23.7	8.1	6.5	0.09	0.32	11.6	3.86	2.12	1.73	13.31	138.1	99.0	39.9
1065.	1.05	0.50	0.55	2.17	23.5	8.1	6.4	0.09	0.26	10.5	3.85	2.12	1.73	12.67	133.7	93.3	38.0
1070.	1.05	0.50	0.55	2.16	23.4	8.1	6.4	0.09	0.22	9.6	3.85	2.12	1.73	12.27	129.5	88.1	36.2
1075.	2.36	1.73	0.63	2.16	23.4	8.2	6.4	0.41	0.26	29.3	8.42	3.29	5.13	11.74	126.9	86.1	35.4
1080.	2.36	1.73	0.63	2.16	23.4	8.2	6.4	0.41	0.30	30.0	8.42	3.28	5.13	11.53	124.7	84.5	34.8
1085.	2.36	1.73	0.63	2.16	23.3	8.3	6.4	0.41	0.33	30.6	8.40	3.28	5.13	11.33	122.6	83.1	34.2
1090.	2.36	1.73	0.63	2.16	23.3	8.4	6.4	0.41	0.35	31.0	8.39	3.27	5.12	11.14	120.5	81.8	33.6
1095.	2.36	1.73	0.63	2.16	23.3	8.4	6.4	0.41	0.36	31.3	8.38	3.26	5.12	10.97	118.6	80.5	33.1
1100.	2.36	1.73	0.63	2.16	23.2	8.5	6.4	0.41	0.37	31.5	8.37	3.26	5.11	10.80	116.8	79.4	32.6
1105.	2.36	1.73	0.63	2.16	23.2	8.5	6.4	0.41	0.36	31.7	8.36	3.25	5.11	10.65	115.1	78.3	32.2
1110.	2.82	2.16	0.66	2.16	23.2	8.6	6.4	0.48	0.40	36.2	9.87	3.62	6.25	10.52	113.6	77.6	31.9
1115.	2.82	2.16	0.66	2.16	23.2	8.6	6.4	0.48	0.42	36.6	9.86	3.61	6.25	10.49	112.6	77.7	31.8
1120.	9.16	6.05	1.10	2.18	23.5	8.7	6.5	1.20	0.54	81.2	29.54	6.23	21.31	11.23	115.6	86.0	34.3
1125.	6.05	4.96	1.09	2.22	23.9	8.8	6.6	0.91	0.70	67.3	17.79	5.39	12.41	12.34	120.2	97.3	37.7
1130.	2.97	2.06	0.91	2.23	23.9	8.9	6.6	0.45	0.64	39.0	7.85	3.04	4.81	12.21	118.5	94.7	36.8
1135.	2.76	1.87	0.89	2.23	23.9	8.9	6.6	0.41	0.59	35.4	7.16	2.87	4.29	11.87	116.4	91.5	35.8
1140.	2.76	1.87	0.89	2.23	23.9	9.0	6.6	0.41	0.54	34.5	7.15	2.86	4.29	11.55	114.4	88.6	34.8
1145.	3.09	2.17	0.91	2.23	23.9	9.1	6.6	0.47	0.51	37.8	8.21	3.12	5.09	11.25	112.5	86.1	34.0
1150.	3.09	2.17	0.91	2.23	23.9	9.2	6.6	0.47	0.50	37.6	8.20	3.11	5.09	11.05	111.0	84.4	33.4
1155.	3.09	2.17	0.91	2.23	23.9	9.3	6.6	0.47	0.50	37.5	8.19	3.10	5.09	10.85	109.5	82.7	32.8
1160.	3.09	2.17	0.91	2.24	23.9	9.3	6.6	0.47	0.49	37.4	8.18	3.10	5.08	10.68	108.2	81.2	32.2
1165.	8.50	7.27	1.23	2.25	24.1	9.4	6.7	1.19	0.58	81.3	25.48	7.13	18.35	10.87	109.7	85.9	33.6
1170.	2.44	1.71	0.74	2.26	24.2	9.5	6.7	0.40	0.57	34.6	7.43	2.93	4.52	11.14	109.3	86.0	33.6
1175.	1.99	1.42	0.58	2.26	24.1	9.5	6.7	0.35	0.52	31.1	7.28	2.92	4.36	10.88	107.7	83.6	32.8
1180.	1.68	1.22	0.46	2.26	24.1	9.6	6.7	0.32	0.48	27.9	7.18	2.91	4.27	10.63	106.2	81.3	32.1

[illegible]

Part I ALTERNATOR DATA

Source: Westinghouse Aerospace Electrical Division, Lima, Ohio¹⁵

Generator part number: 976J936-10

Service: Used in U.S. Navy S3-A aircraft

Physical Constants:	Weight	42.0 lb
	Size	8.0 D x 9.7 long
	Drawing No.	946F907
	Rating	75 kVA at 12,000 r/min
	Number of poles	4
	Insulation	ML-rated at 200°C for 1,000 h (continuous)
	Cooling	Spray oil at 4 gal/min
	Characteristics	3-phase, brushless generator, 115 V(l-n)

Weight breakdown in lb:

Stator steel 11.0

Rotor steel 6.9

Rotor copper 2.9

Stator copper 4.1

Frame plus insulation 17.1

Total weight 42.0

(continued)

	Symbol	PU	Ohms
Armature resistance (200°C)	r_a	0.0495	0.0268
Direct synchronous reactance (unsaturated)	X_d	3.4	1.84
Quadrature synchronous reactance	X_q	1.24	0.67
Direct subtransient reactance	X_d''	0.145	0.078
Armature leakage flux reactance	X_a	0.085	0.046

Losses in Watts

	No Load	100% Load (75.8 kW)	Loss Model Term
Stator copper loss	0	3938	A_1
Rotating field copper	251	1687	A_2
Exciter loss	260	300	A_2
Stator core loss	1230	1255	A_3
Pole face loss	325	346	A_3
Windage loss	2045	2045	A_4
Stray load loss	207	753	A_5
Fan loss	---	---	---
Total	4318	10324	P_7

$$\text{Efficiency} = \frac{75,800}{75,800 + 10,324} \times 100 = 88.0\% \text{ at rated load}$$

Part II DC TRACTION MOTOR DATA

Source: ASEA manual for 70 hp dc motor LAU203M¹⁰

Rating	70 HP
Base speed	2730 Rpm
Armature voltage	420 Volts
Armature current	140 Amps
Field voltage	24 volts
Field current	12 Amps
Number of poles	4
Enclosure	Drip-proof
Standards	Nema
Insulation class	F

The motor is an ordinary, ventilated version with two free shaft ends. It has been provided with specially strengthened feet suitable for ceiling mounting.

The internal fan is mounted opposite the commutator, and the cooling air is drawn in radially at the commutator end and is exhausted radially at the fan end. Furthermore it is provided with a special air duct at the commutator end for tube connection to a separate blower.

The motor is fed from a 3-phase, 390V, 60Hz supply through a fully controlled thyristor controller. The shunt excitation is taken from a 24 Volt DC-supply. This supply is controlled in order to increase the motor speed to 3170 rpm.

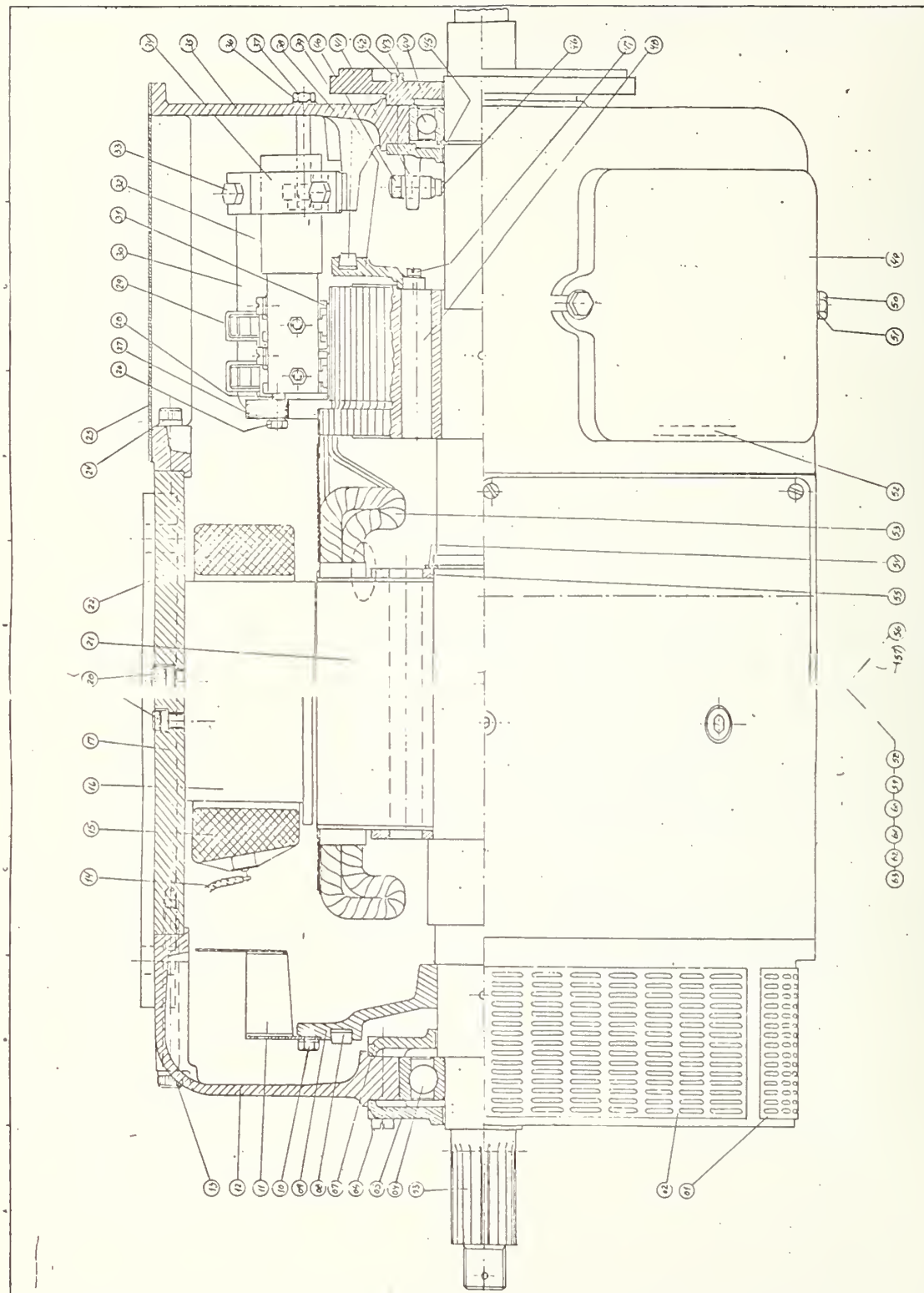


Fig. E-1
Cross Section of 70HP-DC Traction Motor

Table E-1
Parts List For 70 HP-
DC Traction Motor. (See p. E-4)

				DC-motor LAU203M (Morgan town) Parts List (according to drawing) 0808121		Ser. No. 7509322GB	
				Erector Approved 4411		Date 1-15	
				Alt. Dept. HRL		Date 03-05-74	
				Tapped Drift Go		Date 03-05-74	
				Konstruktor Assigned		Cookended Approved	
Serial No.	Part No.	Part Name	Quantity	Part No.	Part Name	Quantity	Part No.
	1 01	Grid plate		0808199			
	2 02	Grid plate		0808180			
	1 03	Shaft		0808091			
	1 04	Ball bearing		SHF 6310-2RS			
	1 05	External bearing cover		0804150			
	4 06	Cheese head screw		0331783	M8x50		
	1 07	Internal bearing cover		062K287			
	1 08	Balance weight clamp		659L001			
	1 09	Fan hub		655L008			
	6 10	Hex. head screw		0126375	M6x10		
	1 11	Fan complete		0282316			
	1 12	End shield drive end		0808172			
	2 13	Socket screw		000E345	3/8"UNC x 4"		
	2 13	Socket screw		000E346	3/8"UNC x 4 1/2"		
	1 14	Hlixon thermostat		1822L-4-4	100°C.		
	1 14	Hlixon thermostat		1822L-6-4	110°C.		
	4 15	Interpole coil		0509221			
	4 16	Interpole piece		0335975			
	1 17	Stator frame		0808148			
	8 18	Socket screw		000F437	1/2"UNC x 3/4"		
	4 19	Main pole piece		0380490			
	8 20	Socket screw		0123277	M8x20		
	1 21	Armature complete					
		consist of item 03-11-30-39-47-48-53-54-55					
	4 22	Main coil		0509248			
	4 24	Socket screw		000E344	3/8"UNC x 2"		
	1 25	Blanking plate		0267155			
	4 26	Hex. head screw		0120405	M6x25		
	1 27	Support ring		0808261			
	16 28	Washer		0101451	464		
	8 29	Brush holder		0570265	HARDENED		
	1 30	Cover with air duct		0814660			
	8 31	Carbon brush, 16x25x40		0808296	QUALITY E.V.B.		
				7509322GB			

				Mr. No.		7509322 GB	
				Ertelster Replaces		Klass 4411	
				Alt. Dept. HRC		Side Page 7-2	
				Tegnet Drafted G.O.		Date Date 03-05-74	
				Konstruktør Designd		Godkendt Apprved	
Enhed	Pos. nr.	Benævnelse	Ident. nr.	Ident. nr.	Udm. Model nr.	Bemærk	
Unit	Item no.	Part name	Ident. no.	Ident. no.	Dim. Part no.	Remarks	
	4 32	Brush holder pin	0140554				1
	8 33	Hex. head screw	0357758		M8x20		2
	4 34	Clamp	6040130				3
	1 35	Endshield-Non drive end	0508950				4
	2 36	Washer	0132594		48.4		5
	2 37	Hex. head screw	0365718		M8x55		6
	1 38	Balance weight clamp	6592001				7
	1 39	Balance disc	0135194				8
	1 40	Brush holder (Earthing)	0518204		Made by Held		9
	1 41	Internal bearing cover	0518255				10
	4 42	Cheese head screw	0331732		M6x50		11
	1 43	Ball bearing	SHF 6209-2RS				12
	1 44	Adapter	0804169				13
	1 45	Circlip ring	0113654		445		14
	1 46	Carbon brush	0518212		Made by Held		15
	2 47	Cheese head screw	0153788		M5x16		16
	1 48	Commutator	0715301				17
	3 49	Inspection cover	0127906				18
	8 50	Hex. head screw	0357728		M8x20		19
	8 51	Washer	0101672		48.4		20
	4 52	Gasket (Emi)			Ø8x690		21
	1 53	Armature coils					22
	1 54	Circlip ring	0113670		460		23
	2 55	Thrust ring	0335681				24
	1 56	Washer	0101508		417		25
	1 57	Eye bolt	6592011				26
	1 58	Adapter	0319902				27
	1 59	Gasket	0326119				28
	1 60	Terminal box	0808164				29
	1 61	Gasket	0326100				30
	1 62	Cover	0326003				31
	12 63	Cheese head screw	0331686		M6x20		32
							33
							34
							35

						7509322 GB	
Udg.	Revision	Dato	St.				

Table E-2
Test Data For 70 HP-DC Traction Motor

E-7

Customer ASEA Inc. 4 New. King St. White Plains N. Y. 10602 U. S. A.				Type LAU 203M		No 2184423	
				Output 70 h.p. kW		Service cont.	
				Voltage 420 V		Current 140 A	
Kind of machine Comp. motor				Excitation 24 V		Speed 2730 rpm	
	Voltage V	Current A arm. exc.		Input kW	Speed rpm	Output kW	Efficiency %
No-load	420	5,1	12,5		3000		
	420	5,1	12,5		3000		clockwise counterclock.
Load	420	140	12,5		2680		
	420	140	12,5		2680		clockwise counterclock.
Resistance between terminals ohms	Winding		At 20				°C
	Arm.		0,0646				
	Comm.		0,0327				
	Series		0,0111				
	Shunt		1,67				
Insul. resistance to frame, megohms		100					
Temperature rise °C	Winding, part of machine		After continuous test at 2680 rpm 420 V 140 A 12,5 A exc.		After at rpm		
			Measured by thermometer	By increase in resistance	By embedded thermometer	Measured by thermometer	By increase in resistance
	Arm.			69			
	Comm.			37			
	Series			29			
	Shunt			38			
	Commutator		32				
High voltage tests	Exc. winding to frame 2000 V 1 min.		Arm. and comm. winding to frame 2000 V 1 min.		Between exc. winding 2000 V 1 min.		
Over-rate tests	Excess voltage V (% incr.) min.		Excess current A (% incr.) min.		Overspeed rpm (% incr.) min.		

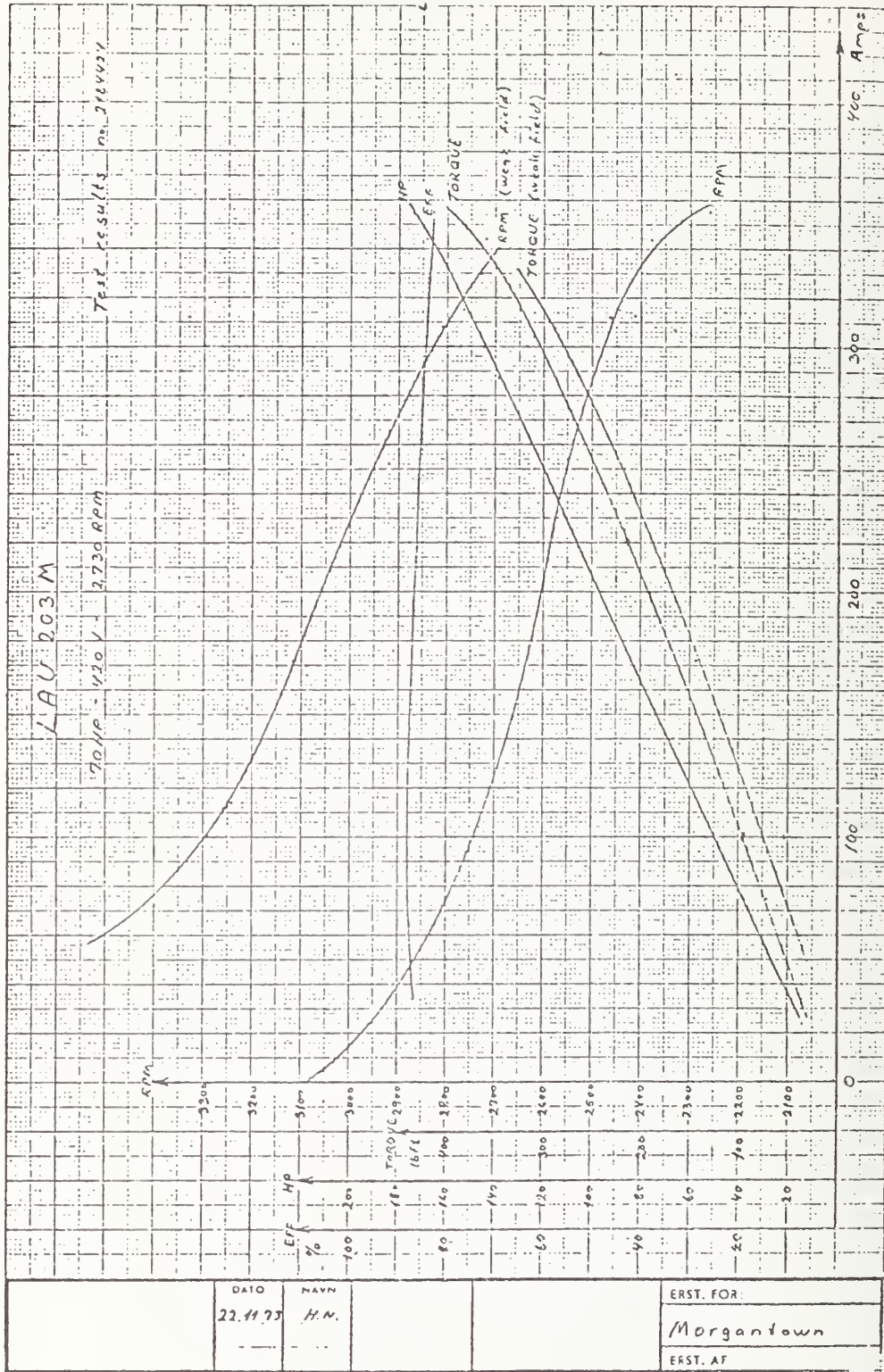


Fig. E-2
Performance Curve For 70HP-DC Traction Motor

WINDING DATA

ARMATURE

43 slots, 129 commutator bars

43 coils (1+2+1) turns of wire 3 par. d=2,0 (insulated with a double coating of enamel).

Weight of copper : 24 lbs.

SHUNT COIL

4 coils, 150 turns of wire d= 2,24 (insulated with a double coating of enamel).

Weight of copper: 30 lbs.

Resistance : 1,7 ohms cold.

SERIES COIL

4 coils, 12 turns of wire 3 x 5 mm (Varnish bonded glass covered rectangular copper).

Weight of copper: 11 lbs.

INTERPOLE COIL

4 coils, 51 turns of wire 3 x 5 mm (Varnish bonded glass covered rectangular copper).

Weight of copper : 33 lbs.

Table E-3
Power Pack Thyristor Data

SOLID-STATE CONTROLLER DATA

Source: Power Semiconductors, Inc. publication: ⁹ PSI-33(909)

TYPICAL CONTINUOUS USABLE D. C. RATINGS

1500 LFM Fan Cooled	I DC Per Leg	KW Output (I DC Leg X 3 X V OC)			DC MOTOR DRIVE - 1.15 SERVICE FACTOR			
		@ 300 V DC	@ 600 V DC	@ 900 V DC	@ 240 V DC	@ 500 V DC	@ 700 V DC	@ 900 V DC
F-180	125	110	225	335	85	200	285	365
F-220	140	125	250	375	110	225	315	405
F-300	170	150	305	460	130	275	385	500
F-400	210	190	375	565	160	340	475	610
F-500	230	205	415	620	180	370	520	670
F-600	250	225	—	—	195	—	—	—
Based on: 6" PSI-3007 Aluminum heatsink (0.08° c/w H. S. - Amb. Thermal Impedance)								

RATINGS:

TYPE PSI-		E or F-180	E or F-220	E or F-300	E or F-400	E or F-500	E or F-600
RMS Fwd. Cur.	I _{RMS}	180A	220A	300A	400A	500A	600A
AVE Fwd. Cur. (180° Cond.)	I _{AVE}	115A	140A	190A	250A	320A	375A
Fwd. Volt Drop @ 500A Peak	V _{FM}	3.00V	2.60V	2.00V	1.50V	1.35V	1.20V
I ² t for fusing @ 8.3 mS	I ² t	35,000	35,000	65,000	80,000	100,000	125,000
Surge Cur. (1) cycle	I _{FM}	3000A	3000A	4000A	4500A	5000A	5500A



APPENDIX F, REPORT OF INVENTIONS

The objective of this work was to develop a computer simulation of electric propulsion systems for flywheel energy storage vehicles. The components that were used to characterize the propulsion system were standard components, therefore the work resulted in no discoveries or inventions.

HE 18.5 .A37 U
no. DOT-TSC-
UMTA-77-15

BORROWER

Form DOT F 172
FORMERLY FORM DC

U. S. DEPARTMENT OF TRANSPORTATION
TRANSPORTATION SYSTEMS CENTER
KENDALL SQUARE, CAMBRIDGE, MA. 02142

OFFICIAL BUSINESS
PENALTY FOR PRIVATE USE, \$300



POSTAGE AND FEES PAID
U. S. DEPARTMENT OF TRANSPORTATION

518

